ScuDo
Scuola di Dottorato ~ Doctoral School
WHAT YOU ARE, TAKES YOU FAR

Doctoral Dissertation
Doctoral Program in Energy Engineering (32nd Cycle)

Exploiting the potential of adaptive building components by means of innovative control strategies

Francesco Isaia
* * * * * *

Supervisors
Prof. Alfonso Capozzoli
Prof. Valentina Serra
Dr. Massimo Fiorentini

Doctoral Examination Committee:
Prof. Per Heiselberg, Referee, Aalborg Universitet
Prof. Francesco Causone, Referee, Politecnico di Milano
Prof. Vincenzo Corrado, Examiner, Politecnico di Torino
Prof. Sergio Sibilio, Examiner, Università degli studi della Campania
Prof. Gianpiero Evola, Examiner, Università degli studi di Catania

Politecnico di Torino
April 30th, 2020

I hereby declare that, the contents and organisation of this dissertation constitute my own original work and does not compromise in any way the rights of third parties, including those relating to the security of personal data.

…….....

Francesco Isaia

Torino, April 30th, 2020

Summary

Reducing building energy consumption while ensuring indoor comfort conditions is becoming everyday more important. Such challenges cannot be approached using traditional solutions, but require a change of paradigm. This transition has already started, as new concepts are arising: *energy flexibility* is gaining importance, demanding improvements in terms of the ability of a building to manage its demand and generation; *responsive building* concepts are replacing the *static* ones, pushing toward building adaptation to changing boundary conditions and requirements.

In this context, *adaptive building façades* represent a promising solution to improve buildings flexibility and responsiveness, providing the building envelope the abilities to change its thermos-optical properties to respond to changing boundary conditions (e.g. weather, occupancy) or requirements (e.g. comfort levels). However, these technologies are rarely implemented in the current building stock.

Control strategies play a central role in the exploitation of adaptive building façades. Despite the widespread use of advanced control strategies in many fields often related to industrial applications, little has been explored for applications involving adaptive façade components.

In this framework, this doctoral dissertation sets out to investigate the opportunities arising from using *advanced control strategies* to operate *adaptive building components*. This endeavour involved different steps. Adaptive building technologies and control strategies were explored through a literature review, with particular focus on components for solar gains modulation and advanced predictive control strategies. Following a pragmatic approach, a Hybrid Model Predictive Control strategy (HMPC) for the operation of an active façade based on electrochromic windows was designed and implemented in two case studies. This activity involved the development of physical models (*white-box*) and simplified

data-driven models (*grey-box*) to accurately describe and predict the thermal dynamics of the systems. Characterization and monitoring of the real case study were carried out to validate the respective physical model and enable the implementation of a real-time control system. A toolchain structure was conceived for the co-simulation and control implementation.

In the first case study, different HMPC strategies were designed to control an electrochromic window with the aim of reducing the heating and cooling energy need. Results based on Key Performance Indicators demonstrated how HMPC strategies outperformed Rule Based Control (RBC) strategies used as baseline and that the possibility to tune HMPC adds flexibility to the controller, which can be regulated according to specific objective functions.

In the second case study, an electrochromic façade was installed in an outdoor test cell (TWINS). The HMPC designed in this case aimed at minimizing the energy need considering the heating, cooling and lighting system. Comparing the HMPC with the baseline strategies, it was demonstrated that the predictive controller was able to better exploit the physical phenomena driving the system evolution, given its prediction abilities and the opportunity to manage contrasting needs

This thesis defines a novel methodology to control active building components using HMPC strategies, able to merge feedback control principles with numerical optimization and to manage both continuous and discrete state variables.

The outcomes of the research activities undertaken in this PhD highlight the importance of control strategies on active building components, showing how an advanced control strategy such as the MPC, on the one hand opens a new set of possibilities (e.g. managing contrasting needs, account for constraints) and on the other hand enhances the performance of these systems.

Acknowledgment

I would like to express my gratitude to my supervisors, Prof. Alfonso Capozzoli, Prof. Valentina Serra and Dr. Massimo Fiorentini, for their insightful comments, encouragements and constant support. I would like to thank Alfonso for always believing in my potential and for helping me to push my own boundaries. I would like to thank Valentina for her scientific and human support and for encouraging my curiosity. I would like to thank Massimo for patiently helping me, sharing his experience and for the precious suggestions.

I would like to thank the TEBE group, in particular the director Prof. Marco Perino, source of inspiration.

I would like to thank Dr. Fabio Favoino for his enthusiastic, inspirational and always constructive suggestions.

I would like to thank Prof. Paul Cooper for hosting me at the SBRC. Thank you to all his research group for welcoming me. Thank you Federico, Neeka, Laia and Steve.

I would like to acknowledge the work of Dr. Luigi Giovannini, crucial for considering lighting requirements in the designed control strategies.

I would like to thank Dr. Stefano Fantucci, whose enthusiasm for research was determinant in convincing me to pursue my PhD.

Contents

List of Tables

List of Figures

Chapter 1

1. Introduction

This Chapter introduces the PhD thesis delineating the background and clarifying the research aims and objectives.

1.1. Background and motivation

During the last decades, the scientific debate has increasingly focused on the need to reduce the global energy consumption, which represents the largest source of greenhouse gas emissions from human activities [1,2]. As stated in many studies and reports, buildings account for up to 40% of the global energy consumption [3,4]. Moreover, an increase in the comfort requirements and the growing accessibility to comfortable buildings pushes the building sector to be more and more energy intensive, both in terms of total energy need and peak loads requirement. To this extent, the concept of *energy flexibility* is gaining importance over the last years, defined in the IEA EBC Annex 67 as *"the ability* [of a building] *to manage its demand and generation according to local climate conditions, user needs and grid requirements. Energy Flexibility of buildings will thus allow for demand side management/load control and thereby demand response based on the requirements of the surrounding grids."* [5,6]. These concepts were also developed in the framework of an increasing need of managing and exploiting energy generation from renewable energy sources (RES), which, because of their discontinuous nature, could jeopardize the energy system stability or at least curb RES market penetration.

Building envelopes account for a significant portion of the overall building energy need. The outdated approach of perceiving the envelope as a barrier that needs to seek a disconnection between the indoor and outdoor environment, can no longer be seen as a viable solution to the current needs. A change of paradigm is increasingly leading to a shift from a *static* conception of the building envelope to *adaptive* concepts [7]. Over the last years, this concept is rapidly meeting reality, given the significant improvements in the building façade systems, which are increasingly able to adapt and respond to changing boundary conditions, in order to meet the users' comfort needs while reducing the building energy demand.

This is made possible by building technologies that are able to modulate heat and mass transfer between the indoor and outdoor environments in many different ways, for example:

- adaptive cladding in opaque façades can exploit variable solar absorption coefficient to control heat fluxes through the opaque building envelope or even energy storage in massive opaque components [8];
- dynamic insulation modulates heat fluxes through the opaque building envelope, with the possibility of allowing or reducing heat gains and heat losses [9];
- double skin façades of advanced multifunctional façades can operate in different modes, exploiting wind action or solar radiation to accumulate or dissipate heat [10,11];
- smart glazing technologies can allow solar gains modulation, with effects on both thermal and lighting [12].

Amongst the many available technologies, *active* building components are particularly promising, since ad-hoc control strategies can be designed to shape the desired behaviour. However, ineffective control strategies applied to powerful active building components could lead to not only nullify the advantages potentially brought by the component, but even worsen the overall performances of the considered system with respect to a traditional, static technology.

Despite the advances in the *hardware* solutions, little is explored on the *software* side [13]. Many advanced control strategies have been used and are currently applied in various fields, often linked to production processes or mechanical systems. A great potential resides in declining these *software* solutions for the previously introduced *hardware* (i.e. active building components). This potential is boosted by the increasing availability of affordable electronic components, powerful computational devices, reliable weather forecast data and data-analytics tools, that provide the needed information and sub-structure to support the application of advanced control strategies in active building elements.

1.2. Research aims and objectives

Nowadays, the need of reducing building energy consumption while guaranteeing comfort condition, better exploiting energy generation from RES and increasing building flexibility is becoming more and more urgent.

A significant contribution in meeting these requirements can come from active building components, which are gaining importance in a world where technology is opening to new possibilities and electronic components are becoming every day more accessible. The inherent potential of active building components systems is enormous, especially if compared with the traditional, static ones.

Today's challenge is that of exploring advanced control strategies in order to fully exploit adaptive building components potential and overcome the cost-effectiveness barrier.

In this context, the presented PhD thesis aims at investigating the new possibilities arising from merging the adaptive abilities of modern building components technologies with powerful advanced control strategies. This endeavour can be summarised as follows:

- Investigation on adaptive (*active*) building components and building control systems, with a particular focus on advanced predictive control strategies;
- Development of validated physical models (*white-box*) and calibrated simplified models (*grey-box*), able to describe and predict the thermal dynamics of the considered systems;
- Characterization and monitoring of a real case study, which allowed the validation of the respective physical model and the implementation of real-time control strategies;

- Conception of a toolchain structure to enable the co-simulation of building systems equipped with active components under advanced-control based operation;
- Definition of a novel methodology to control active building components using Hybrid Model Predictive Control (HMPC) strategies, able to merge feedback control principles with numerical optimization and to manage both continuous and discrete-state variables.

Summarising, this PhD thesis sets out to investigate the use of advanced control strategies for active building components. The design and implementation of HMPC strategies for active façades represent a novel approach to better exploit promising active technologies while considering all these hybrid systems key characteristics.

1.3. Thesis outline

Chapter 2 provides an overview of the current advances in the fields of active building components and building control systems and strategies. The state-of-the-art is described and new opportunities are identified. This literature review constitutes the basis from which the following parts of the thesis developed.

Chapter 3 describes the workflow of the first application of an advanced Model Predictive Control strategy in a simulative case study. An electrochromic window was considered as the active component to be controlled, and results show comparisons between different MPC strategies and between Rule Based Control (RBC) strategies and MPC. This work was developed in the framework of a visiting research program at the Sustainable Buildings Research Centre (SBRC) of the University of Wollongong (UOW), during which, the development of the presented work ran in parallel with the design of a comparative experimental facility composed of two test cells, now built and functioning.

Chapter 4 presents a second case study, characterized by both numerical and experimental activities. The case study considered is a test cell part of the TWINS (Testing Window Innovative System) facility of Politecnico di Torino. In particular, the test cell was equipped with next-generation electrochromic glazing units, characterized by reduced faster transitions between states and improved aesthetics (more neutral colour rendering) and provided in the framework of a research collaboration with a cutting-edge smart-glazing manufacturer. A similar methodological approach of the one carried out in Chapter 3 was applied, resulting in the implementation of a Model Predictive Control strategy considering thermal and lighting requirements. Also in this case, results compare different MPC and RBC control strategies.

Chapter 5 concludes the present thesis, providing an overview on the main findings and results and suggesting perspective for future works.

A schematic of the thesis outline is shown in *Figure 1.1*.

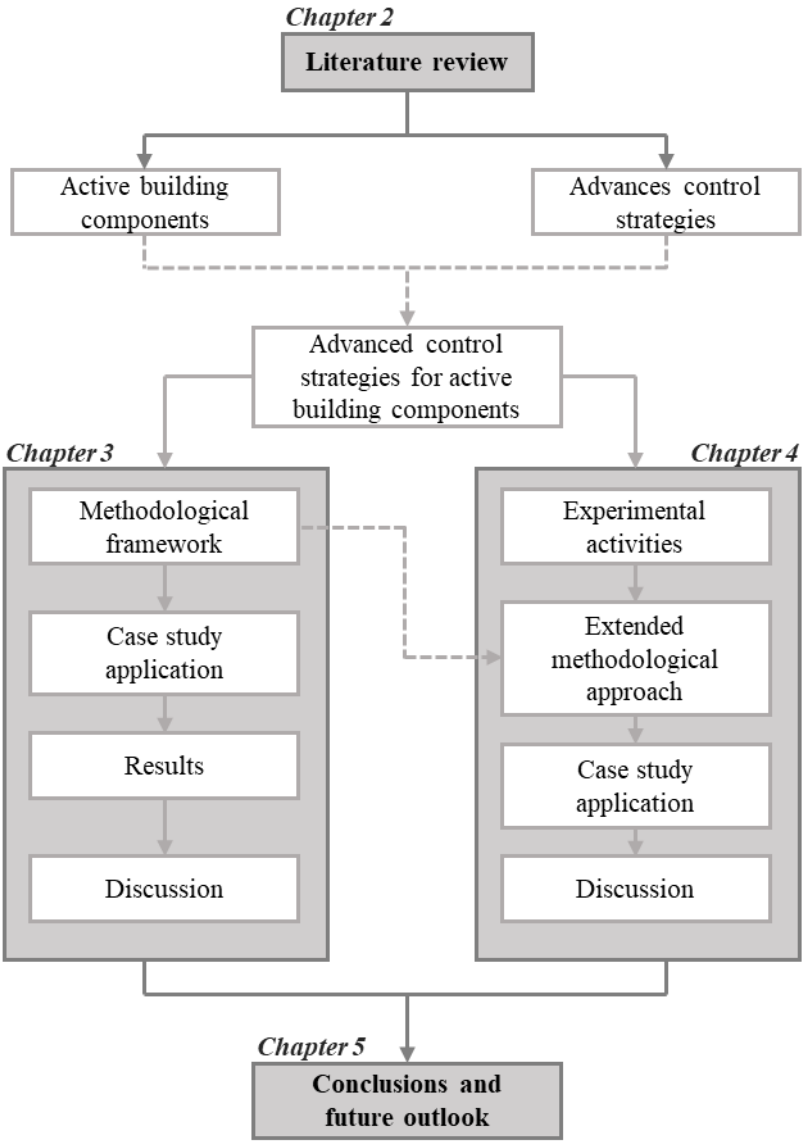

Figure 1.1. PhD thesis outline

Chapter 2

2. Literature Review

This Chapter provides the literature background in which the thesis is developed. Literature review on adaptive building components and building control is reported.

2.1. Introduction

This chapter provides an overview of the literature review carried out in this thesis with the aim of providing a background in the fields of adaptive building components and building control.

A first section focuses on the state-of-the-art building adaptive components, particularly on active components. Specifically, active technologies able to actively modulate solar radiation by means of variable thermo-optical properties are investigated.

A second section reviews current advances on building control including existing hardware architectures, control algorithms and control-oriented modelling. Particular attention was given to papers related to Model Predictive Control, as this control approach was used by the author in this thesis.

2.2. Building adaptive components

Adaptive building components include a variety of building-related technologies and many authors tried to provide a clear definition. Using the terminology of Climate Adaptive Buildings Shells (CABS), Loonen et al. defined it as an element *"able to repeatedly and reversibly change some of its functions, features or behavior over time in response to changing performance requirements and variable boundary conditions, and does this with the aim of improving overall building performance"* [14]. This definition describes precisely the key features of an adaptive building component while being general enough to be applicable to the several ways in which these components can work as stated. From the technological point of view, many reviews have tried to provide classifications, separating them in sub-classes, including opaque components, solar façades, shape-morphing solar shadings, etc. [8,12,15–20]. These can also be divided in *passive* and *active*. *Passive* technologies naturally respond to changing environmental conditions, without the need of an external input. The mechanical or chemical processes that trigger this response can be influenced by different factors, as air humidity [21] or temperature [22]. The advantage of these components is that during operation they operate independently, reducing the system complexity and effort during operation. This, on the other side, is also a weakness: the inability control the adaptive component might lead to unwanted behaviours, which not necessarily always meet the design or occupants' expectations.

Active components, change their properties in accordance with an external stimulus that acts as a control input. These technologies can be mechanically operated, such as shading devices, blinds, vents, or electrical/electronic systems, such as liquid crystal devices (LCD), electrochromic glazing and suspended particle devices (SPD). This category of adaptive components is more flexible than the passive ones, since their behaviour can be altered in accordance to specific needs during operation as they change over time. However, there are several additional installation requirements and precautions to be implemented for the correct integration of these components in a building. An appropriate control infrastructure

needs to be designed in order to connect the active technology with the Building Automation and Control Systems (BACS); the control strategy implemented needs to choose the correct control actions to be delivered to the active component and the necessary sensors to provide feedback to the control algorithm need to be installed in the right location. The increasing presence of automation in buildings is a sign that also the building sector is moving in the direction of the current digital revolution. *Information and Communication Technologies* (ICT) are getting more and more applied in the building sector and new concepts as the *Internet Of Things* (IoT) are shaping the new ways in which physical problems are approached. In this framework, active building components can help pushing this industry in the same direction, finding fertile ground for their application.

2.2.1. Active modulation of solar radiation

Active building components that able to modulate solar radiation affect multiple physical domains, such as thermal comfort, visual comfort and building energy performance. Moreover, ad-hoc control strategies can be conceived to manage the component in order to achieve specific objectives. Furthermore, modulating the incoming solar radiation has both immediate and longer time-span effects on the system, which can both be exploited. For example, in the short term, solar gains can be modulated to affect the immediate effects on thermal comfort due to people exposed to solar radiation, or visual comfort issues; longer-term effects include the heating of the building thermal mass, and use it to allow better thermal comfort conditions while lowering the building energy demand [23]. Of course, this is possible if the control strategy implemented is able to take into account these delayed effects and sometimes conflicting objectives.

Active glazing technologies change their thermo-optical properties in response to an electric impulse. Suspended Particle Devices (SPD) and Liquid Crystal Devices (LCD) require a continuous voltage application to be activated [20]. In SPD, when no potential difference is applied, randomly oriented dipolar particles suspended in an organic fluid block light transmission; when the voltage is applied, these particles align, thus increasing light transmission (*Figure 2.1 a* [24]). LCD work thanks to a layer made of nematic liquid crystal droplets dispersed in a polymer matrix; this composite material is constituted by two materials with different refractive index, which normally results in light scattering, but with a voltage application, the alignment of the crystals allow light transmission (*Figure 2.1 b* [24]). One of the main differences between the devices is that while LCD scatter light and appears translucent when no voltage is applied, SPD absorb light, thus appearing darker.

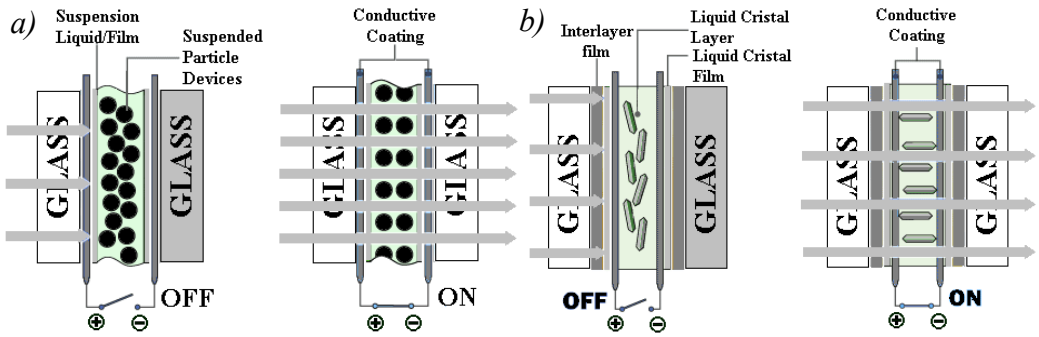

Figure 2.1. Working schematics of a) SPD and b) LCD [24]

Electrochromic materials mainly exploit oxidation and reduction chemical processes to change their optical properties. These materials can be organic-based (as bipyridilium systems, conducting polymers, phthalocyanines, tetrathiafulvalenes, quinones, terephthalates, and cyanobiphenyls) or inorganic-based (mostly W and Ni) [25]. When an external voltage is applied, these chemicals reactions drive electrons to move between the two electrochromic materials, causing a change in the way the solar radiation is absorbed and reflected. It is particularly interesting to observe that when there is no electric voltage applied, the electrochromic glazing maintains the optical properties (*Figure 2.2* [24]). This means that energy is required only to drive a state change, making this technology way less energy intensive than the previously described LCD and SPD. The transition time between two states, however, are slower in electrochromic than in LC and SP devices. Nonetheless, from one side advances in the technology are reducing time response (in the order of few minutes), and from the other side applications in architecture can more easily accept these responses because of the usually slow building thermal dynamics.

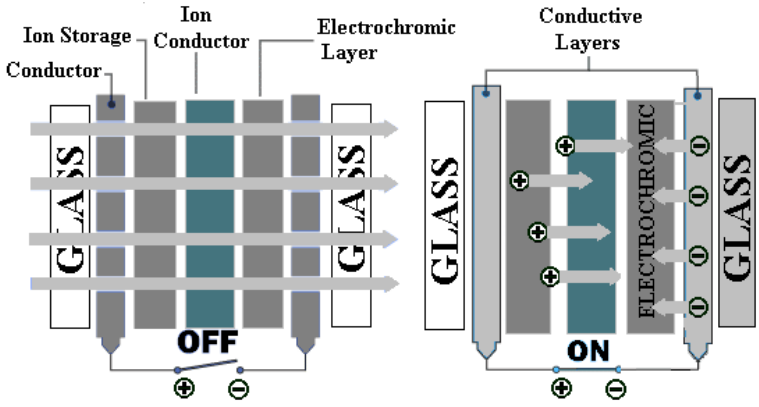

Figure 2.2. Working schematic of an electrochromic glazing [24]

Photovoltachromic couple electrochromic and photovoltaic materials, allowing solar radiation modulation and energy generation. However, further development is needed for these technologies to be implementable for building purposes [26,27].

Many technologies are available for solar radiation modulation in buildings. Each has its advantaged and drawbacks, but electrochromic seems to hold the most potential in the short-mid term: a low energy expense is needed during operation, the adaptation range allows potentially high energy savings and better comfort conditions and the technological readiness level is already mature. Many studies have analysed the electrochromic technology according to the material used ([28–30]), the glazing colour rendering [31] and building applications [32].

Granqvist [33] defines the electrochromic-based fenestration as the most advanced and currently being used in innovative buildings, with the ability of improving energy efficiency, enhancing indoor comfort and providing financial benefits.

Baetens et al. [12] reviewed smart windows technologies for daylight and solar energy control in buildings, concluding that electrochromic windows seem the most promising technology for daylight and solar energy purposes. They also highlight how control affects the effectiveness of electrochromic windows.

As pointed out in literature, control strategies dramatically affect performances in terms of energy consumption and comfort levels. As a result, there is a clear necessity of adopting advanced control strategies to fully exploit the potential of the presented active technologies [12,27,34–36].

2.3. Overview and general description on building control

Active building components are generally controlled using relatively simple Rule Based Control (RBC). As will better discussed in the next subsection, RBC consists of simple *if-then* rules based on endogenous or exogenous parameters which are expected to influence the building performance in terms of indoor comfort conditions or energy consumption. However, more advanced control strategies, which are already been studied in other building systems contexts, can provide an opportunity for a more effective operation of adaptive building components. The following subsections outline the main characteristics and features of building control system and strategies.

2.3.1. Rule Based Control strategies

Rule Based Control (RBC) strategies are currently the most widespread control algorithms applied to building active glazing systems. They are formulated to enable operations that, *if* a condition occurs, *then* a given control action is applied; this is translated in practice by choosing certain parameters and the relative thresholds to establish which conditions lead to what actions are to be applied. While the control actions are related to the technology used (e.g. glass tinting states in case of electrochromic windows), the controlled parameters, acquired via the sensing system, can encompass endogenous (e.g. indoor temperature) and exogenous (e.g. solar radiation) variables. These can also result from a mathematical elaborations of multiple measurements (e.g. comfort indices such as

the Predicted Mean Vote). The most used parameters are the indoor temperature [37,38], outdoor temperature [39], solar radiation [34,35,37,38,40–42], illuminance [35,37–39,43], heating or cooling need [40] and occupancy levels[35,40].

Karlsson [44] applied two control strategies to for switchable glazing control in an office module. One strategy is based on solar radiation, linearly varying the switchable glazing between 50 and 300 W/m^2; the other strategy is based on indoor air temperature and occupancy presence.

Scorpio et al. [38] used three strategies to control a crystal based electrical driven window, which could switch from a transparent to an opaque (translucent) state. The control strategies were based on the indoor air temperature (*thermal strategy*), the daylight illuminance inside the room (*daylight strategy*) and the solar radiation on the vertical surface (*solar strategy*).

Jonsson and Roos [40] tested four control strategies: one based on the heating or cooling need, one on transmitted solar radiation and two strategies based on schedules and combining the previous logics with information on occupancy.

Ritter et al. [37] based their five control strategies on solar radiation, internal illuminance, indoor air temperature and two controls based on the PMV-index.

Gugliermetti et al. [34] developed an ON-OFF and a linear controller based on the incident solar radiation.

Lee et al. [45] modulated the tinting level of an electrochromic window based on the incident solar radiation or on the work plane illuminance.

Fendandes et al. [43] controlled an elecrochromic window with blinds to satisfy visual comfort parameters.

Assimakopoulos et al. [36] used a learning-based approach, different from Rule Based Control. They implemented adaptive neuro-fuzzy inference system (ANFIS) using window and work-plane illuminance, vertical solar radiation, and room temperature.

Lee et al. [46] used a simulation-based optimal control to operate electrochromic glazing in commercial buildings considering different climatic conditions. The optimization is based on the minimization of an objective function containing the cooling and heating needs over the year.

All these studies have shown that even using simple rules it is possible to obtain satisfactory results. However, more advanced control strategies as Model Predictive Control have a great potential in further improving the effectiveness of these technologies while allowing more flexibility in operation.

2.3.2. Model Predictive Control strategies

Model Based Control strategies approach the control problem in a completely different way compared to RBC. In MBC, the controller uses a generally linear and differentiable model of the system, used to simulate the behaviour of the system to choose the best strategy to reach predefined goals. This result in a much higher flexibility compared to RBC strategies, since instead of using pre-defined strategies, an *indirect logic* approach is exploited, which consists of employing

models to simulate the system behaviour under different control strategies and choose the best one [47,48].

When MBC strategies are enhanced with predictive abilities, future scenarios can be taken into account, potentially increasing the controller performance. This formulation, called Model Predictive Control (MPC), is considered one of the most promising advanced control strategies [47,49].

Serale et al. [49] developed an extensive review on MPC for building and HVAC system energy efficiency.

In MPC, the underlying model is able to predict the response of the dynamic system, called *outputs*, from information on the manipulated variables (*inputs*) and uncontrolled inputs (*disturbances*). The MPC looks for the best sequence of future inputs to minimize a given cost function. This optimization procedure is performed for a pre-defined prediction horizon, and constraints on inputs and outputs are taken into account by the controller. The first inputs of the optimized sequence are applied, and the procedure repeats itself at the following control time-step. This makes the MPC a feedback, closed-loop control, and the peculiar procedure of moving the prediction horizon forward at each time-step is known as *receding horizon* (*Figure 2.3* [49]).

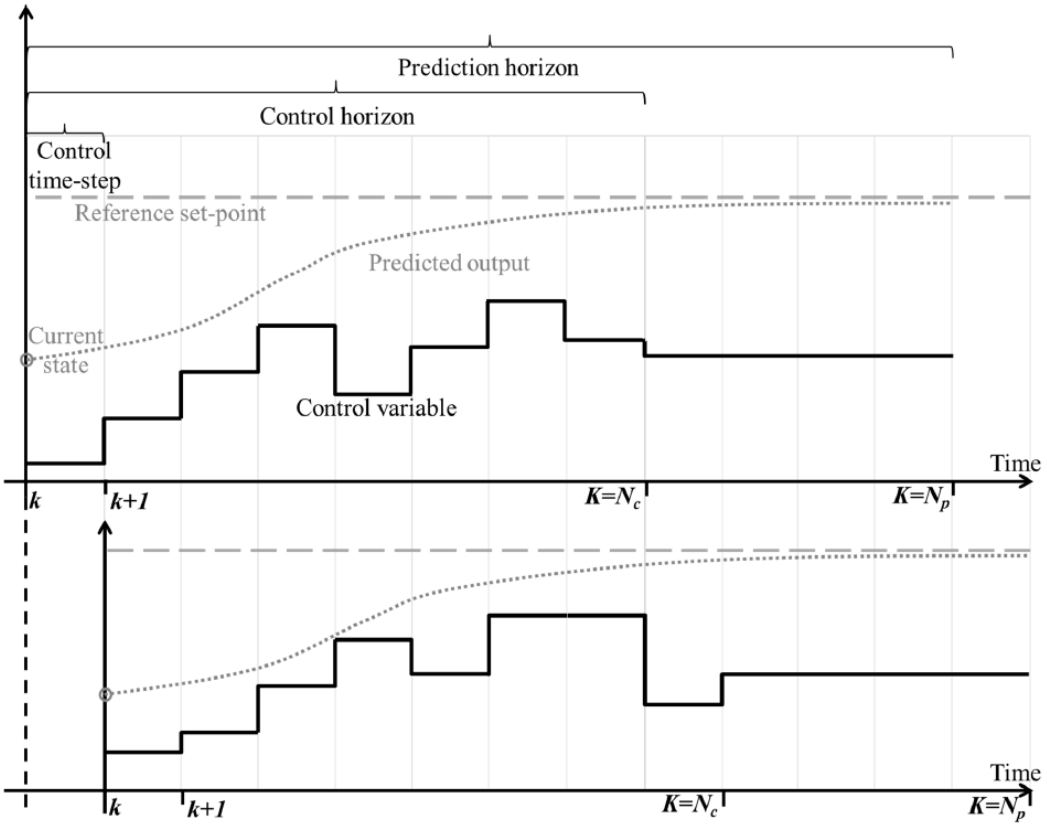

Figure 2.3. Receding horizon schematic [49]

In *Figure 2.3* [49], *k* is the current moment, the *control time-step* is the time at which the control is updated, the *control horizon* is the time in which the manipulated variables can assume different values and the *prediction horizon* refers to how much ahead in the future the looks to optimize the cost function. Often the control horizon and the prediction horizon can be found equal.

An exhaustive framework pointing out all the elements composing an MPC is found in [49] and reported in *Figure 2.4*.

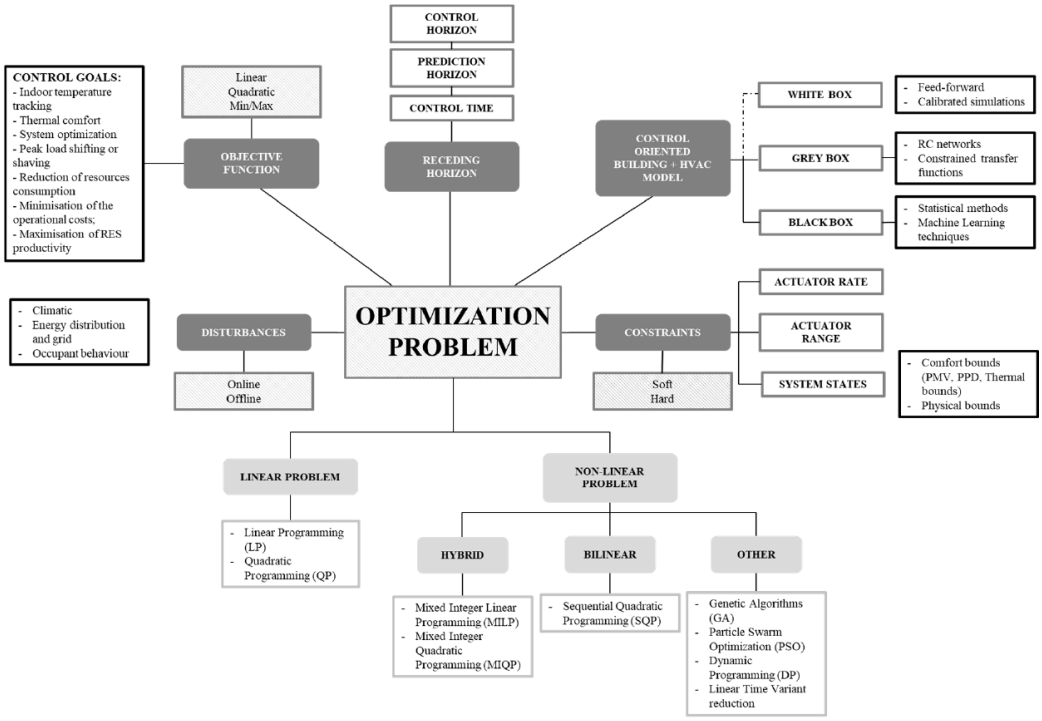

Figure 2.4. Framework of the MPC optimization problem [49]

From *Figure 2.4* it is clear that MPC is much more complex to design than direct RBC strategies. The dark grey rectangles point out all the working elements of an MPC, specifically conceived for building and HVAC system. If adaptive components are also considered, the overall complexity of the MPC formulation increases, but the same constituting blocks are needed. The functional pieces of an MPC strategy are now described.

Disturbances

Disturbances are related to all the input variables affecting the system that cannot be controlled; in the case of building applications, weather conditions are always considered, but additional disturbances as occupancy levels, energy pricing and occupants' behaviour can be considered. On one side, this increases the complexity of the problem and adds uncertainties to the future prediction on the used disturbances; on the other side, however, improvements in the controller performance could be seen. This because a better exploitation of potential benefits provided by the disturbances or a better planning to anticipate unfavourable changes can be foreseen by the controller.

Objective function

The *objective function* defines the goal to be sought; multiple factors can be taken into account at once, even contrasting. This feature makes the MPC

particularly interesting for applications in buildings with adaptive components, in which the multiple needs to satisfy are often in contrast. For example, increasing the transparency of a switchable glazing, leads to an increase of natural daylight in the indoor environment, thus reducing the energy needs for artificial lighting; on the other hand, an increase in exogenous heat gains via solar radiation occurs, leading to potential increases in cooling energy needs. It is indeed essential to find a trade-off solution to satisfy the overall need of energy reduction. This is possible to be defined in the objective function of the MPC, with the added feature of associating a *weight* to each involved controlled variable, allowing to tune a given MPC strategy according to specific needs. Following the previous example, by tuning in different ways the relative weights associated with the energy usage and the transparency level of the switchable glazing, the MPC will find different strategies while seeking the same goal. If the energy usage is associated a much higher cost (or weight) than the related to the transparency level of the switchable glazing, MPC will consume as little energy as possible, almost regardless of the transparency level. However, if a lower cost is associated with energy usage, the MPC strategy will allow a higher energy usage than the previous case, but ensuring higher transparency levels.

The objective function can be written in the form [50]:

$$\begin{aligned} min \sum_{k=1}^{N_p} \left[W_x \| x(k) - x(k)_r) \|_{n_x} + W_y \| y(k) - y(k)_r) \|_{n_y} \right] \\ + \sum_{k=0}^{N_{p-1}} \left[W_u \| u(k) - u(k)_r) \|_{n_u} \right. \\ \left. + W_{\Delta u} \| u(k) - u(k-1)) \|_{\Delta u} \right] \end{aligned} \tag{2.1}$$

Where:

- $x(k)$ is the vector of the system states
- $y(k)$ is the vector of the outputs
- $u(k)$ is the vector of the manipulated inputs
- r (use as subscript) refers to the reference values of the relative vector
- $W_x, W_y, W_u, W_{\Delta \mathrm{u}}$ are the weight matrices
- N_p is the prediction horizon
- k is the discrete time step

Receding horizon problem

The *receding horizon* parameters need to be conceived as a function of the specific needs, the time-span in which the system physical phenomena take place and the characteristics of the controlled components. For example, the control time-step for a switchable glazing needs to be chosen considering the time needed for the change in state to occur. At the same time, the prediction horizon depends on

the time-spans involved in a specific case, so strategies designed for high thermal mass buildings will need to consider longer (minimum) prediction horizons than cases related to lightweight buildings. It is worth to be noted that setting long prediction horizons and short control time-steps will lead to high computational effort, which could result in needing more time to compute a single control time-step than its real duration (i.e. impossible to implement).

Constraints

Constraints are a key characteristic of MPC strategies, and allow to put boundaries on the manipulated inputs and the system states. Constraints on manipulated inputs can include physical limitations, as the maximum power of a HVAC system, or preferences, as avoiding switchable glazing state variation during the night. Constraints on the system states are usually used to define the target conditions, as the indoor air temperature. Another feature adding flexibility to MPC is the possibility to define hard constraints and soft constraints. Hard constraints set strict boundaries that cannot be violated; soft constraints, instead, allow the violation of the boundary, penalizing the cost function by means of a *slack variable* that measures the entity of this violation. Since the slack variable plays a role in the cost function, also in this case a relative weight is associated. Relatively high weights associated with the slack variable result in a soft constraint behaving as a hard one.

Control-oriented models

Control-oriented models are used to predict future system states based on future disturbances and controlled inputs. It is thus of paramount importance to conceive reliable control-oriented models, since otherwise the MPC strategy would be based on wrong future predictions, resulting in failing of achieving the goal or even to find feasible solutions at all [51,52]. Building models are generally dived in three categories: white-box, grey-box and black box models [47,49,51,53]. *White-box* models describe the physical model through detailed physical laws, thus solving algebraic and differential equations to assess the system dynamics. On the opposite end, *black-box* models are empirical, data-driven models that are not based on the laws governing the physical system. *Grey-box* models can be considered as in-between the two previous groups, since they are based on a simplified physics of the system, which can be solved through algebraic or first order differential equations (ODE). The parameters used to describe the simplified physical model need to be identified using measured data or data obtained from white-box simulations. An overview of the positive and negative aspects of these models is presented in *Table 2.1*.

Table 2.1. Main Advantages and Disadvantages of the different model typologies for control applications (adaptation from [47]*)*

Models	Advantages	Disadvantages
White-box	Accuracy Reliability Describe detailed physical phenomena	Computational effort Error-prone modelling Not suitable for control and real-time applications
Grey-box	Describe physical phenomena in a simplified way Easy to implement Low computational effort Suitable for control and real-time applications	Lower accuracy than white-box Not generalizable
Black-box	Low computational effort Flexibility Suitable for control and real-time applications	Physical phenomena are not described Application specific

In *Figure 2.5* a comprehensive schematic of this classification, according to ASHRAE [53], is provided.

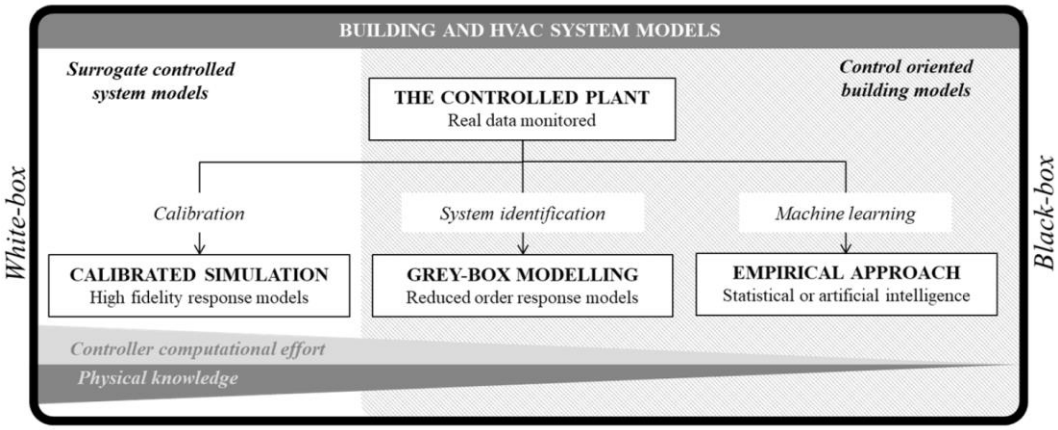

Figure 2.5. Schematic of the different modelling approaches according to ASHRAE classification [49]

As Aste et al. suggest, *"the basic conditions that a model for MPC should satisfy are simplicity, stability, accuracy and precision in the estimation of system dynamics"* [47]. For these reasons and for the effectiveness in modelling the thermal response of a building [54], grey-box models are widely used in MPC applications [55–57]. Grey-box models *"retain the physical description of the system they represent and their parameters can be estimated using system identification methods"* [49]. The "retained physical description" is approached using the analogy between the thermodynamics of a system and an analogue Resistance-Capacitance (R-C) electrical network.

An example of the R-C analogy is presented in:

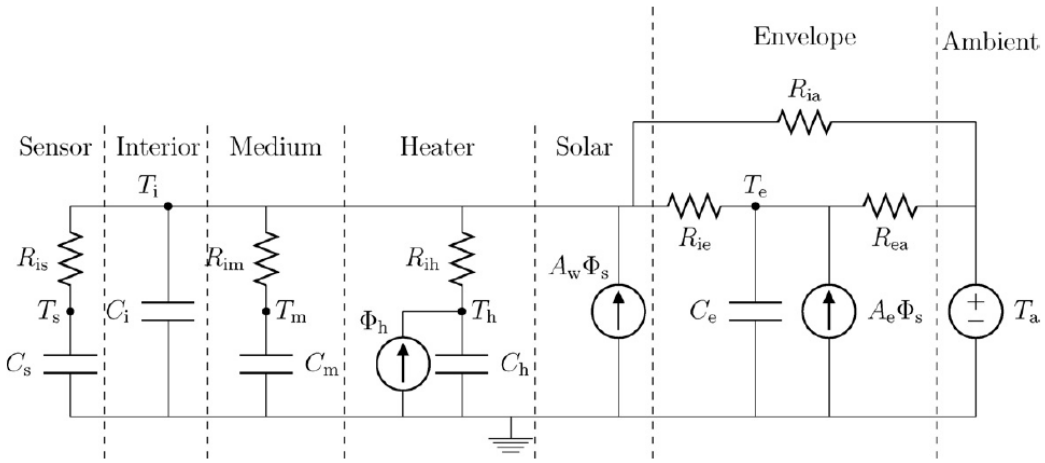

Figure 2.6. An example of an R-C network describing a building thermal system [58]

Figure 2.6 represents an example of the R-C analogy, as described by Bacher et al. in a research work aimed at identifying suitable models for the heat dynamics of buildings: increasingly complex grey-box models were considered in a case study and statistical and physical analyses were used to evaluate the models. It was found that starting from a certain level of complexity (specifically, from the model called $T_iT_eT_h$), that residuals were found similar and the models were able to well describe the dynamics of the system [58]. The outcome of this study was greatly considered in the case studies presented in this thesis.

Grey-box models are usually written using a state-space representation of Linear Time Invariant systems (LTI) [50]:

$$\begin{cases} x(k+1) = Ax(k) + B_u u(k) + B_v v(k) + Gw(k) & (2.2) \\ y(k) = Cx(k) + D_u u(k) + D_v v(k) + d(k) & (2.3) \end{cases}$$

Where:

- $x(k)$ is the vector of the system states
- $y(k)$ is the vector of the outputs
- $u(k)$ is the vector of the manipulated inputs
- $v(k)$ is the vector of the uncontrolled inputs (disturbances)
- $w(k)$ is the random noise on the states measurement
- $d(k)$ is the random noise on the outputs

The matrices $A,\ B_u, B_v, C, D_u, D_v$ and G are, respectively, the state matrix, the manipulated input matrix, the disturbances matrix, the output matrix, the direct transmission matrix for manipulated inputs, the direct transmission matrix for disturbances, the matrix of the random noise on states. These matrices are estimated through system identification techniques.

2.3.3. Applications of MPC for buildings

In literature, many research studies have involved the application of MPC strategies in buildings, receiving a continuously increasing interest in the scientific community. It is in fact widely accepted that MPC strategies can lead to significant performance improvements, depending on the specific application, if compared to conventional control strategies.

A demonstration of the increasing interest in this control approach for building applications is the emergence of tools as *MPCPy* [59], an open-source software platform for allowing non-experts of MPC to apply these strategies in buildings.

Building systems

Simulative and experimental applications involve MPC strategies for the control and operation of building HVAC systems.

Oldewurtel et al. [60], for example, designed a Stochastic Model Predictive Control strategy for building climate control through a HVAC system and considering weather prediction and the relative uncertainty.

Experimental studies were conducted by Sturzenegger et al. [61], which applied linear and non-linear MPC strategies in test rooms and buildings with different heating and cooling systems (as HVAC, TABS, radiators, fan-coil).

The Czech Technical University (CTU) has implemented an MPC strategy for the control and operation of the heating system of the university building. Their extensive research activity demonstrated how MPC strategies, compared to weather-compensated control systems, improved energy savings up to 24% [62–64].

Researchers at the University of California, Berkeley have been developing different MPC strategies for building temperature regulation. Morosan et al. used a distributed predictive control approach considering intermittently operating mode, and the occupation profile [65]. A non-linear stochastic approach was used by Ma & Borrelli, considering prediction of weather and occupancy, with energy savings of 30% compared to conventional RBC and PID strategies [66]. MPC strategies for cooling systems with thermal energy storage were also experimentally tested, showing improvements in the system COP with respect to the baseline control logic [57,67].

Adaptive components

There are few examples of MPC strategies used to control active building components.

An extensive research activity was developed by ETH Zurich and other commercial partners in the OptiControl project [68]. An integrated control of blinds, lighting and HVAC system was considered for different buildings, climates and systems. The most significant energy saving potentials were found in high

thermal mass buildings and in climates with high and variable energy fluxes (as solar gains).

Favoino et al. used a non-linear Receding Horizon Control (RHC) strategy to control photovoltachromic glazing in different climates and demonstrates the energy saving advantages compared to RBC strategies [26]

One of the most active contributor in the field is the LNBL of the University of California, Berkeley. Coffey used a near-optimal MPC to control a dynamic façade and radiant slab heating and cooling system for energy use minimization. Near-optimal rules for some class of buildings are developed by extrapolating from the results of optimal offline control results from prototypical buildings [69]. In recent publications by Gehbauer et al., an MPC approach was developed [70] and used [71] to control a dynamic façade. A gradient-based, non-linear programming problem solver derives the control strategy, and a second step is needed to convert the solution to a discrete state for façade actuation. As declared by the authors, weaknesses of the approach include that continuous and differentiable models are required, precluding *"the use of integer variables, tables, and other complex modeling structures such as if-statements"* [70].

The possibility to take into account discrete and continuous variables can be provided by the Hybrid Model Predictive Control, the MPC formulation used in the case studies of this PhD thesis.

2.4. Discussion

Technological advances in the field of adaptive components is leading to increasingly performing solutions to be integrated into buildings. In particular, *active* components can be exploited to explicitly control their thermos-optical properties changes, potentially improving their effectiveness. The use of *active* components in buildings implies appropriate control infrastructures (as BACS), which are increasingly widespread in modern buildings. *Active* components consist of a plethora of different technologies with different properties and adaptability ranges, and although many are still in their early stages of prototyping, many mature technologies are ready to be implemented. Many studies have explored the opportunity of implementing these technologies, with the result of a promising future for many of those. As it has been clearly stated by many researchers, control strategies greatly affect the performance of *active* building components. However, the majority of the studies use conventional RBC strategies to control these systems. Moreover, by controlling active building components, multiple physical domains can be affected, as thermal comfort, visual comfort, lighting energy need, heating or cooling energy need and so on. This leads to the necessity of considering different and often contrasting needs while designing a control strategy, which it is not possible to be achieved using simple rule-based strategies.

On the other hand, extensive research has exploited the potential of advanced control strategies to control building systems. In particular, MPC has demonstrated to be particularly suitable for building applications. Despite the many applications for building mechanical systems, very few studies have explored the opportunities

to exploit MPC strategies for active building components. However, these applications are characterized by weaknesses linked to the adoption of sub-optimal solutions or limitations as the preclusion of using certain variables.

This PhD thesis aims at exploring the opportunities to control active building components using advanced control strategies. In particular, the electrochromic technology was taken into account given its potential in terms of performance and development stage. Since Model Predictive Control strategies are widely considered to hold great potential in buildings, and given the importance of predicting future disturbances when controlling active building components, these strategies were identified as the most suitable. This thesis goal is to cover the literature gap of using promising and advanced control strategies as MPC for an active building component technology which demonstrated great performances in building applications as electrochromic glazing. In particular, Hybrid Model Predictive Control strategies were used, which enabled to merge feedback control principles with numerical optimization and to manage both continuous and discrete-state variables. This study represents a first attempt to fully decline MPC strategies to intrinsically hybrid systems, which need both continuous and discrete variables to be considered.

Chapter 3

3. MPC formulation in a case study: a methodological approach

This chapter introduces the first case study in which a Model Predictive Control strategy was designed and applied.

3.1. Introduction

In the framework of a research collaboration between the Politecnico di Torino and the Sustainable Buildings Research Centre (SBRC) of the University of Wollongong (UOW), an outdoor experimental facility consisting of a set of two identical test cells has been designed with the aim of running comparative testing on different envelope components or systems in a real outdoor environment.

During the design phase of the test cells, a research activity on electrochromic glazing was specifically carried out, with a particular focus on the control strategy applied to the glazing system. The short-term objective was to test Model Predictive Control strategies in a numerical simulation environment, with a longer-term objective of testing those outcomes through experimental campaigns. Control strategies play a central role in the performance of adaptive façades (as stated in literature and in Chapter 2 of the present thesis). To this purpose, different control strategies were designed, belonging to two groups: Rule Based Control (RBC), conceived as benchmark cases, and Model Predictive Control (MPC) strategies.

In order to accomplish the aforementioned objective, a first step focused on the development of a building simulation model of the designed test cell, to enable an accurate energy performance simulation of the system. A dataset with the input and output variables of the test cell system (e.g. glass state, internal temperature, transmitted solar radiation, etc.) was then generated via the simulation of this model. In a third step, a state space formulation of the system was developed and, using a Resistance-Capacitance (RC) analogy of the thermal system, a second order grey-box model of the system was developed. With a reliable reduced complexity model, it was then possible to design different MPC strategies, which were later implemented using co-simulations tools. This was achieved by coupling via the Building Controls Virtual Test Bed (BCVTB) [72] the physical model (in EnergyPlus), used to obtain the most reliable results on the test cell response to changing boundary conditions, and an advanced numerical computing tool (Matlab), to solve the designed MPC problems and embed the reduced grey-box model.

3.2. Case study description

The case study experimental facility consists of two identical test cells, allowing comparative tests to be performed [73–75], located at the University of Wollongong, New South Wales, Australia (Innovation Campus - Latitude: 34°24′01″S; Longitude: 150°53′58″E). Each test cell consists of a cube with internal sides' length of 2.4 m (*Figure 3.1*).

The three walls and the roof are made of an external layer of Cement board, an insulation layer made by three panels of Expanded Polystyrene (EPS) (for a total thickness of 30 cm) and an internal layer made of two plasterboards. The floor is made similarly, but with a plywood inside layer instead of the plasterboard, to provide a walkable surface. The thermal transmittance of each side of the cube (U_{wall}) is approximately 0.127 W/m^{2}K.

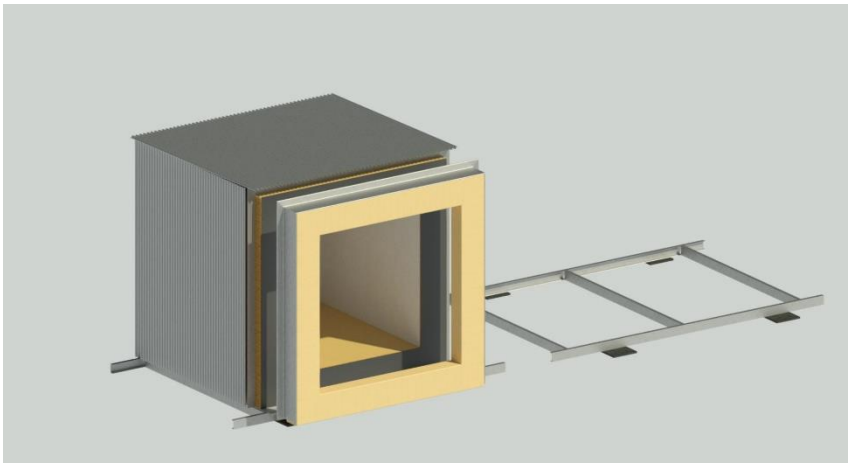

Figure 3.1. Test cell 3D model developed during the design phase

The faces that are not used for façade testing and are exposed to direct or indirect solar radiation (the three sides and the roof) are shaded using external metal cladding panels. The surface that hosts the test façade faces north in order to maximize its incident solar radiation. A frame was designed to support the test façade and to be attached to the test cell in an airtight manner, using multiple air gaskets.

The cell sits on a steel frame structure, which provides proper support, the possibility to anchor the whole structure to the ground in various ways and enables the transportability of the test cell using a forklift. These features were required as the test cells are expected to be moved in different locations for testing and operational reasons.

During the author's stay at UOW, one of the undertaken activities involved the test cells design process, starting from the basic requirements definition to the detailed design and construction procedures. *Figure 3.2* shows some of the details of the test cells. For example, the assembly methods to limit air permeability can be noticed: the red airtight sheets covering the sides of the test cells and the black gasket in the interface between the movable frame hosting the test façade and the

rest of the structure. In the same figure the substantial thickness of the walls can also be noticed, mostly due to the thermal insulation requirements.

Figure 3.2. Assembly of the test cells. On the left, a test façade is being fixed to the test cell with the help of a forklift. On the right, the interior of the test cell.

Figure 3.3 shows a picture of the test cells completed. It can be noticed how the metal cladding shades all the sides and except the test one (green ones in this figure). The test façades presented here are not the one described in this Chapter, as they were only used to run preliminary performance tests on the test cells (airtightness, oscillation of the inside temperature, consistency of the results between the two cells, etc.).

Figure 3.3. Completed test cells

The case study presented in this chapter considers the test cell energy model as developed to support the design phase, thoroughly described in the next paragraph. The test façade is composed of an opaque and a transparent part. The opaque part is identical to the other faces of the test cell, while the transparent part is made of two SageGlass Insulated Glazing Units (IGUs) with dimensions of 1.1 x 0.42 m (*Figure 3.4*). The IGU is composed of two glass panels separated by a gas gap: an electrochromic panel is placed on the external side (7 mm laminated), a low-emissivity glass pane (4 mm) on the inside, divided by 12 mm of Krypton gas. Its thermal transmittance (U_{window}) is 1.267 W/m^{2}K.

Figure 3.4. SageGlass Insulated Glazing Unit (IGU)

3.3. Energy model definition

An energy model of the above described test cells was developed using the building energy simulation software EnergyPlus [76,77].

The test cell was modelled as the final design, considering the three fixed walls and the roof as not exposed to solar radiation, due to the metal cladding designed and built to shade those surfaces.

As previously stated, the opaque part of test façade under investigation consists of the same layers of the fixed test cell faces. These surfaces are characterised by a thermal transmittance (U_{wall}) of 0.127 W/m^{2}K and thickness of about 33 cm (excluding the metal cladding).

Being the transparent part of the test façade adaptive, it was necessary to model it differently than the opaque, static part: multiple *Constructions*, as defined by EnergyPlus, were used in order to take into account all the possible states that the adaptive component could assume. Each *Construction* is made of up to 10 layers, consisting of the defined materials (which, for windows, are divided in *WindowMaterial:Glazing* and *WindowMaterial:Gas*).

In this case, the IGU is composed by two static components and one adaptive component: the internal clear glass panel and the 12 mm gas spacing are static, while the external electrochromic glazing can change state, assuming different light and solar transmission properties. Hence, for each possible state that the electrochromic layer could assume, a different *Construction* needs to be defined. For each *Construction* object, the static layers are the same, but different *WindowMaterial:Glazing* objects are used to describe the electrochromic layer.

To perform accurate simulations, the glazing spectral data sets were necessary. These data specify the normal-incidence measured values of transmittance, front reflectance and back reflectance at 800 wavelengths covering the solar spectrum (from about 0.25 to 2.5 μm). These datasets were exported from the International Glazing Database (IGDB) published by the Lawrence Berkeley National Laboratory (LBNL).

In this database, the *SageGlass_Classic* panel properties are referred to five different states:

Table 3.1. SageGlass states in the IGDB with the relative optical properties

State	g-value [-]	τ_{vis} [-]
Fully clear 64%	0.548	0.728
Int state 18%	0.287	0.203
Int state 11%	0.260	0.119
Int state 6%	0.244	0.063
Fully tinted 1%	0.228	0.014

The *g-value* (or SHGC) and τ_{vis} (visible solar transmission) were evaluated for the single panel using the LBNL Window program, while the states were named as in the database.

The g-value span for the tinted and intermediate states is quite uniform. However, there is a big gap between *Int state* 18% and the *Fully clear* state. A new intermediate state, named *Int state* 41%, was created to fill the gap. This was done by creating a new spectral data set obtained by linearly interpolating each spectral value of the two adjacent states (*Fully clear* and *Int state* 18%).

To simplify the problem while considering the wide adaptability range of the electrochromic glazing, four states were selected: the two extremes (*Fully clear* and *Fully tinted*) and two intermediates (*Int state* 18% and *Int state* 41%).

In the *Construction* section of EnergyPlus, therefore, four different objects representing the electrochromic window were considered. These objects differ one another from the external layer, which corresponds to each of the four considered states of the electrochromic layer.

The constructions that were used are reported in *Table 3.2*:

Table 3.2. Correspondence between the chosen construction states and the glazing properties

State name	Electrochromic state	g-value [-]	τ_{vis} [-]
Clear	Fully clear 64%	0.436	0.634
Int1	Int state 41%	0.287	0.405
Int2	Int state 18%	0.138	0.176
Dark	Fully tinted 1%	0.066	0.012

To know how each surface of the building is made, EnergyPlus associates a *Construction* name to each surface object. Thus, whenever a glass state change is wanted, the *Construction* object associated with the window needs to be changed. This can be done through:

- predefined schedules;
- simple rule-based instructions;
- external inputs.

Obviously, predefined schedules are not a solution when control purposes are sought, but can be extremely useful to perform tests and generate surrogate datasets.

A very useful feature of EnergyPlus is the Energy Management System (EMS), which allows giving simple instruction to the simulated models. As described in the EnergyPlus documentation, *"EMS provides high-level, supervisory control to override selected aspects of EnergyPlus modelling"* [78]. The instructions were written using the EnergyPlus Runtime Language (Erl), which allows simple Rule Based Control (RBC) strategies to be implemented directly into the simulation program.

Another crucial feature in EnergyPlus is the *ExternalInterface* class. It *"allows coupling EnergyPlus to the Building Controls Virtual Test Bed (BCVTB)"* [79]. BCVTB is a software that can link different simulation programs (as EnergyPlus, Matlab, Modelica, etc.) in order to run co-simulations. In this particular case, while EnergyPlus simulates the energy model, powerful numerical software as Matlab can run complex control algorithms to choose the most appropriate electrochromic window state as a result of an optimisation process. This is possible because BCVTB ensures data exchange between the two programs as the simulation moves forward. This last option is clearly the most complex one, but surely the one that unlocks a whole new set of possibilities from a control perspective.

3.4. Simplified model and System Identification

Complex model-based control algorithm as Model Predictive Control need fast-to-solve yet reliable numerical models.

Grey-box models are often used for these purposes, since they carry the basics of the thermal interactions happening in the described model, they can be identified using real datasets, and they are sufficiently accurate without carrying the complexity and non-linearity of the complete physical equations that describe all thermal phenomena occurring in a building.

In this case, following the most commonly used approach, the R-C network analogy and the state-space representation are used to describe the grey-box model [58,80,81].

3.4.1. R-C network definition

As in [58], different R-C networks were developed in order to find the one that best described the real system dynamics. It is in fact true that increasing the system complexity enriches the description of the underlying thermal phenomena, but at the same time leads to an increase of the number of parameters to be identified, undermining the system identification process.

Figure 3.5 represents the R-C model used to describe the test cell.

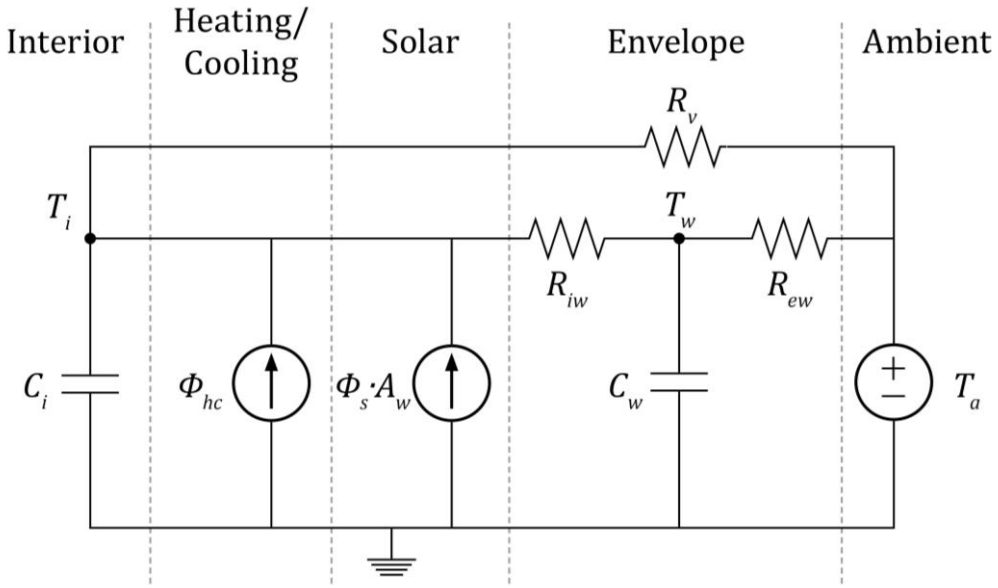

Figure 3.5. Second order R-C network chosen to the describe the test cell

Where:

- T_i – average inside temperature;
- T_w – equivalent wall temperature;
- T_a – ambient temperature;
- R_v – equivalent infiltration resistance;
- R_{iw} – internal half of the wall equivalent resistance;

- R_{ew} – external half of the wall equivalent resistance;
- C_i – equivalent internal capacitance;
- C_w – equivalent wall capacitance;
- ϕ_{hc} – energy flux from the heating/cooling system;
- ϕ_s – energy flux from solar radiation;
- A_w – effective window area.

The R-C network presented in *Figure 3.5* is virtually divided in five parts: Interior, Heating/Cooling, Solar, Envelope and Ambient.

The *Interior* part represents the inside of the test cell, with its average inside temperature node (T_i) and an equivalent internal capacitance (C_i) to describe its thermal inertia.

The *Heating/Cooling* part includes an energy flux (ϕ_{hc}) that is positive when sensible thermal energy is provided to the system (i.e. heating) and negative when sensible thermal energy is subtracted from the system (i.e. cooling).

The *Solar* part represents the solar radiation entering the built environment through the transparent component. It is proportional to the effective area of the window (A_w) and to the energy flux of the solar radiation (ϕ_s). It is thus affected by the electrochromic glazing state: as the electrochromic glazing reduced its solar transmission properties (becomes darker), the portion of solar radiation "entering" the built environment gets smaller. This can be taken into account in different ways; in this case, it was found that the most effective is to consider ϕ_s as the incident solar radiation to the considered façade ($\phi_{s,i}$) multiplied by the g-value of the transparent component that it needs to pass through.

The opaque *Envelope* is represented as two resistances (one internal and one external, R_{iw} and R_{ew}), an equivalent capacitance (C_w), to take into account its thermal inertia and, consequently, a node describing the wall equivalent temperature (T_w).

The outside environment is described in the *Ambient* section by the external (ambient) temperature (T_a).

Lastly, the equivalent infiltration resistance (R_v) was taken into account to describe the "thermal connection" between the internal environment and the external one happening because of the infiltration/exfiltration phenomena.

The stochastic differential equations describing the dynamics of the presented model are:

$$\frac{dT_i}{dt} = \frac{1}{R_{iw}C_i}(T_w - T_i) + \frac{1}{R_v C_i}(T_a - T_i) + \frac{1}{C_i}\phi_s A_w + \frac{1}{C_i}\phi_{hc} \tag{3.1}$$

$$\frac{dT_w}{dt} = \frac{1}{R_{iw}C_w}(T_i - T_w) + \frac{1}{R_{ew}C_w}(T_a - T_w) \tag{3.2}$$

Where T_i and T_w are the state variables.

3.4.2. State-space representation

A *state-space* representation was used to describe the Linear Time Invariant (LTI) system. It is defined by the following system of equations:

$$\begin{cases} \dot{x}(t) = Ax(t) + Bu(t) & (3.3) \\ y(t) = Cx(t) + Du(t) & (3.4) \end{cases}$$

Where:

- $\dot{x}(t)$ - state vector;
- $y(t)$ - output vector;
- $u(t)$ – input vector;
- A, B, C, D – time invariant matrices.

In this case, using Equations (3.1) and (3.2):

$$x = [T_i,\ T_w]^T \tag{3.5}$$

$$u = [T_a, \phi_s, \phi_{hc}]^T \tag{3.6}$$

$$A = \begin{bmatrix} -\left(\frac{1}{R_{iw}C_i} + \frac{1}{R_v C_i}\right) & \frac{1}{R_{iw}C_i} \\ \frac{1}{R_{iw}C_w} & -\left(\frac{1}{R_{iw}C_w} + \frac{1}{R_{ew}C_w}\right) \end{bmatrix} \tag{3.7}$$

$$B = \begin{bmatrix} \frac{1}{R_v C_i} & \frac{A_w}{C_i} & \frac{1}{C_i} \\ \frac{1}{R_{ew}C_w} & 0 & 0 \end{bmatrix} \tag{3.8}$$

$$C = [1 \quad 0] \tag{3.9}$$

$$D = [0 \quad 0 \quad 0] \tag{3.10}$$

The parameters to be identified are: R_{ew}, R_{iw}, R_v, C_i, C_w and A_w.

3.4.3. System identification

The system parameters need to be identified using simulated datasets, hence using the results of the EnergyPlus white-box model simulations.

The simulation period was set to four-weeks. The first half of the dataset was used to estimate the grey-box parameters values and the second half to test the accuracy of the model. Random schedules for the Heating/Cooling system and for the electrochromic glazing states were generated, paying attention in having impulses of variable magnitude and duration, and ensuring a heating, cooling and

free-running period in both halves of the simulation period. In *Figure 3.6* it is possible to see how the Heating/Cooling system forcing on the system is operating as the g-value is dynamically modified, with various durations and magnitude. In this way, the resulting dataset takes into account a wide range of possible situations that the modelled system cab encounter.

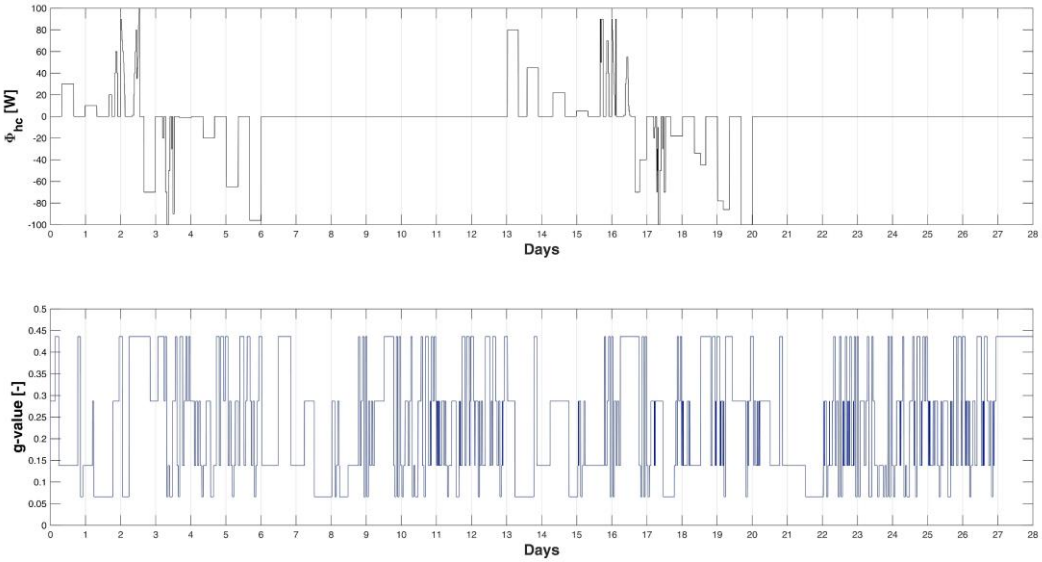

Figure 3.6. Heating/Cooling system and glass state schedules used to generate the input dataset

Using the schedules shown in *Figure 3.6*, the input dataset used for the system identification was generated.

Figure 3.7 shows the input dataset used to identify the LTI system, with the time evolution of the three input variables, Ambient temperature (T_a), heating/cooling power (ϕ_{hc}) and solar gains (ϕ_s). It is worth noting that ϕ_s is calculated as the solar radiation incident on the test façade (G_g) multiplied by the window g-value, which changes according to the schedule shown in *Figure 3.6*.

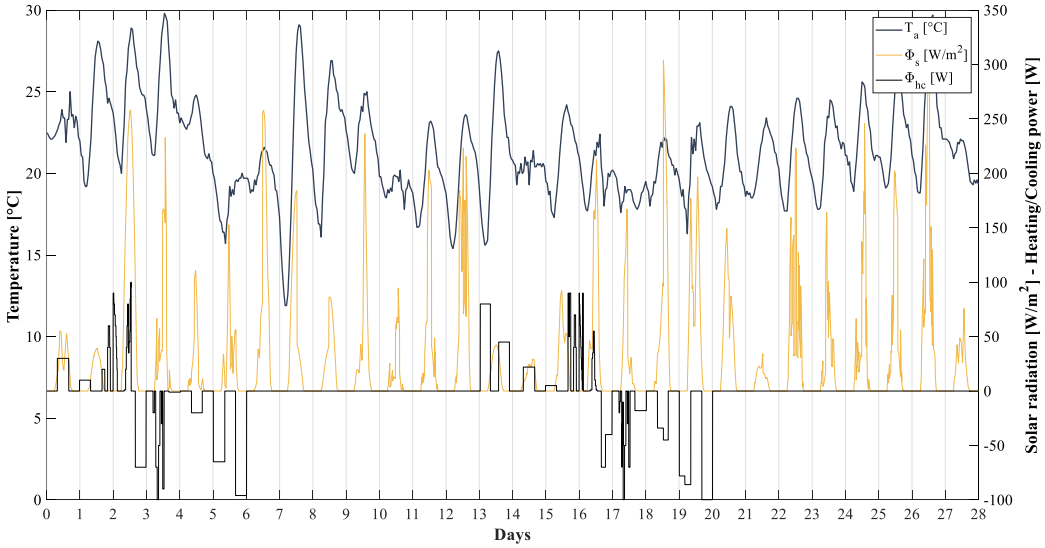

Figure 3.7. Input dataset for the system identification of the grey-box model

The Linear Grey-Box modelling tools readily available in Matlab were adopted to estimate the parameters of the time invariant matrices.

Table 3.3. Parameters identification

	R_{ew} (K/kW)	R_{iw} (K/kW)	R_v (K/kW)	C_i (kWh/K)	C_w (kWh/K)	A_w (m^2)
Identified value	**176.78**	**11.36**	**3796.49**	**0.011**	**0.1293**	**0.616**
Upper boundary	513.36	14.3	3800	0.0132	0.35	1.848
Initial guess	256.68	7.15	1265.5	0.0053	0.175	0.924
Lower boundary	128.34	3.58	421.83	0.0021	0.0875	0.462

Table 3.3 shows the identified values for each parameter in the first row, along with the initial guess, a lower and an upper boundary.

The parameters to identify are lumped, representing thermo-physical characteristics of the model. Some are more straight-forward, such as the equivalent internal capacitance (C_i), that can be estimated by calculating the thermal capacitance of whatever is enclosed in the built environment or as the equivalent window area (A_w), which is the area of the transparent component.

Other lumped parameters are less straight-forward, as the equivalent thermal resistance of the walls (R_{ew}, R_{iw}), which represents an average resistance of the opaque and transparent areas, weighted on the respective areas. In this way, all the elements contributing to the wall resistance are lumped in a single element of the R-C network. Another way of considering this analogy is to see the opaque components as parallel resistors of an R-C network ($R_1, R_2, \dots, R_n$), which can be simplified in one equivalent resistor (R_w) as:

$$\frac{1}{R_w} = \sum_{i=1}^{n} \frac{1}{R_i} \tag{3.11}$$

The internal half of the wall equivalent resistance (R_{iw}) is much lower than the external half (R_{ew}) because the wall section is not symmetrical, and the median capacitance point was estimated at the very internal part of the wall section. This means that the majority of the wall section is on the external side of the median capacitance point, resulting in a R_{ew} much higher than R_{iw}.

The estimated parameters were compared using the second half of the dataset (testing data set), and the fit goodness evaluated using Matlab System Identification Toolbox through the Normalised Root Mean Square Error (NRMSE), resulted to be 89.19% in this case.

The simulated response comparison between the simulated data (EnergyPlus) and the identified model is shown in *Figure 3.8*.

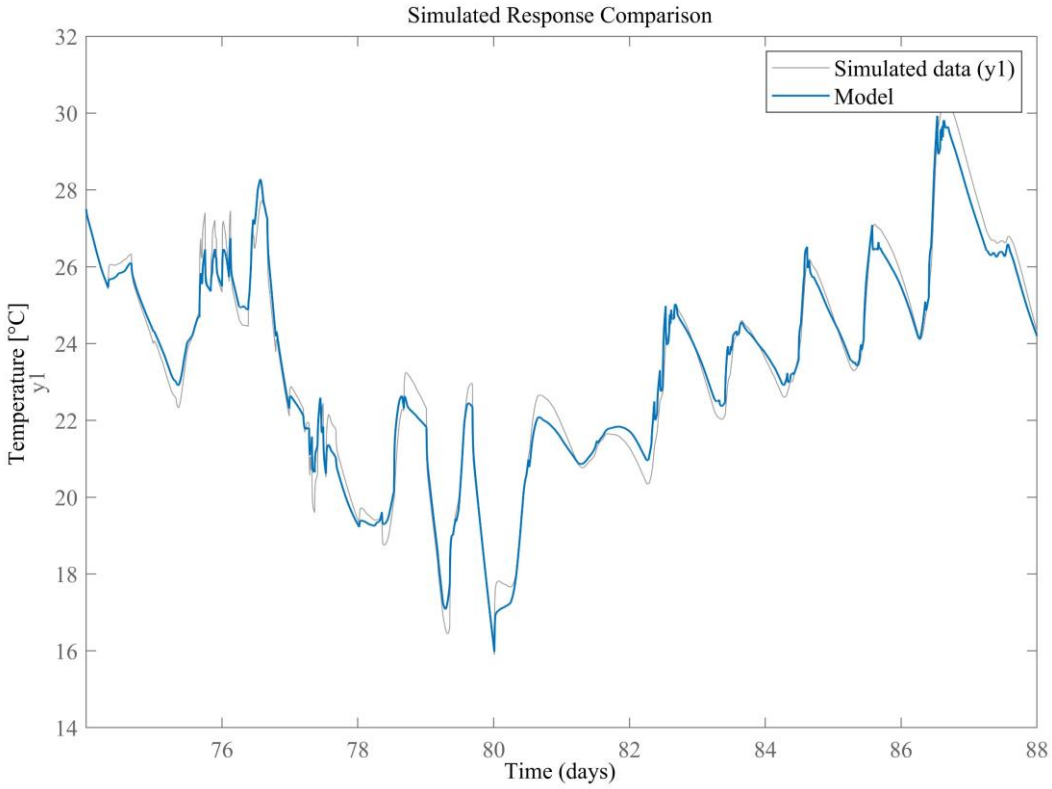

Figure 3.8. Comparison of the simulated response of the identified grey-box model with data simulated in EnergyPlus

3.5. MPC formulation

The presented case study can be seen as a dynamic system in which the output response is influenced by manipulated variables and disturbances. The manipulated variables are, as the name suggests, inputs that can be controlled, while the disturbances cannot be managed. In this case, the manipulated variables are the glass states and the heating/cooling energy, while solar radiation and ambient temperature are disturbances.

The grey-box model previously described works as a control-oriented model, since it can be used by the controller to predict the system future response, which is a function of the future manipulated variables and disturbances. In particular, the MPC can choose the best sequence of manipulated variables, over a defined control horizon, according to a given cost function. MPC uses a numerical optimisation process to find the best control actions, taking into account the present system states and the future disturbances and constraints on both input and output variables. Once the optimal sequence is obtained, the controller applies the first set of values, discards the rest of the control sequence and the whole block moves one control time-step forward (the so-called “receding horizon”).

3.5.1. Constraints

Constraints can be defined as *hard* or *soft*. Hard constraints cannot be violated, while soft constraints are defined so to penalize the cost function whenever its limits are violated (but still allowing the inputs or outputs variable to exceed those limits).

For example, hard constraints are useful to put limits on variables such as the heating/cooling system, which of course cannot exceed their maximum power supply. Soft constraints can be used to describe a preferable range of a certain variable; for example, the internal temperature (T_i) can be defined as preferably ranging from 20°C to 26°C, meaning that whenever these limits are violated, the cost function increases proportionally to this violation. Since the cost function minimization is sought, these violations can occur if this increment is over-compensated by another element in the cost function (e.g. allowing T_i to rise above 26°C but using less cooling energy ϕ_{hc})

The constraints adopted in this case study are summarised in the following equations:

$$\phi_{hc,min} \leq \phi_{hc} \leq \phi_{hc,max} \tag{3.12}$$

$$\sim (\delta_1 \,\&\, \delta_2) \,\&\, \sim (\delta_1 \,\&\, \delta_3) \,\&\, \sim (\delta_2 \,\&\, \delta_3) \tag{3.13}$$

$$\sim (\delta_1 \,\&\, night) \& \sim (\delta_2 \,\&\, night) \& \sim (\delta_3 \,\&\, night) \tag{3.14}$$

$$T_{i,min} - e \leq T_i \leq T_{i,max} + e \tag{3.15}$$

In Equation (3.12), an upper and a lower limit to the heating/cooling load (assuming heating as positive and cooling as negative) are set. Equation (3.13) states the not possible to activate two different window states at the same time (the Boolean variables $\delta_1, \delta_2, \delta_3$ are better explained in the next section). Equation (3.14) forces the system to choose the clear window state at night time, where $night$ is a Boolean value that is equal to 1 when solar radiation is below a predefined threshold. Equation (3.15) sets a soft constraint on the internal temperature T_i: it is in fact possible for the system to violate the boundaries $T_{i,min}$ and $T_{i,max}$, but in those cases the slacking variable e will penalize the objective function. Limits on the absolute value of e are also defined.

3.5.2. Hybrid Model Predictive Control Problem formulation

In the presented case, a Hybrid Model Predictive Control (HMPC) is defined, since both continuous and discrete variables are taken into account: solar radiation, ambient temperature, indoor temperature and the heating/cooling power are of continuous variables, while the electrochromic window state assumes discrete states. In these cases a Mixed Logic Dynamical formulation is required, that can be generally written as:

$$x(t+1) = Ax(t) + B_1u(t) + B_2\delta(t) + B_3z(t) \quad (3.16)$$

$$y(t) = Cx(t) + D_1u(t) + D_2\delta(t) + D_3z(t) \quad (3.17)$$

Where $x(t) = [x_c^T(t)\ x_d^T(t)]$ is the state vector, with a continuous part ($x_c(t) \in \mathbb{R}^n$) and a discrete part ($x_d(t) \in \{0,1\}^{n_d}$); $y(t) = [y_c^T(t)\ y_d^T(t)]$ is the output vector, with $y_c(t) \in \mathbb{R}^m$ and $y_d(t) \in \{0,1\}^{m_d}$ the respective continuous and discrete parts; $u(t) = [u_c^T(t)\ u_d^T(t)]$ with $u_c(t) \in \mathbb{R}^l$ and $u_d(t) \in \{0,1\}^{l_d}$ the respective continuous and discrete parts; $z(t) \in \mathbb{R}^r$ is a continuous auxiliary and $u_d(t) \in \{0,1\}^{r_d}$ represents discrete variables; A, B_i, C, D_i are the real constant matrices [50,82].

3.5.3. Objective function

Writing the problem using the Mixed Logic Dynamical systems, allows to take into account the discrete states of the electrochromic window, and can be seen as multiple linear systems that vary according to the discrete state variable.

The objective function can be written as follows:

$$min_{\{u\}_0^{N-1}} J = \sum_{t=1}^{N-1} \|Q(x(t) - x_r)\|_p + \|R(u(t) - u_r)\|_p \quad (3.18)$$

Where Q is the weighted matrix of the states and R is the weighted matrix of the controlled inputs; $x(t)$ is the state vector, x_r the reference state vector, $u(t)$ the controlled inputs vector and u_r the reference controlled input vector.

In this case, only the controlled inputs are considered for the cost function. The controlled input vector is $u = [e,\ \phi_{hc}, \delta_1, \delta_2, \delta_3]^T$, where e is a slacking variable used to define a soft constraint, ϕ_{hc} is the heating/cooling energy, δ_1, δ_2, δ_3 are three Boolean variables related to the first intermediate (*Int 1*), second intermediate (*Int 2*) and dark states of the electrochromic window respectively. The following table summarizes the Boolean actions:

Table 3.4. Correspondence between the Boolean variables and the relative states action

δ_1	δ_2	δ_3	State	g-value
0	0	0	*Clear*	0.436
1	0	0	*Int1*	0.287
0	1	0	*Int2*	0.138
0	0	1	*Dark*	0.066

The Boolean variables δ_1, δ_2, δ_3 can thus be activated one at the time and when none are active, the electrochromic window is in the *Clear state*.

Summarizing, the cost function takes into account:

- The slacking variable e, which depends on the violation of the soft constraint defined on the output (allowing the relaxation of the internal temperature T_i);
- The heating/cooling energy ϕ_{hc}, which measures the energy needed to warm up or cool down the indoor environment in order to maintain the indoor temperature T_i within the defined range;
- The glass state, defined by the Boolean variables δ_1, δ_2, δ_3 according to the logic shown in *Table 3.4*. The glass state affects the window g-value, which in turn influences the solar gains.

In this study, a control (and prediction) horizon of 6 hours and a control time-step of 30 minutes were chosen. The reasons behind this choice are both linked to the system dynamics and computational effort. It was in fact found that reducing the control time-step, the control horizon needed to be lowered to have reasonable solving durations. At the same time, with longer control horizons, a higher time-step was necessary. The best compromise was found in the before mentioned values for control (and prediction) horizon and control time-step, since it allows the system to correctly deal with its dynamics and consider a sufficiently long horizon to take into account the external dynamics (solar radiation variation over the day). Moreover, lower control time-steps translates to potentially higher state-changes, that in this case study are not preferable considering a user's comfort perspective (uniform conditions are usually considered preferable).

A more precise description of the main characteristics is shown in *Table 3.5*, while the costs associated with the input variables (i.e. the weighting matrices) are shown in *Table 3.6*. With the aim of assessing the weight influence on the controller, different matrices were defined. In each matrix the proportion between the weights associated with the input parameters are different, therefore the cost function minimization will lead to different results from case to case.

Table 3.5. Input variables description

Variable	Description	Variable typology	Limits	
			Lower	Upper
$\boldsymbol{e}$	Slacking	Continuous	0 °C	2 °C
$\boldsymbol{\phi_{hc}}$	Heating/Cooling	Continuous	-100 W	100 W
$\boldsymbol{\delta_1}$	*Int1* State	Boolean	0	1
$\boldsymbol{\delta_2}$	*Int2* State	Boolean	0	1
$\boldsymbol{\delta_3}$	*Dark* State	Boolean	0	1

Table 3.6. Weights associated with the input variables

Variable		Weights				
		W1	W2	W3	W4	W5
$\boldsymbol{e}$	[W/K]	1	1	1	1	0.1
$\boldsymbol{\phi_{hc}}$	[-]	10	10	10	100	1
$\boldsymbol{\delta_1}$	[W]	3E-08	3E-02	3E-01	3E-08	3E-08
$\boldsymbol{\delta_2}$	[W]	4E-08	4E-02	4E-01	4E-08	4E-08
$\boldsymbol{\delta_3}$	[W]	5E-08	5E-02	5E-01	5E-08	5E-08

In *Table 3.6* is possible to notice that the chosen sets of weights follow this logic: starting from a given cost associated with the ϕ_{hc} variable, the slacking variable e weight is at least one order of magnitude lower and the Boolean variables δ_1, δ_2, δ_3, that describe the glass states other than the clear one are, are various order of magnitude lower. This is because ϕ_{hc} is directly linked to an energy cost (the higher the absolute value of ϕ_{hc}, the higher the energy consumption), while the slacking variable e and the Boolean variables δ_1, δ_2, δ_3 are not. The difference between the slacking variable and the Boolean variables is determined by the fact that violating the preferred average inside temperature T_i range, described by the variable e, was considered less preferable than changing the glass state towards lower solar transmission properties. Among the Boolean variables δ_1, δ_2, δ_3, a relatively small weight difference was associated in order to drive the controller to choose the clearest possible state, assuming this is preferable from a visual comfort point of view. An important remark is that the order of magnitude and the nature of the different input variables (summarised in *Table 3.5*) are very different from each other. This aspect influences the choice of the weights, since, as in Equation (2.1), the cost function is influenced by the multiplication between the weighting matrix and the input vector values.

Another important remark is that, while in this study the main objective is to prioritize the energy consumption reduction (of course excluding the always-dark condition), in other applications different weighting matrices can be defined in order to prioritize other aspects. For example, by increasing the cost associated with the slacking variable e, so that the inside temperature control gains importance with respect to the energy consumption or choosing darker glass states.

3.5.4. Programs and setup

The Mixed Logic Dynamical System was formulated in HYSDEL[83]. The MPC algorithm was developed using the Multi-Parametric Toolbox 3.0 (MPT3) [84] in Matlab. The optimization software CPLEX was installed to take care of the Mixed Linear Programming (MILP) problem. The machine in which all of the above was implemented and run is a DELL XPS15, with an Intel Core i7 @ 2.8Ghz processor and 16GB of RAM.

3.6. Co-simulation infrastructure

As anticipated in Section 3 of the present Chapter, co-simulations capability is a key factor for the presented study. Different simulation programs run simultaneously and multiple information needs to be exchanged between the different actors in a synchronised manner. In particular, the MPC algorithm runs on Matlab and uses the grey-box model; at each control time-step the updated state vector is required, along with the future weather conditions; lastly, the control actions chosen by the MPC need to be passed to EnergyPlus, that will apply it on the white-box model until the next control time-step.

This synchronised information exchange, which also involves the pausing and running of different programs, was managed by BCVTB. A comprehensible workflow is shown in *Figure 3.9*.

In *Figure 3.9*, on the left side, the white-box model is represented, and EnergyPlus is its engine. All the physical laws describing the thermodynamics are taken into account, and its results can be seen as measures taken through sensors.

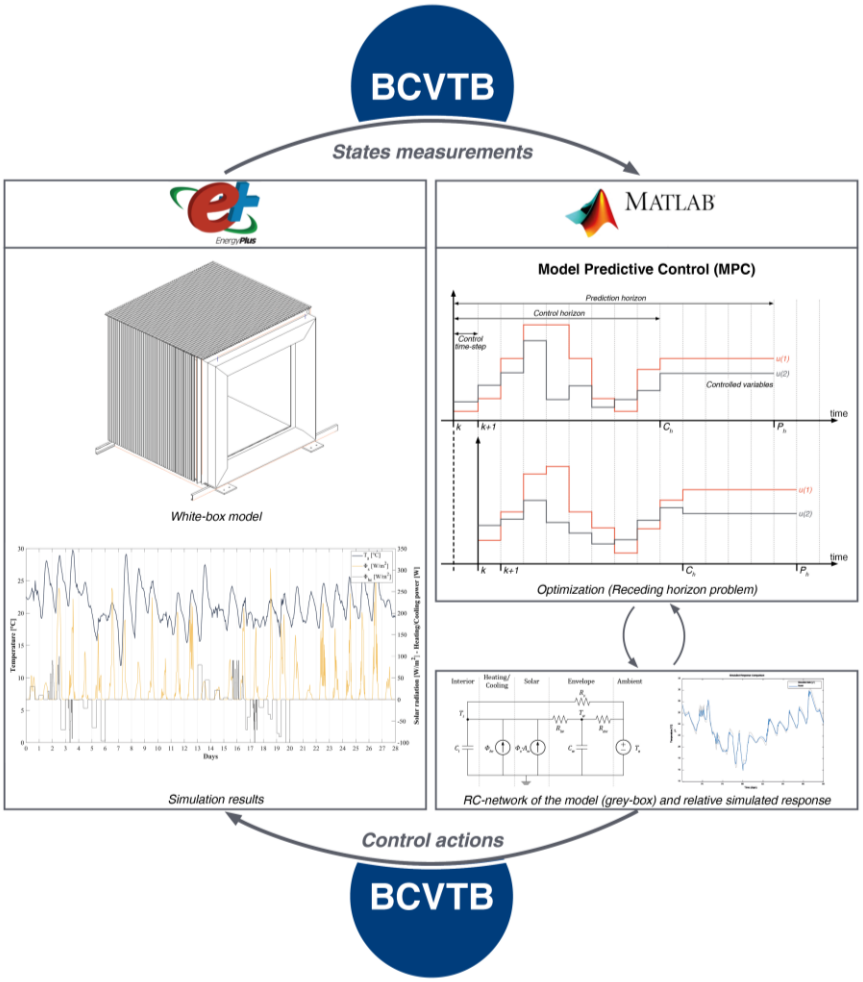

Figure 3.9. Simulation Workflow

On the right side, the MPC problem is formulated in Matlab (with the support of other programs, as stated in the previous section), where an optimization is run based on future estimations performed by means of a grey-box model, which embeds the thermal relationships between the elements, but can be solved rapidly. BCVTB ensures that:

- when a new control time-step is reached, EnergyPlus pauses the simulation,
- the new state measurements are provided to the MPC controller,
- the optimization process takes place, resulting in a control action to be maintained until the next control time-step,
- the control action (input vector) is passed to the physical model,
- the Energy Management System of EnergyPlus implements the control,
- the simulation continues until the next control time-step.

3.7. Baseline controllers

To assess the effectiveness of the previously described MPC strategies, simulations using simple control strategies were performed to set a baseline for the MPC approach.

Firstly, a base case with a static window in the Clear state was simulated

Then, different RBC strategies were implemented, using widely adopted control algorithms. The majority of studies found in the literature consider thresholds on solar radiation or illuminance, while few on indoor temperature. Usually, energy consumption minimization or visual comfort are sought. These IF-THEN strategies are typically implemented on commercial applications [85].

For these reasons, two RBC strategies were designed: one based on the incident solar radiation ($\phi_{s,i}$) and one based on the average inside temperature of the test cell (T_i). In each case, three thresholds were defined, in order to exploit the full adaptability range of the electrochromic window, consisting of four different states as described before. Threshold values are summarised in *Table 3.7*.

Table 3.7. Baseline control strategies summary

RBC strategy	Thresholds	Electrochromic state
$\phi_{s,i}$	$\phi_{s,i} \leq 100$ W/m^2	*Clear*
	100 W/m^2 < $\phi_{s,i} \leq 150$ W/m^2	*Int1*
	100 W/m^2 < $\phi_{s,i} \leq 400$ W/m^2	*Int2*
	$\phi_{s,i} > 400$ W/m^2	*Dark*
T_i	$T_i \leq 24.5$ °C	*Clear*
	24.5 °C < $T_i \leq 25$ °C	*Int1*
	25 °C < $T_i \leq 25.5$ °C	*Int2*
	$T_i > 26$ °C	*Dark*

3.8. Results

In this section, results are presented. Both results related to a given control application and radar charts comparing different control strategies are shown.

Plots show the variation of the main variables over a week period. In particular, weather disturbances (incident solar radiation, $\phi_{s,i}$ and ambient temperature, T_a) are plotted in the upper part of the figures, while the controlled inputs (glass state and heating/cooling system power, ϕ_{hc}) on the bottom. Glass states are represented through the g-value (the lower the g-value, the darker the glass state), while the heating (ϕ_h) and cooling (ϕ_c) powers were split for a better representation.

Radar charts are used to compare different control strategies using five performance indicators:

- *total energy consumption [Wh]*: the energy request of the heating/cooling system over the week period;
- *peak power [W]*: the peak load of the heating/cooling system over the week period;
- *dark states [%]*: the amount of time in which the window was in dark states (i.e. *Int 2* or *Dark*) with respect to the total simulation period;
- *Percentage of Discomfort Hours (PDH) [h]*: as defined in EN 16978-1:2019 [86], it is the percentage amount of time in which the operative temperature T_{op} is above or below threshold values, in this case 20°C and 26°C respectively (Category II)
- *glass state changes [-]*: total number of times in which the glass state changes.

It is possible to notice that the most preferable situation is when all these performance indicators are the lowest possible. Therefore, the bigger the polygon shown in the chart, the worse the correspondent control strategy. The radar chart can rapidly provide an insight on how well certain control strategy behave with respect to some parameters (energy consumption, comfort, etc.) or on a comparison between different control strategies.
To provide an additional tool to compare different control strategies, a new Key Performance Indicator (KPI) was defined. It consists of the normalised area of the polygon: each axis was normalised using its maximum value, so to have all axis ranging from 0 to 1; then, the polygon areas were evaluated for each case. The comparison between the calculated areas provides a fast tool to have an indication on which control strategy can work best: since all the radar charts parameters are best when closer to 0, smaller areas can be associated with better strategies. Whereas the areas of different strategies do not differ much, the radar chart can be analysed to get more insight. It is worth to be noted that similar areas do not result in similar strategies, but strategies with similar performances as long as all the previously described parameters are considered equivalent in terms of importance.

3.8.1. Results – Summer week in Wollongong

From *Figure 3.10* to *Figure 3.14*, results of MPC strategies with the different weights matrices reported in *Table 3.6* are shown for a typical summer week in Wollongong.

In *Figure 3.15*, a radar chart is represented to compare these strategies.

The results related with the control logics used as baseline are shown in *Figure 3.16* to *Figure 3.18*, while in *Figure 3.19* a comparison between benchmark and best performing MPC results is displayed.

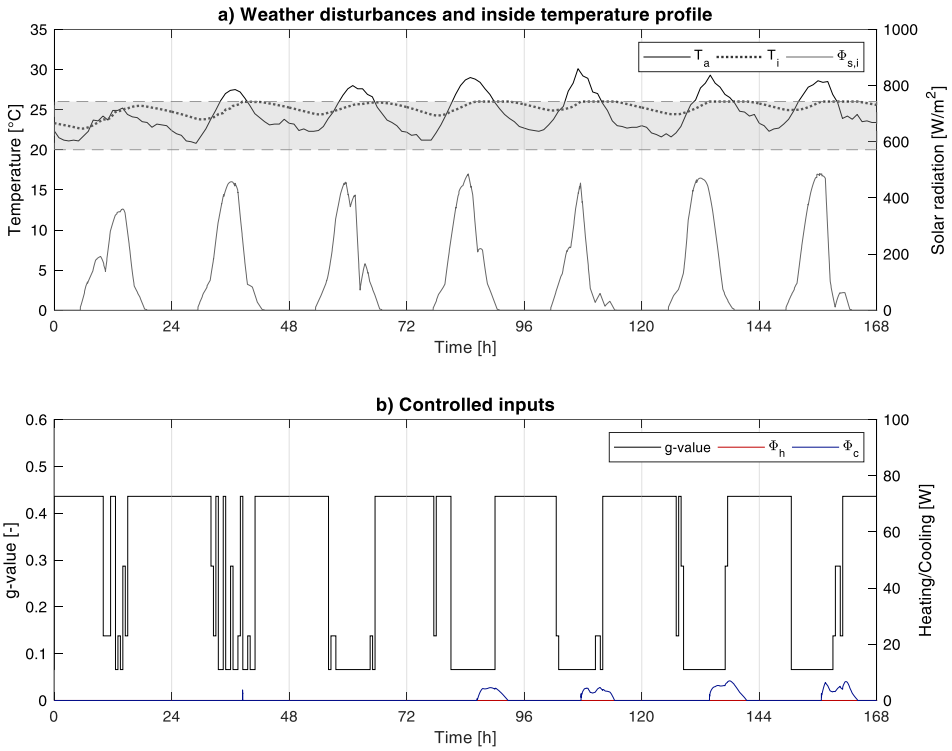

Figure 3.10. MPC control in Wollongong during a summer week. Weights W1

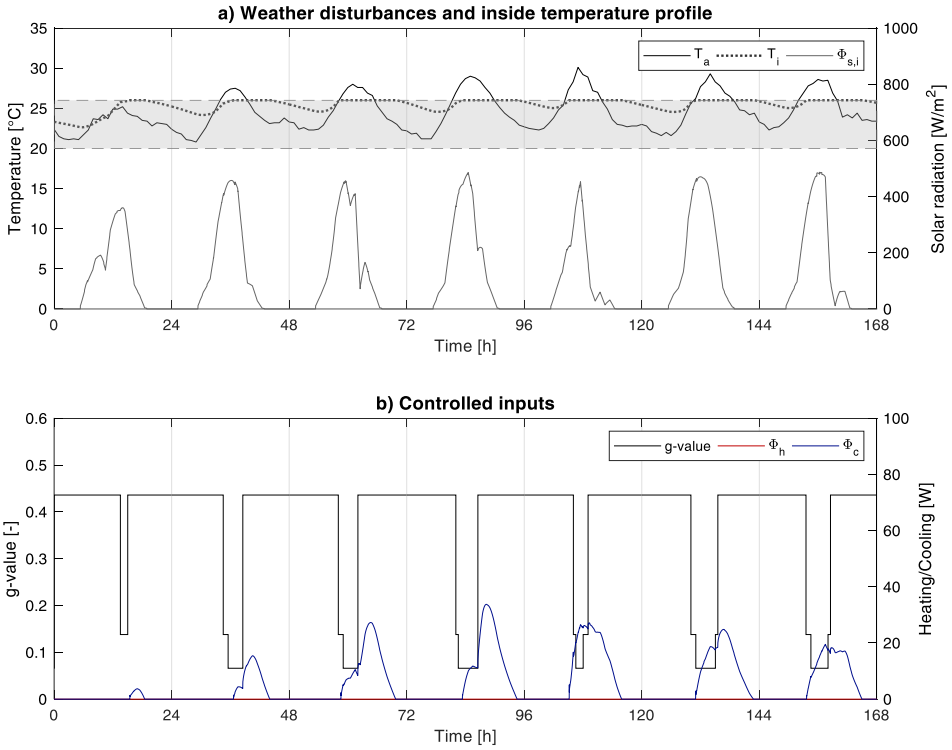

Figure 3.11. MPC control in Wollongong during a summer week. Weights W2

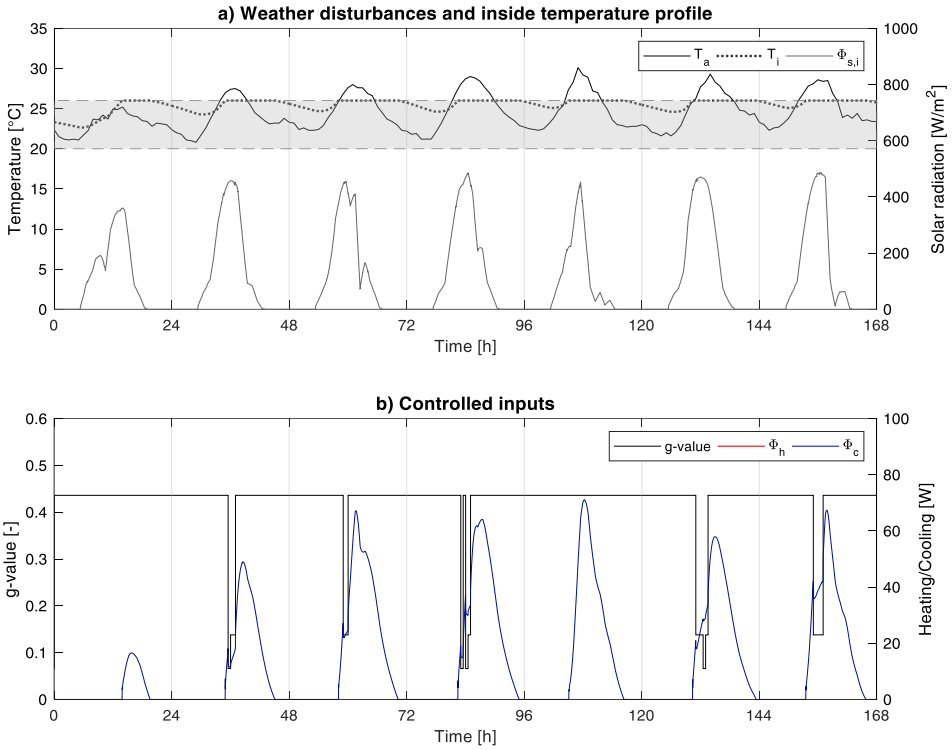

Figure 3.12. MPC control in Wollongong during a summer week. Weights W3

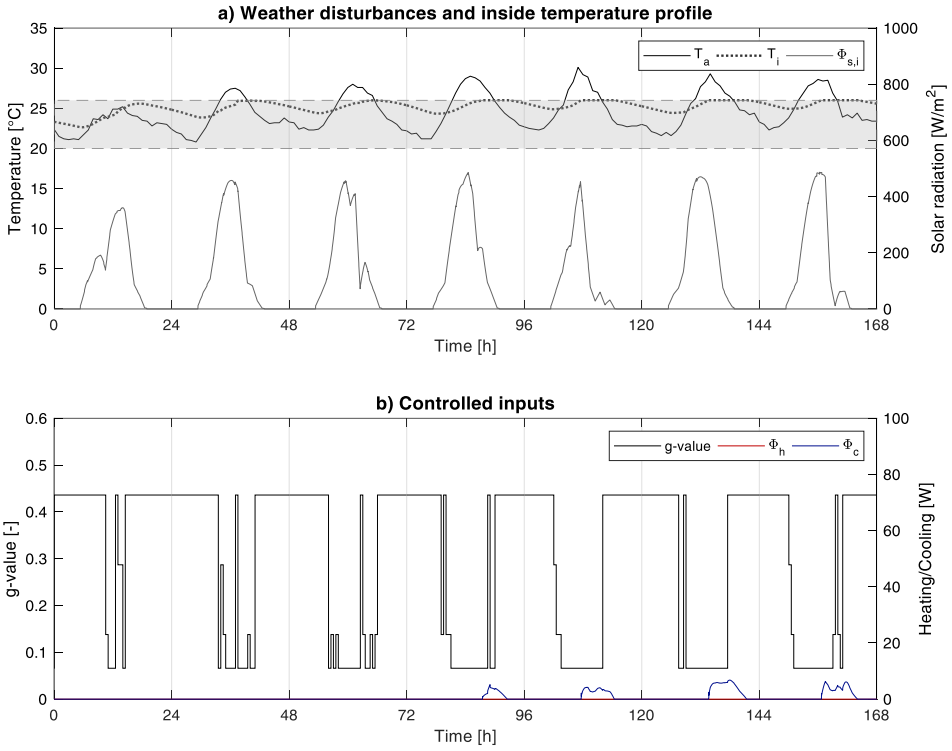

Figure 3.13. MPC control in Wollongong during a summer week. Weights W4

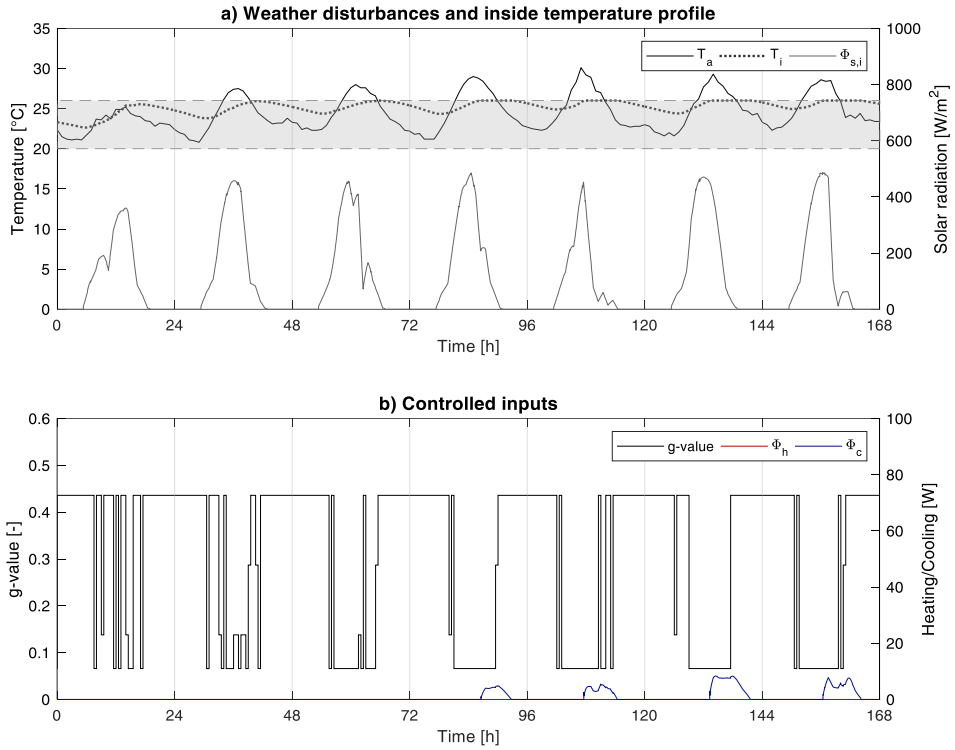

Figure 3.14. MPC control in Wollongong during a summer week. Weights W5

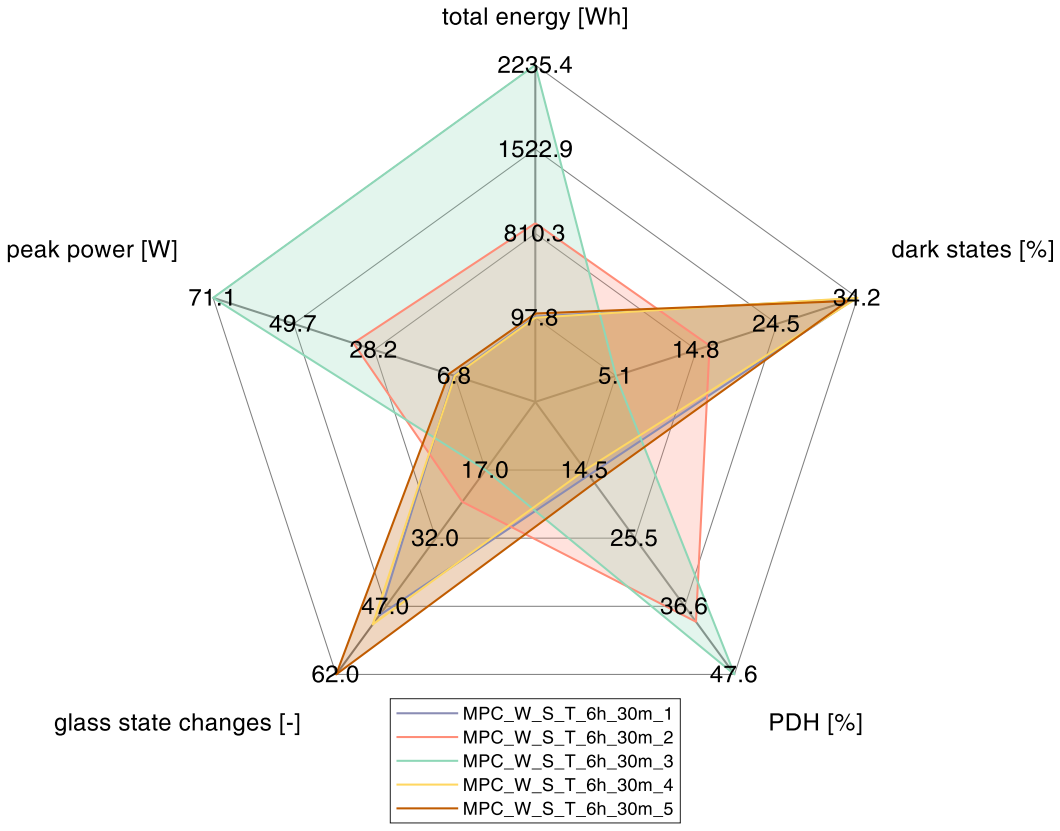

Figure 3.15. Comparison between MPC controls in Wollongong during a summer week with different weight matrices

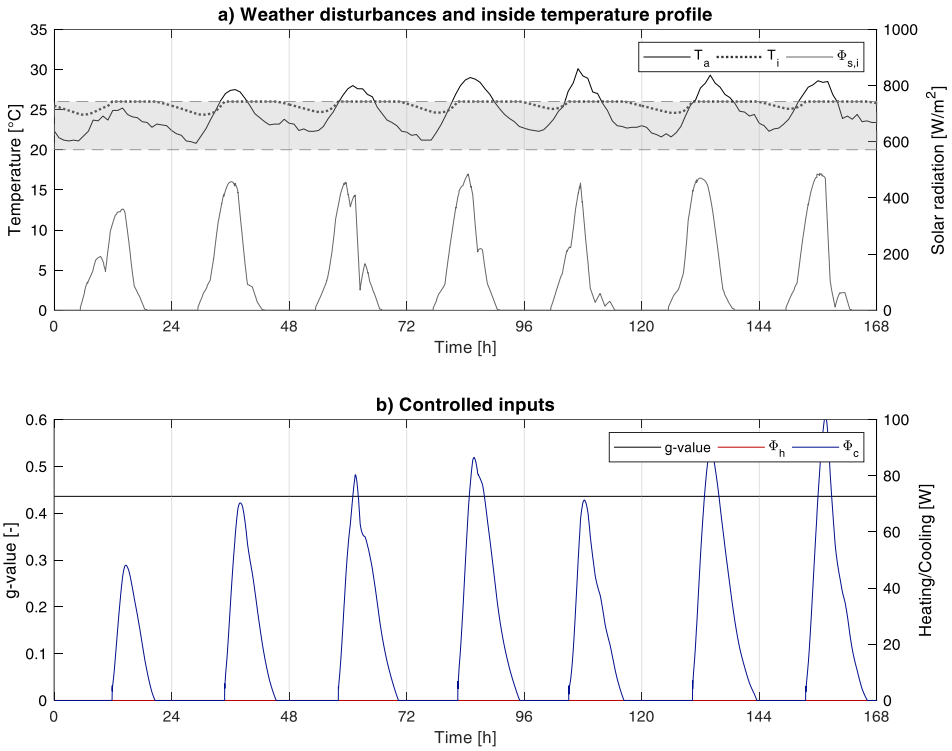

Figure 3.16. Static window (as Clear State) in Wollongong during a summer week

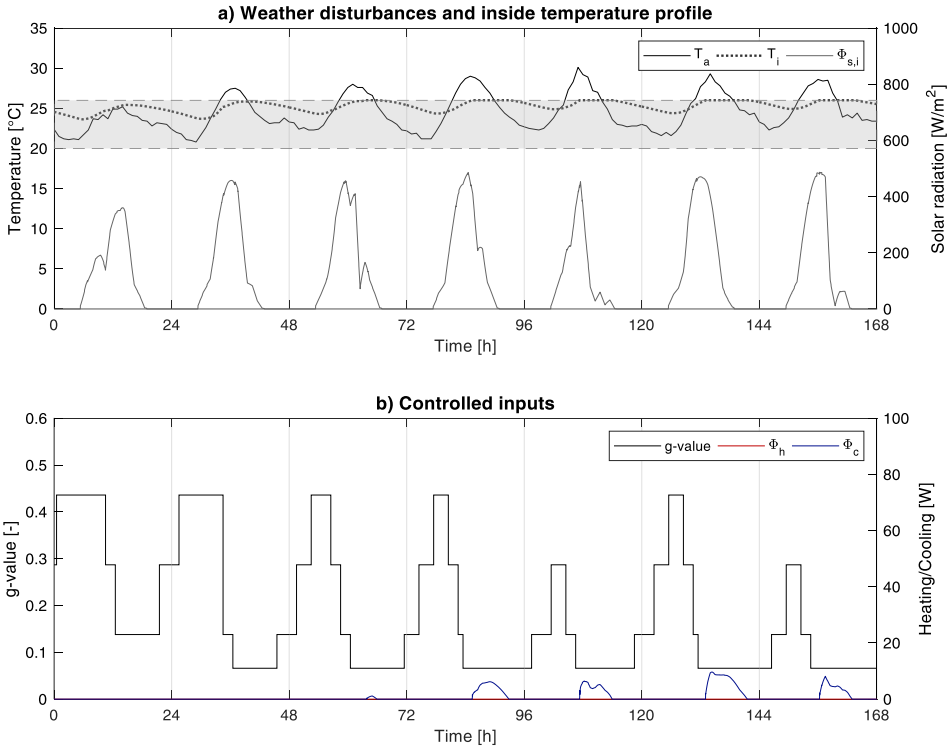

Figure 3.17. Rule Based Control based on internal temperature (T_i) in Wollongong during a summer week

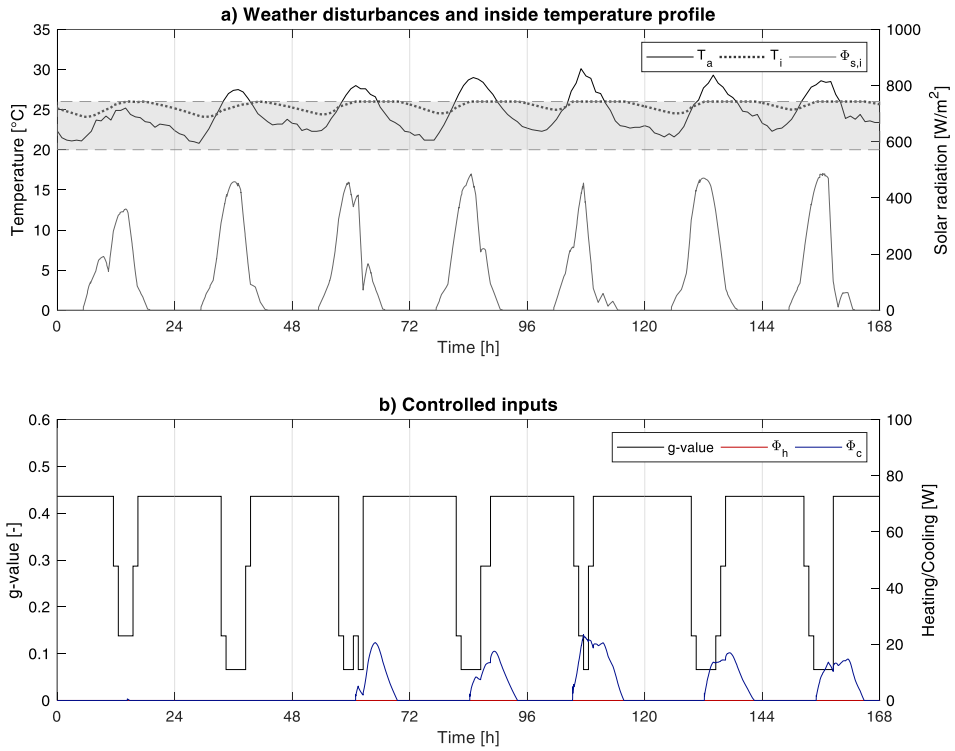

Figure 3.18. Rule Based Control based on incident solar radiation ($\phi_{s,i}$) in Wollongong during a summer week

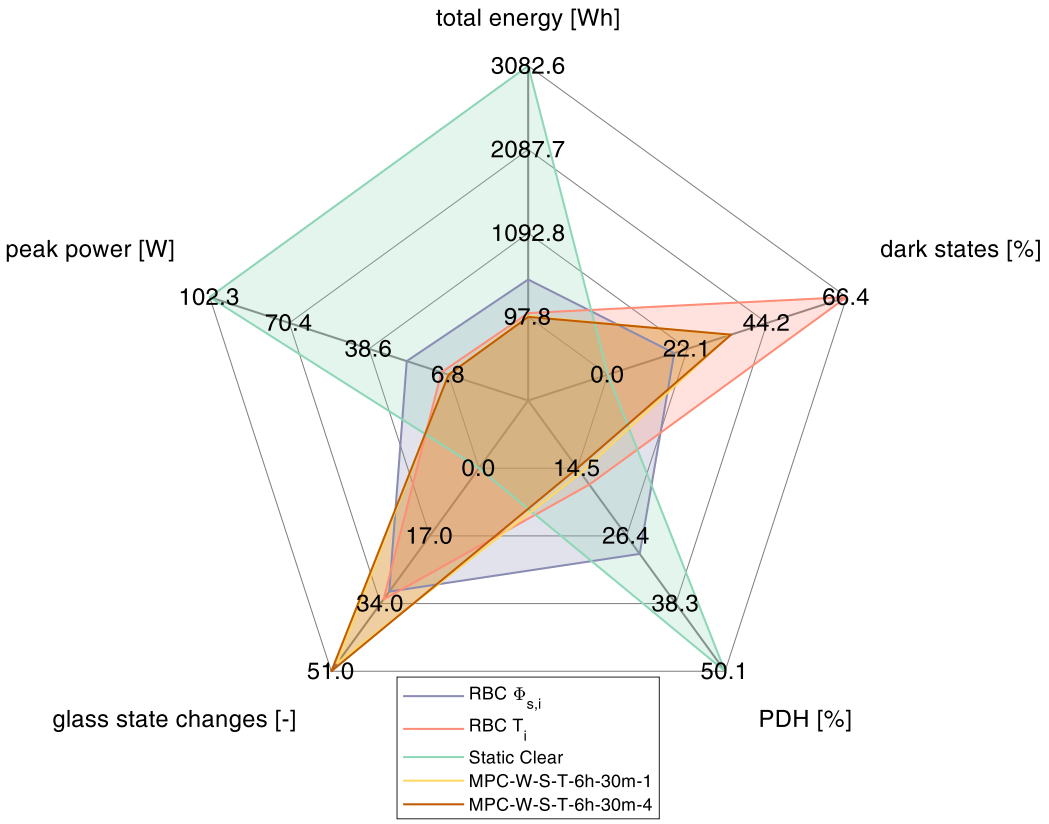

Figure 3.19. Comparison between MPC and RBC control strategies in Wollongong during a summer week

Results shown in *Figure 3.15* are summarised in *Table 3.8*, along with the areas of each polygon.

Table 3.8. Performance parameters and polygon areas - MPC controls in Wollongong during a summer week

	Total Energy [Wh]	Peak Power [W]	Dark States [%]	PDH [%]	State changes [-]	Polygon Area [-]
Weights W1	107.19	6.97	33.95	15.32	49	0.334
Weights W2	897.31	33.75	16.39	39.10	24	0.607
Weights W3	2235.40	71.09	5.08	47.64	17	0.877
Weights W4	97.81	6.78	34.25	14.48	51	0.324
Weights W5	133.25	8.35	33.06	16.57	62	0.412

Results shown in *Figure 3.19* are summarised in *Table 3.9*, along with the areas of each polygon.

Table 3.9. Performance parameters and polygon areas - MPC and RBC controls in Wollongong during a summer week

	Total Energy [Wh]	Peak Power [W]	Dark States [%]	PDH [%]	State changes [-]	Polygon Area [-]
RBC $\phi_{s,i}$	542.13	23.49	18.45	29.53	31	0.357
RBC T_i	142.86	9.64	66.37	17.36	33	0.324
Static Clear	3082.63	102.26	0.00	50.15	0	0.476
MPC - W1	107.19	6.98	33.95	15.32	49	0.255
MPC - W4	97.81	6.78	34.25	14.48	51	0.249

From *Figure 3.15* (and *Table 3.8*) it is clear that when the weights matrices are such that changing the glass state has a relatively high cost, as in W2 and W3, glass state changes and the percentage of time with dark states is significantly lower than in the other cases. However, unsatisfactory indoor conditions (PDH) increase as well as energy consumption and peak power, which are better managed in cases W1, W4 and W5. This conclusion is also supported by comparing the areas of each polygon, which results significantly higher in the cases W2 and W3. This outcome should be interpreted as a demonstration of the MPC flexibility: by tuning the weights, it is possible to obtain different results. This feature can be exploited to adapt the controller to specific and possibly changing requirements. For example, W2 and W3 cases could be temporarily preferred to enhance daylight. It is worth to note that a not correctly tuned MPC strategy could lead to trivial solutions: in this case, for example, choosing the darkest state in presence of solar radiation would certainly lower the energy consumption. On the other hand, balanced MPC strategies act as the previously shown ones, taking into account the contrasting goals of reducing the energy need and preferring clear states according to the relative weights.

Results relative to the best performing MPC strategies (W1 and W4) are then compared to the above described baseline strategies (*Figure 3.19* and *Table 3.9*). Observing the polygon areas, it results clear that the MPC strategies perform better as far as the chosen KPIs are concerned. An average percentage of time in dark states (if compared with the RBC strategies), allows the system to lower the total energy consumption and peak power, while keeping the environment inside the comfort conditions for a longer period. Prediction plays an important role: foreseeing the system future states, the MPC is able to lower the cooling energy need by choosing darker states before RBC strategies. This curbs the increase of the indoor air temperature, resulting in reduced energy needs and peak loads.

3.8.2. Results – Spring week in Wollongong

From *Figure 3.20* to *Figure 3.24*, results of MPC strategies with different weights are shown for a spring week in Wollongong. These results demonstrate how the previously shown control strategies behave in a period of the year in which both heating and cooling could be needed. In *Figure 3.25*, moreover, a radar chart is reported to compare these strategies.
As in the previous case, also results related to the benchmark controllers are shown (*Figure 3.26* to *Figure 3.28*), along with the comparative radar chart (*Figure 3.29*).

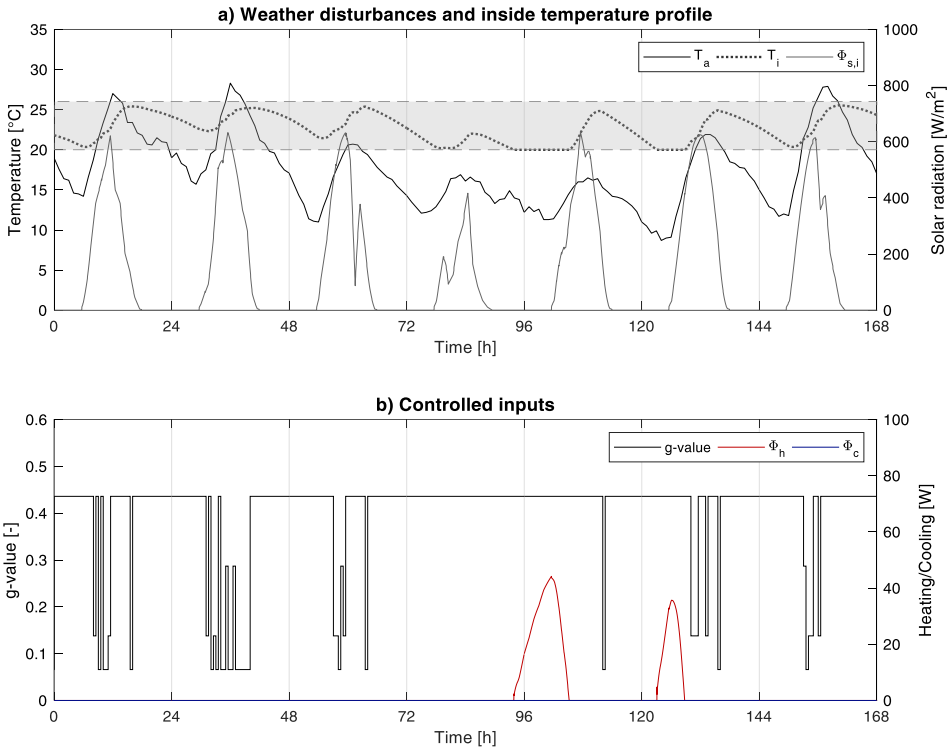

Figure 3.20. MPC control in Wollongong during a spring week. Weights W1

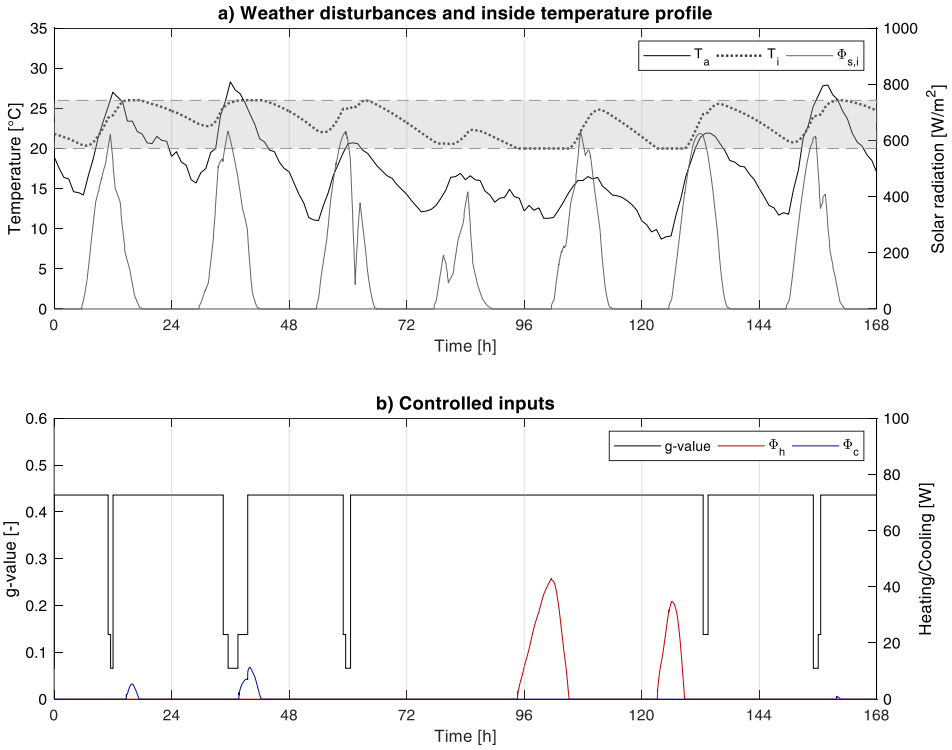

Figure 3.21. MPC control in Wollongong during a spring week. Weights W2

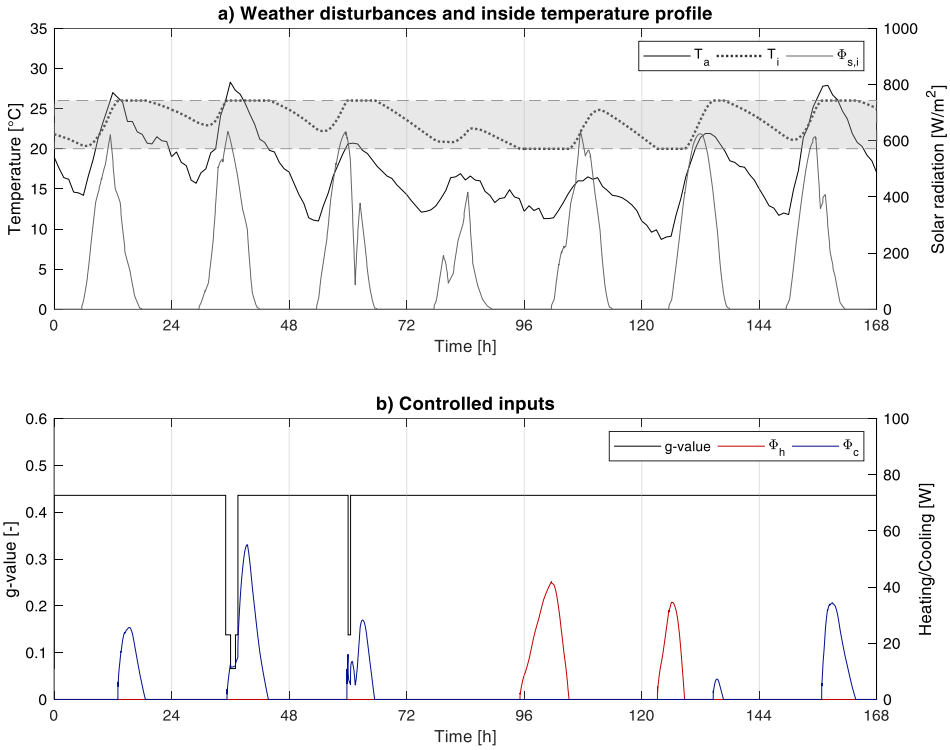

Figure 3.22. MPC control in Wollongong during a spring week. Weights W3

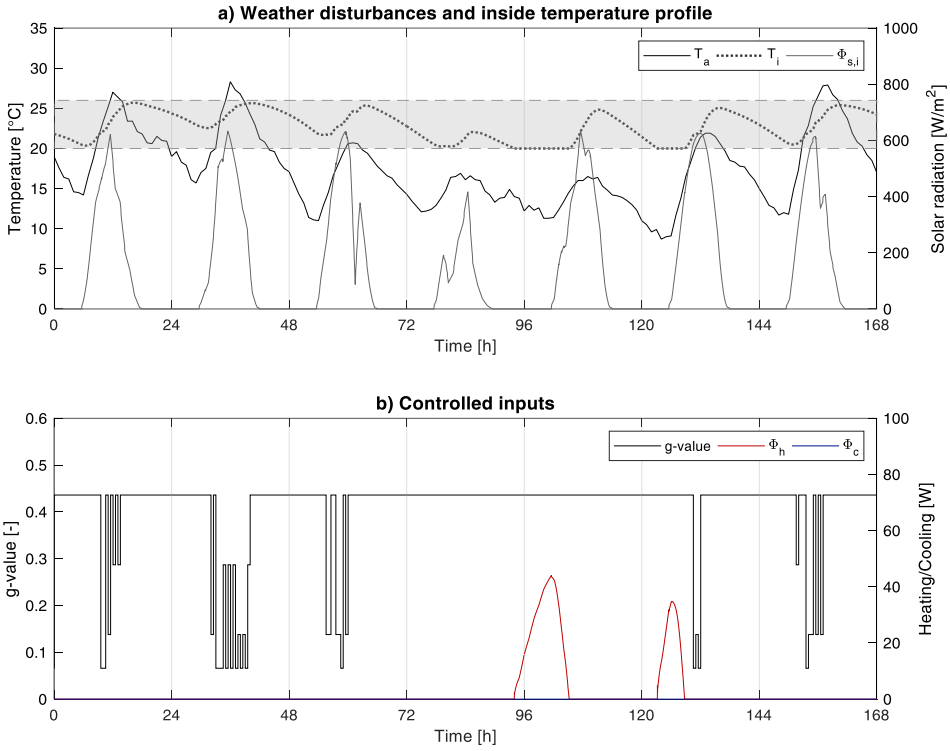

Figure 3.23. MPC control in Wollongong during a spring week. Weights W4

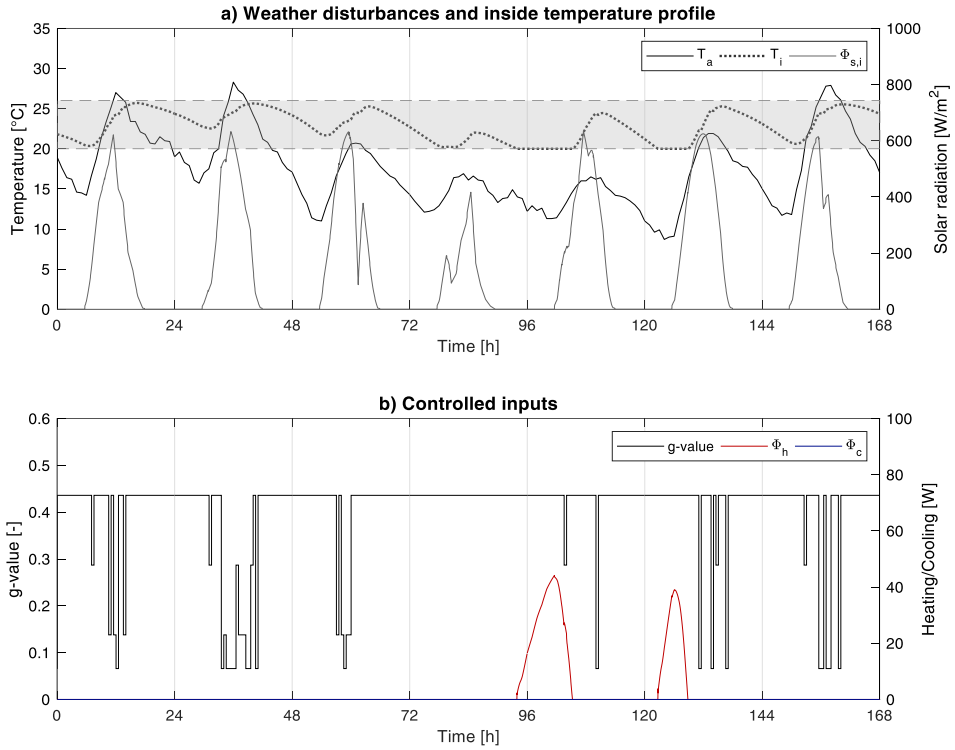

Figure 3.24. MPC control in Wollongong during a spring week. Weights W5

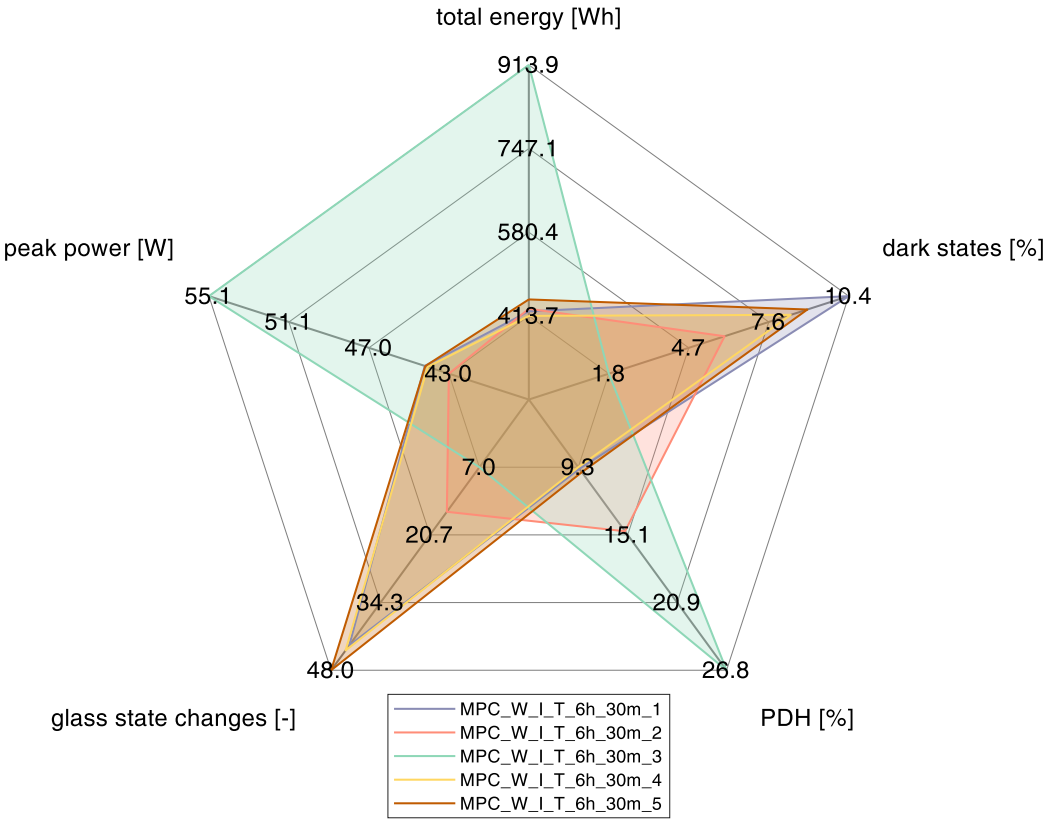

Figure 3.25. Comparison between MPC controls in Wollongong during a spring week with different weight matrices

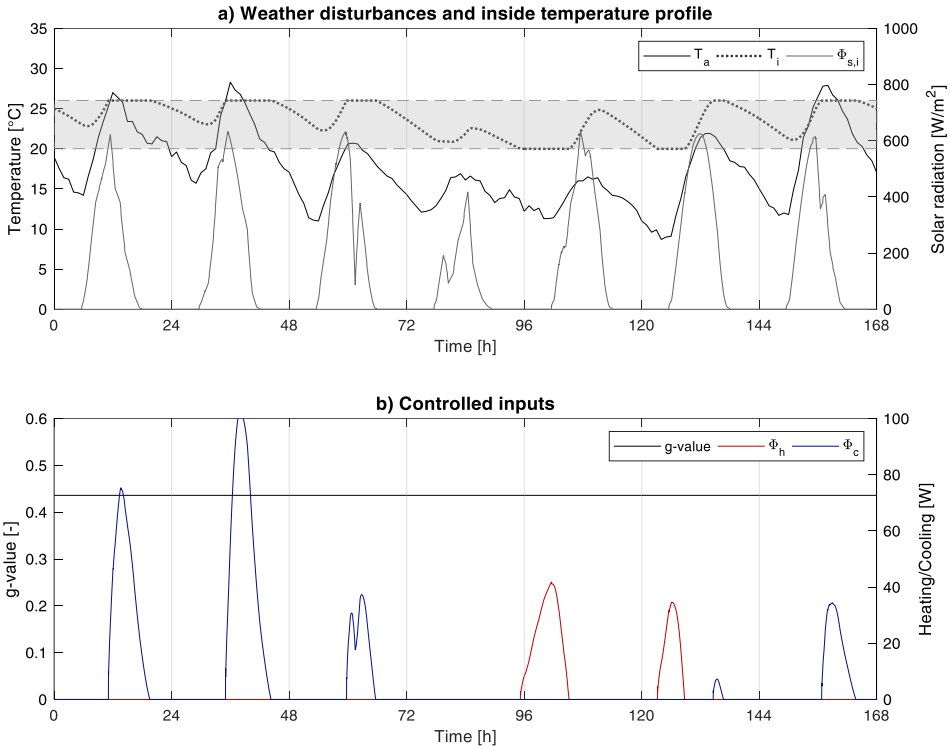

Figure 3.26. Static window (as Clear State) in Wollongong during a spring week

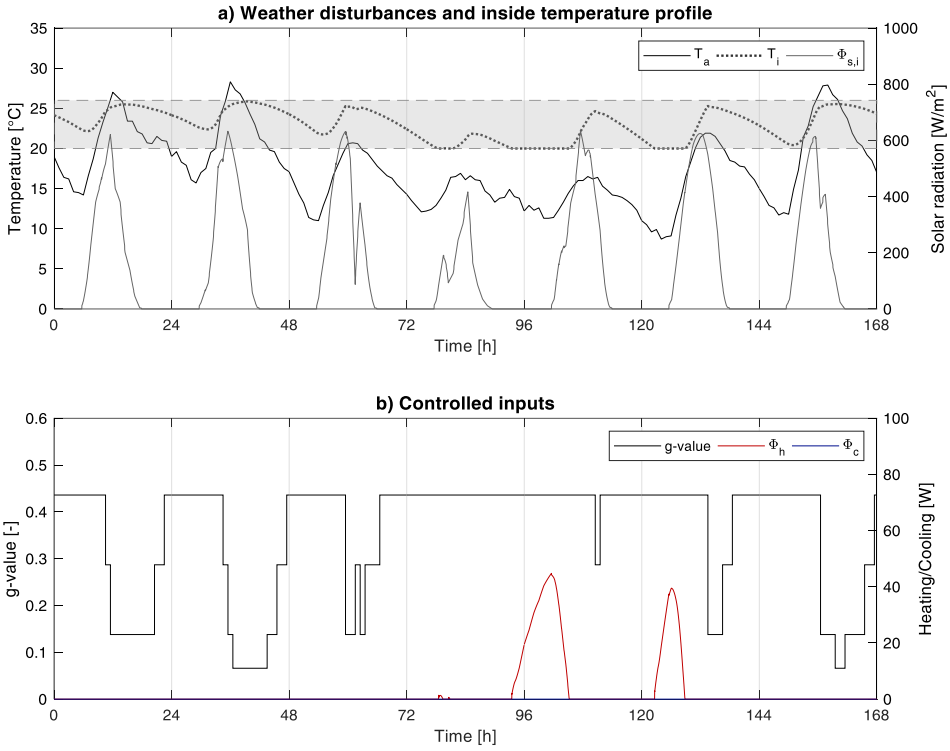

Figure 3.27. Rule Based Control based on internal temperature (T_i) in Wollongong during a spring week

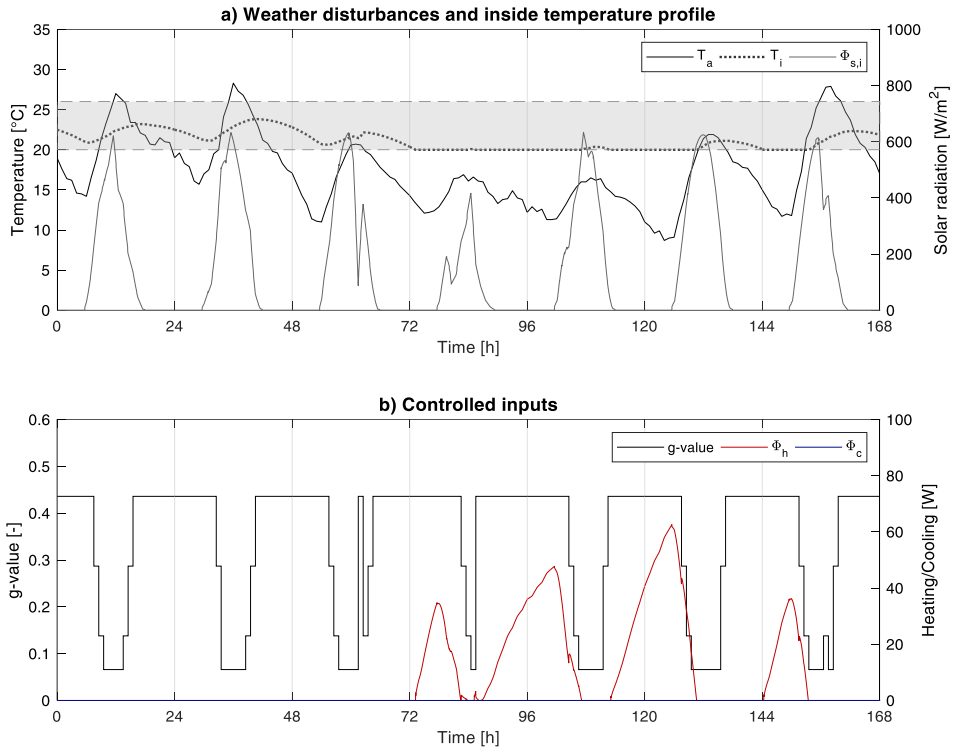

Figure 3.28. Rule Based Control based on incident solar radiation ($\phi_{s,i}$) in Wollongong during a spring week

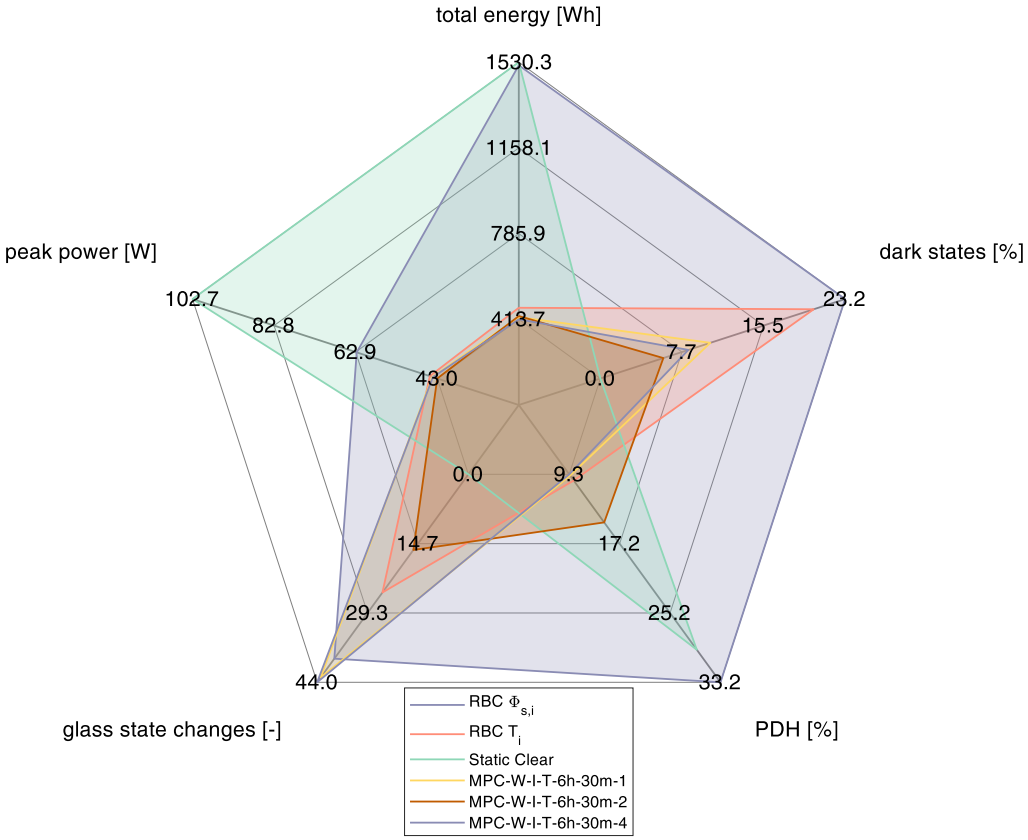

Figure 3.29. Comparison between MPC and RBC control strategies in Wollongong during a spring week

Results shown in *Figure 3.25* are summarised in *Table 3.10*, along with the areas of each polygon.

Table 3.10. Performance parameters and polygon areas - MPC controls in Wollongong during a spring week

	Total Energy [Wh]	Peak Power [W]	Dark States [%]	PDH [%]	State changes [-]	Polygon Area [-]
Weights W1	422.82	44.20	10.44	9.40	43	1.055
Weights W2	427.84	42.98	5.97	14.79	16	0.663
Weights W3	913.86	55.09	1.81	26.79	7	0.779
Weights W4	413.70	44.05	8.35	9.27	44	0.975
Weights W5	446.46	44.17	8.95	9.69	48	1.086

Results shown in *Figure 3.29* are summarised in *Table 3.11*, along with the areas of each polygon.

Table 3.11. Performance parameters and polygon areas - MPC and RBC controls in Wollongong during a spring week

	Total Energy [Wh]	Peak Power [W]	Dark States [%]	PDH [%]	State changes [-]	Polygon Area [-]
RBC $\phi_{s,i}$	1516.99	62.62	23.21	33.16	39	1.913
RBC T_i	463.78	44.79	20.24	9.98	25	0.512
Static Clear	1530.28	102.67	0.00	29.42	0	0.476
MPC - W1	422.82	44.20	10.44	9.40	43	0.508
MPC – W2	427.84	42.98	5.97	14.79	16	0.294
MPC - W4	413.70	44.05	8.35	9.27	44	0.486

From *Figure 3.25* and *Table 3.10* it can be observed that cases W1 and W4 perform and act in a similar way, while W2 acts in a completely different way: being related to higher costs concerning the choice of darker states, it adopts an apparently trivial yet effective strategy to keep clear states for longer periods. It results in slightly higher energy consumption if compared with cases W1 and W4, but it is equilibrated by the other KPIs, so much so that it has the lowest polygon area. However, it is worth to notice that W2 is characterized by both heating and cooling needs throughout the week, which could be considered as a downside depending on the specificities of the relative system. On the other hand, strategies W1 and W4 were able to completely eliminate the cooling needs and to guarantee better indoor comfort conditions. As in the summer case, these different behaviours represent a useful resource to be exploited: W2 could be preferred when the system easily allows the switching between heating and cooling modes and when daylight is preferred to comfort conditions. Similarly, W1 and W4 could provide a better solution when switching between heating and cooling is not possible (or not preferred), and when comfort conditions are prioritized to daylight.

Although the conditions are very different from the summer case, since some heating is always required, MPC strategies were able to meet the goals and perform better than the benchmark cases. This can be observed from *Figure 3.29* and *Table 3.11*, which show how the MPC strategies are characterised by lower normalised polygon areas. The predictive control strategy proves to be able to prevent or mitigate from the over-heating phenomena, while exploiting solar gains when needed.

3.8.3. Results – Summer week in Torino

From *Figure 3.30* to *Figure 3.34*, results of MPC strategies with different weights are shown for a summer week in Torino.

In *Figure 3.35*, moreover, a radar chart is represented to compare these strategies.

In *Figure 3.36* to *Figure 3.38*, results on the benchmark controllers are plotted, compared in *Figure 3.39* with the best performing MPC strategies.

It is worth to be noted that, in this case, the control-oriented model needed to be identified again, given the different weather conditions. As Torino weather conditions are extremely different from the one found in Wollongong, it was preferred to perform the grey-box model system identification using as dataset simulation run using the climatic file of Torino. The same methodological approach described in the previous sections of the present chapter was followed. The new system identification leads to comparable fit results to the previous case (in terms of NRMSE) and identified parameters within the same range, which was defined based on the physical meaning of the lumped parameters. The slight changes in the grey-box parameters, however, resulted in a more suitable model for the presented application.

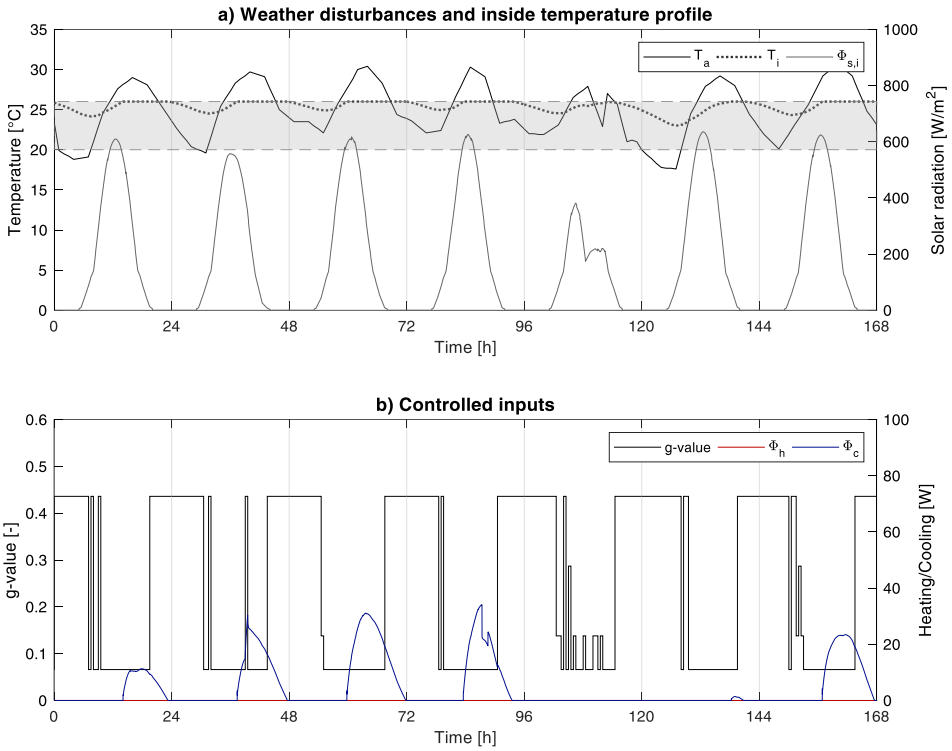

Figure 3.30. MPC control in Torino during a summer week. Weights W1

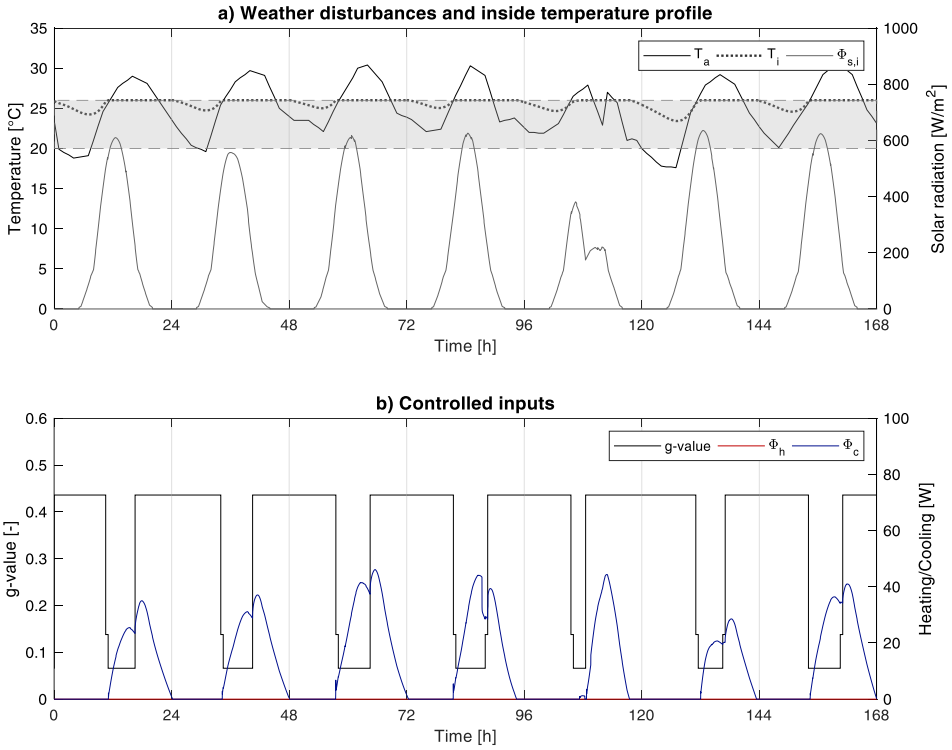

Figure 3.31. MPC control in Torino during a summer week. Weights W2

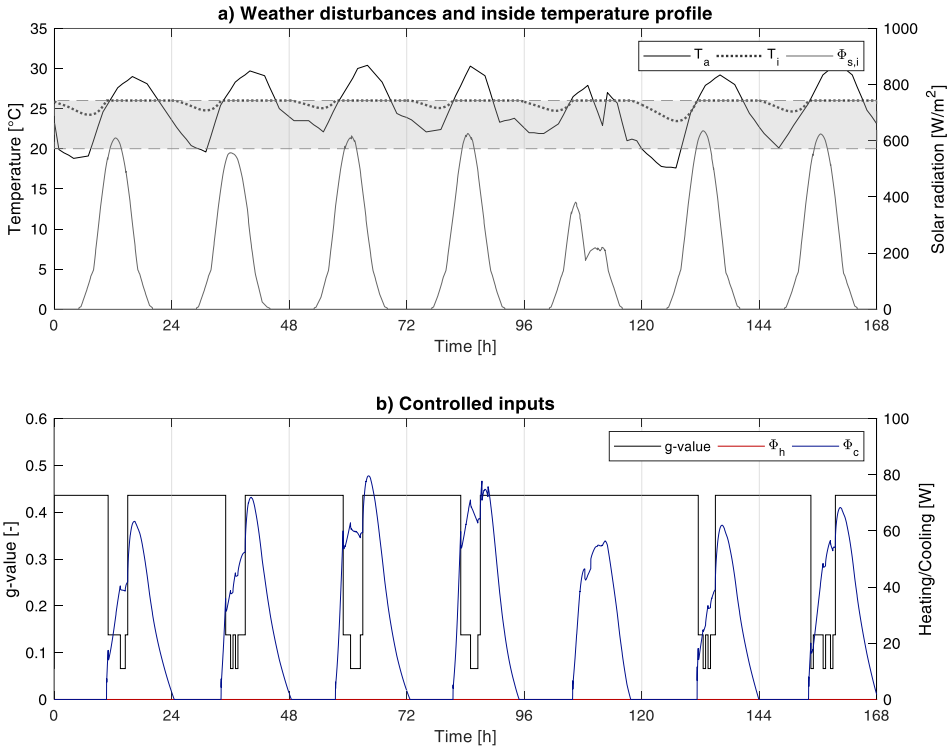

Figure 3.32. MPC control in Torino during a summer week. Weights W3

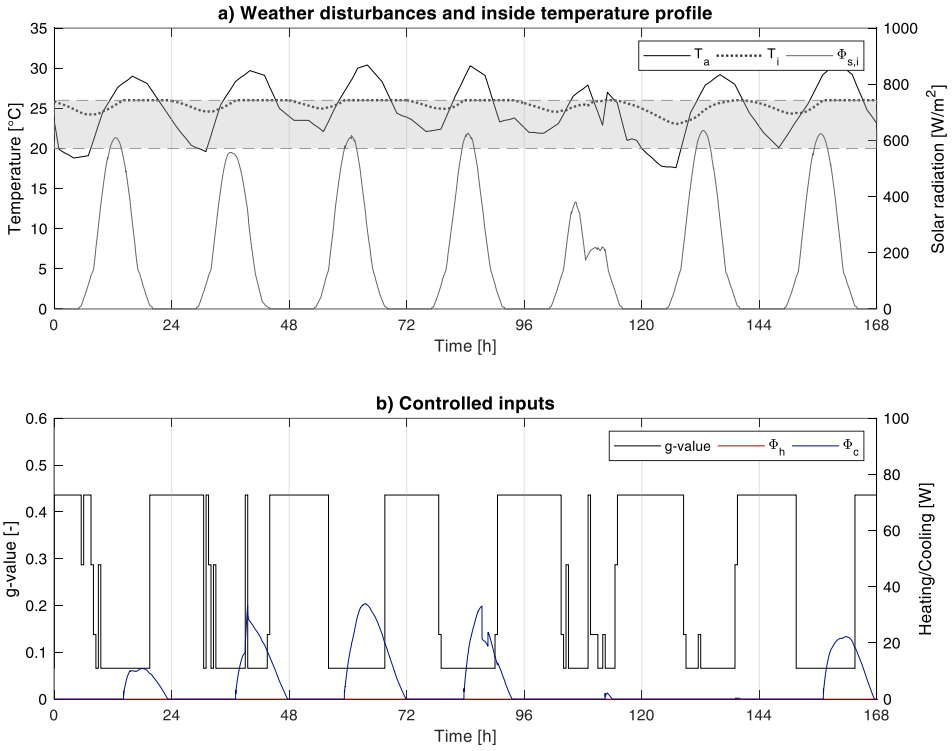

Figure 3.33. MPC control in Torino during a summer week. Weights W4

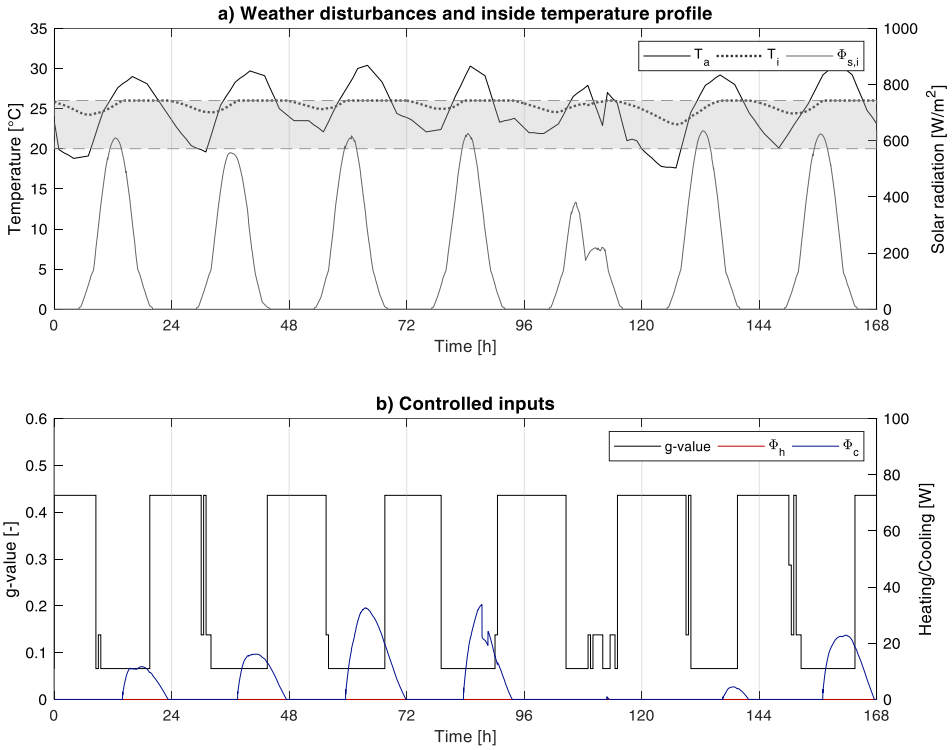

Figure 3.34. MPC control in Torino during a summer week. Weights W5

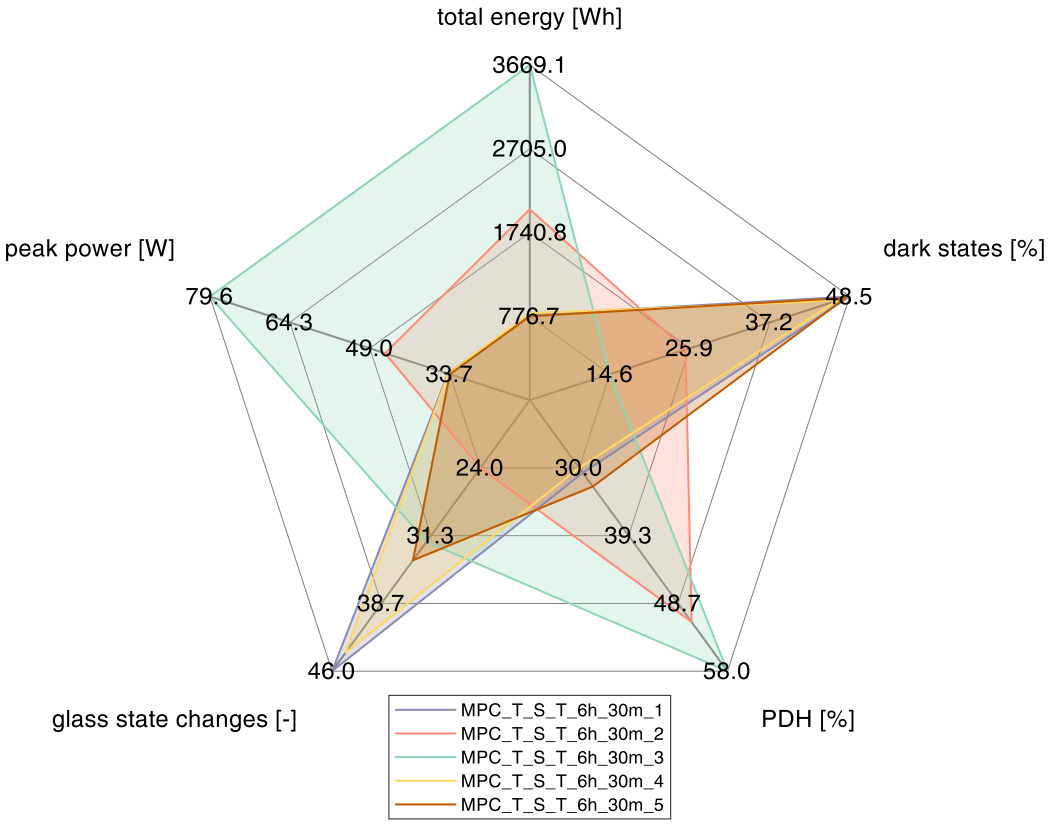

Figure 3.35. Comparison between MPC controls in Torino during a summer week with different weight matrices

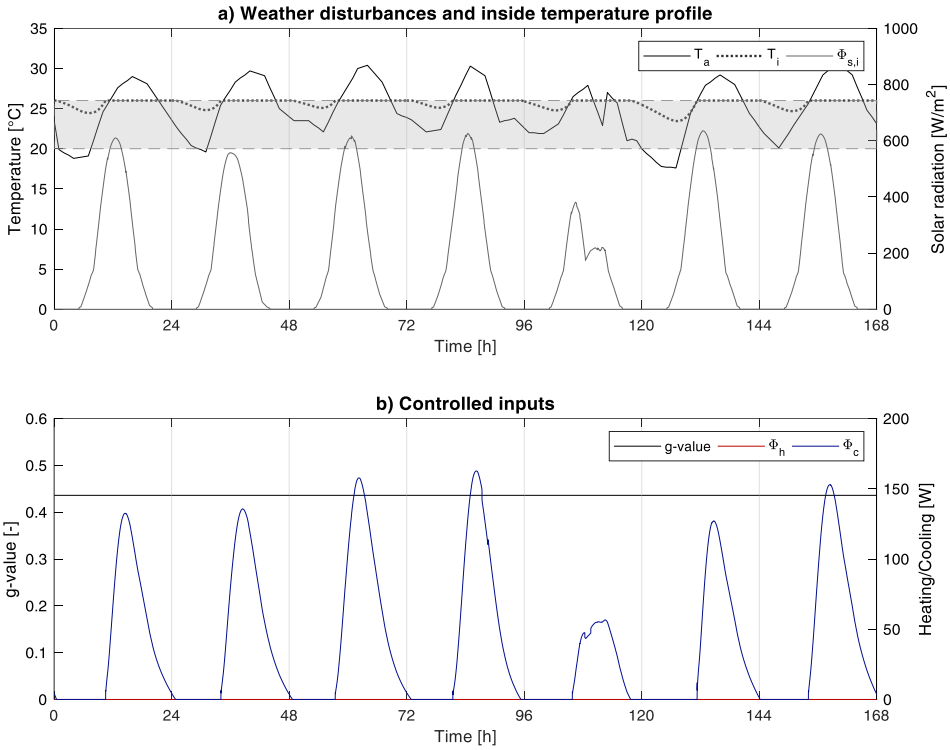

Figure 3.36. Static window (as Clear State) in Torino during a summer week

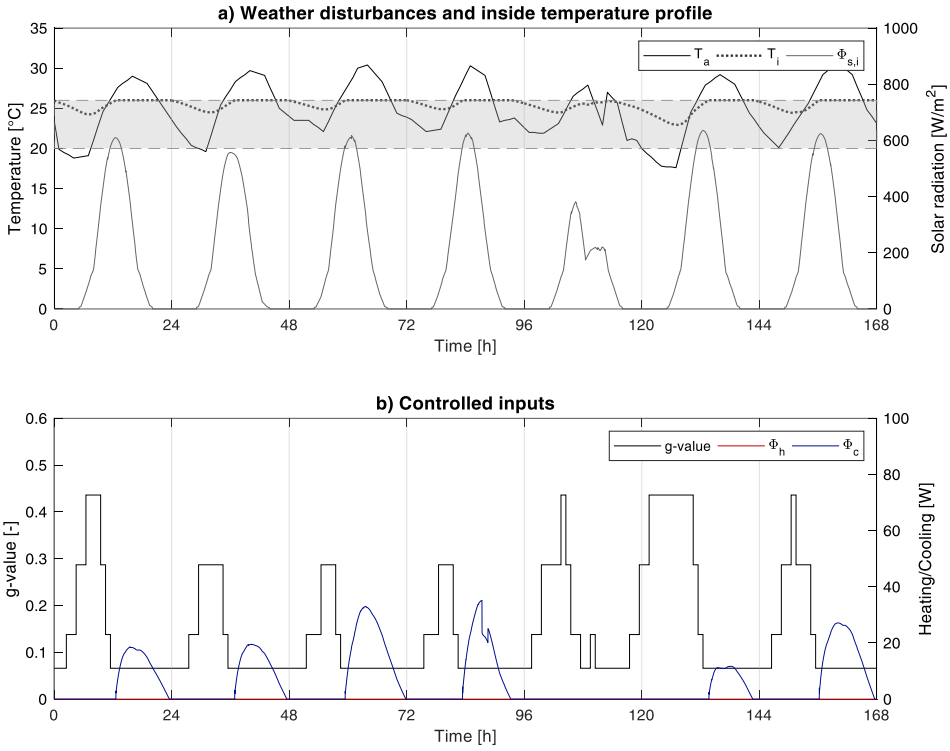

Figure 3.37. Rule Based Control based on internal temperature (T_i) in Torino during a summer week

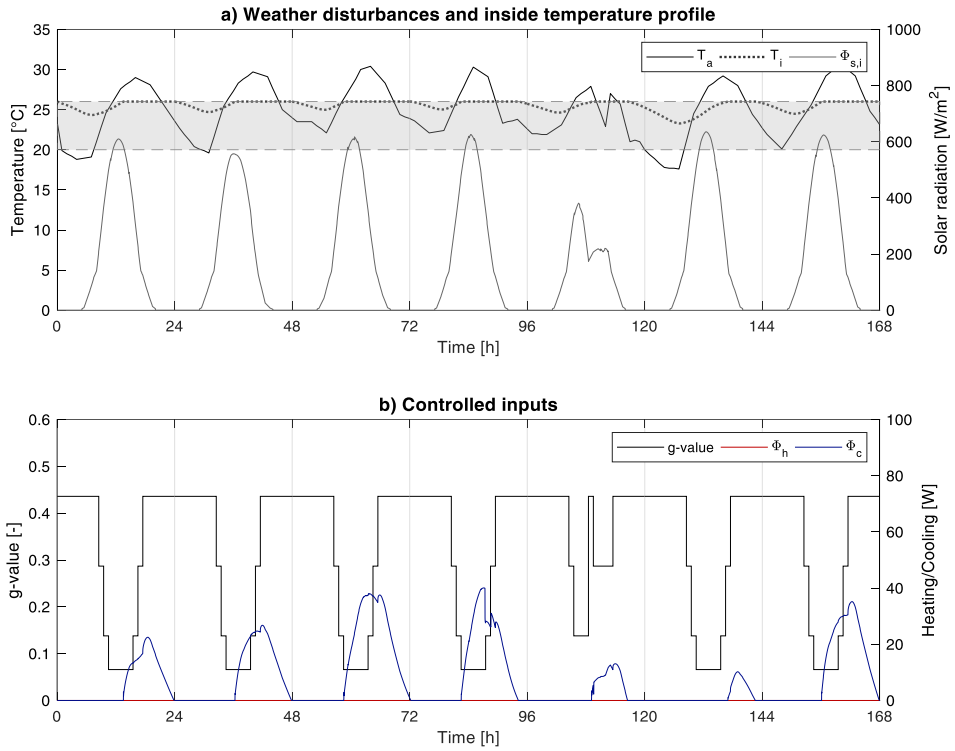

Figure 3.38. Rule Based Control based on incident solar radiation ($\phi_{s,i}$) in Torino during a summer week

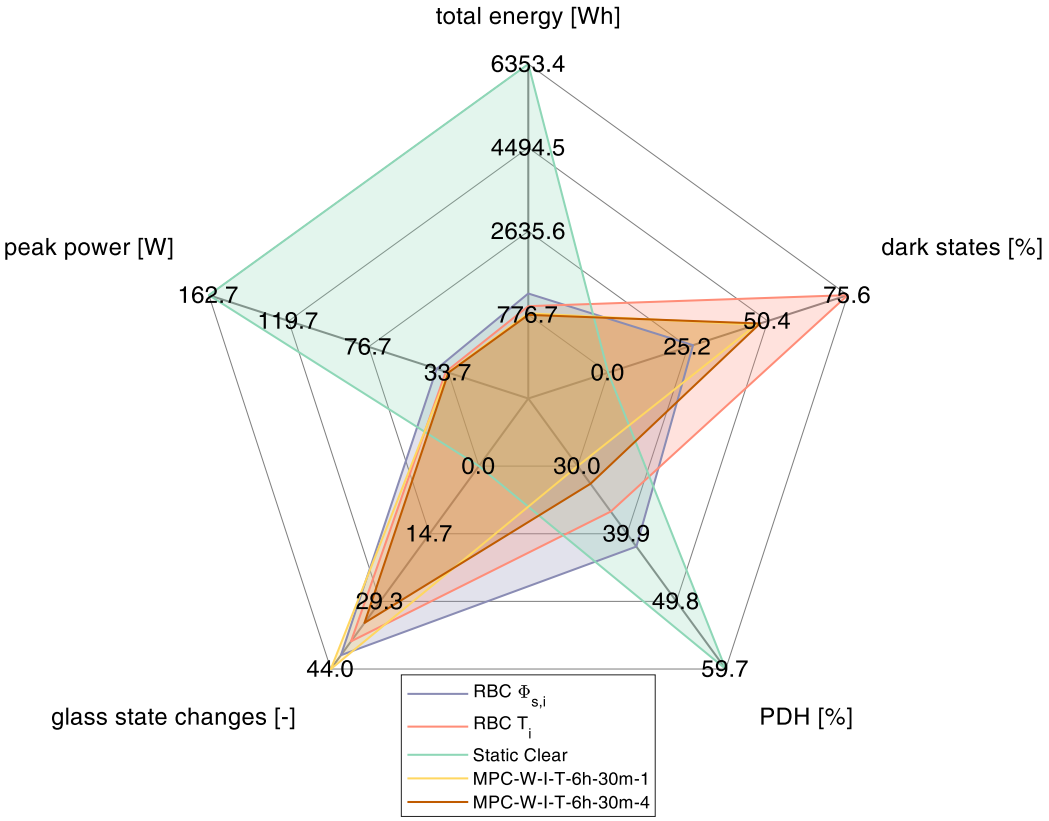

Figure 3.39. Comparison between MPC and RBC control strategies in Torino during a summer week

The results shown in *Figure 3.35* are summarised in *Table 3.12*, along with the areas of each polygon.

Table 3.12. Performance parameters and polygon areas - MPC controls in Torino during a summer week

	Total Energy [Wh]	Peak Power [W]	Dark States [%]	PDH [%]	State changes [-]	Polygon Area [-]
Weights W1	792.74	34.08	48.53	30.65	46	0.853
Weights W2	2008.93	46.11	25.32	51.25	24	0.869
Weights W3	3669.14	79.59	14.60	58.04	32	1.423
Weights W4	811.59	33.99	46.75	29.97	44	0.812
Weights W5	776.70	33.74	47.94	32.55	34	0.752

Results shown in *Figure 3.39* are summarised in *Table 3.13*, along with the areas of each polygon.

Table 3.13. Performance parameters and polygon areas - MPC and RBC controls in Torino during a summer week

	Total Energy [Wh]	Peak Power [W]	Dark States [%]	PDH [%]	State changes [-]	Polygon Area [-]
RBC $\phi_{s,i}$	1252.03	40.06	26.79	41.75	41	0.593
RBC T_i	969.94	35.15	75.60	36.62	38	0.721
Static Clear	6353.38	162.68	0.00	59.66	0	0.476
MPC – W4	811.59	33.99	46.75	29.97	44	0.536
MPC – W5	776.70	33.74	47.94	32.55	34	0.490

Even though the same MPC strategies applied in Wollongong were applied in Torino, different results are found. Being the climatic conditions heavily influencing the MPC behaviour, this was an expected outcome. The flexibility of this approach is once again demonstrated, since the strategies are adapted according to the specific climatic conditions: in Torino, the incident solar radiation ($\phi_{s,i}$) is characterized by higher peaks and the outdoor temperature is subjected to higher oscillations and similar peaks.

From *Figure 3.35* and *Table 3.12* it is possible to notice that W4 and W5 perform better than the other cases, being the relative areas smaller and being almost all the key performance indicators lower. Given the climatic conditions, strategies in which darker states are particularly penalized (as W2 and W3), resulted in penalizing too much the rest of the KPIs.

When compared with the baseline cases, it can again be stated that the MPC strategies are able to reduce energy consumption and peak power while ensuring the desired indoor conditions. RBC strategies can be defined as less balanced: the RBC based on solar radiation ensures clear states for a longer period, but by doing so more cooling energy is required; the strategy based on the internal temperature

lowers the energy need for cooling by keeping dark states for a big portion of the time.

3.9. Discussion

This Chapter investigated the opportunity to apply advanced control strategies to adaptive façade components. The complexity of the thermal phenomena underlying even the simplest test cell had to be translated in an agile model for the Model Predictive Control strategy: a fast yet reliable control-oriented model able to predict future states from a series of future inputs and disturbances.

This methodological approach starts with the energy model definition, and following a replicable path allows a reliable implementation of a Hybrid Model Predictive Controller for enhancing the performances of an active component for solar gains modulation integrated in the building façade.

Moreover, the co-simulation toolchain presented enables the required benchmarking of the advanced controller by coupling at time-step level the physical model simulation and the controller itself.

MPC strategies have demonstrated to be suitable for electrochromic façades, since a better performance if compared to traditional controllers was found in the presented cases. These findings can be seen as an opening to the possibility of applying predictive control strategies to transparent adaptive components or, more in general, *solar gains modulators*. The HMPC formulation allowed to capture the hybrid nature of the case study, characterized by an electrochromic glazing able to switch between discrete states and a continuous heating/cooling system.

If these approaches are combined with specific cases particularly suitable for MPC applications, moreover, the described positive effects could be enhanced. This means, for example, largely transparent buildings with high thermal mass.

Furthermore, the demonstrated flexibility of the MPC formulation can be exploited to achieve different goals: for example, in some scenarios comfort requirements are more important than the energy need, while in others energy saving has the priority. Using the same structure and simply changing the objective function weights (or using a different objective function altogether), it is possible to address the correct needs. This control flexibility can be also exploited to improve the overall building energy flexibility and demand management: considering variables as the availability of renewable energy resources, energy pricing, electric or thermal storages availability and so on within the objective function, it is possible to apply strategies beneficial to an electric grid.

Chapter 4

4. Control application in the TWINS (Testing Window Innovative Systems) test facility

This chapter describes the research activity carried out in a case study. Experimental and numerical activities were carried out to design Model Predictive Control strategies for the control of an electrochromic façade and a heating/cooling system taking into account thermal and lighting aspects.

4.1. Introduction

The research activity presented in this chapter was carried out within the TEBE group (Technology Energy Building Environment) of the Department of Energy (DENERG) of Politecnico di Torino and in the context of a collaboration with a smart glass manufacturer, which provided next-generation electrochromic Insulated Glazing Units (IGUs), characterized by reduced time-responses for the transition between two states and improved, more neutral colour rendering.

In particular, two electrochromic and one static IGUs were provided. The glazing units were installed on the Testing Window Innovative Systems (TWINS), an outdoor test facility located at the rooftop of the Department of Energy of Politecnico di Torino. These units were integrated on the east test cell, on its south facade.

An extensive experimental campaign was carried out with the aim of characterizing the test cell and validating its relative numerical model. These activities were carried out in the framework of two master's theses [87,88] (one of which co-tutored by the author) and a research grant funded by Prof. Alfonso Capozzoli. A closed-loop control system was set up to control the electrochromic IGUs. Since it was not possible to use the HVAC system of the test cell, the measurements were performed in free-running conditions or in heating conditions through a simple convection heater.

With the validated EnergyPlus model of the test cell, it was then possible to simulate the test cell under different control strategies and same disturbances. Moreover, a detailed lighting simulation was performed to evaluate the energy required for lighting at each hour of the year and for each glass state. This information was used to design a predictive model strategy taking into account thermal aspects.

4.2. Case study description

4.2.1. Test cell

The case study experimental facility consists of a test cell with internal dimensions of 1.6 m (width), 3.5 m (length) and 3 m (height). It is located on the rooftop of the Department of Energy of Politecnico di Torino (Latitude: 45°03′28″N; Longitude: 7°39′23″E).

The walls, the roof and the floor are made of sandwich panels composed by metal sheets and polyurethane insulation, for a total thickness of 48 mm. Only the floor has an additional layer of linoleum in the internal side to provide a walkable surface. The thermal transmittance of each side is approximately 0.5 W/m^2K.

The south face of the test cell hosts the testing façade, in this case composed by three IGUs arranged as in *Figure 4.1*.

Figure 4.1. TWINS facility

The top unit is a static glazing system, while the central and lower ones are electrochromic. The static glazing unit has the same thermo-optical characteristics as the electrochromic units in their bleached state. The static IGU has dimensions of 1.3 m in width and 0.77 m in height, while the electrochromic IGUs of about 1.3 m in width and 0.83 m in height.

The width dimension of the glazing units was not enough to cover the entire width of the test cell façade, leaving a gap of about 10 cm. Plexiglas strips were

used to cover those gaps, both on the internal and the external side of the façade. In *Figure 4.1* it is possible to see these strips on the left side of the façade, while *Figure 4.3* provides an overall view from the inside of the test cell.

On the north façade there is a door, and its thermal characteristics were assessed in the experimental campaign in order to take into account its influence on the overall heat exchange.

The east façade is completely free from obstructions, while in the west façade, an obstruction of 2 x 2 x 2.2 m of dimensions casts a shadow on the test cell in the late afternoon.

As visible in *Figure 4.1*, the whole structure sits on a steel frame structure that elevates the test cell of about 14 cm from the pavement.

4.2.2. Data gathering

The experimental setup of the test cell consists of several different sensors and a data logger:

- *Type T thermocouples*, used to measure both surface and air temperatures (*Figure 4.2 (a)-(e)*);
- *Heat flux plates*, to measure heat fluxes through every surface dividing the internal and external environment (walls, floor, door, windows, etc.) (*Figure 4.2 (c)*);
- *Pyranometers*, to measure solar irradiance, located both inside the environment and outside and oriented both horizontally and vertically (*Figure 4.2 (b)*);
- *DataTaker DT85*, a data logger used to collect data of every sensor used in the case study.

The thermocouples used to measure the surface temperatures were placed on the indoor and outdoor surfaces of each envelope component, matching their relative positioning and trying to avoid singularities as corners or structural elements, which would lead to misleading measurements. The heat flux plates were positioned on the internal side of the envelope surfaces, next to the corresponding thermocouple; in this way the measured thermal flux and surface temperatures lead to better estimations of key parameters to be characterized (i.e. the envelope conductance).

The outside air temperature was measured using one thermocouple placed outside the test cell and underneath it, in order to be naturally shielded from direct solar radiation. The internal air temperatures were measured using four thermocouples mounted on supports at 1.5m height, centred in the sense of the test cell width and spaced along its length.

To measure the transmitted solar radiation through the test façade, one pyranometer was installed for each one of the three IGUs. The sensors were centred with each pane. To measure the external solar radiation, one pyranometer was positioned vertically on the south façade, using an angular steel frame as a support,

and a second pyranometer was installed horizontally. In this way, it was possible to obtain the solar radiation incident on the south façade and the global horizontal solar radiation, essential parameters to define the outdoor conditions.

Given the extensive experience of the research group on experimental campaigns run on these test cells, some precautions were taken to avoid distorted measurements caused by direct or reflected solar radiation hitting the above described sensors [11,89–92]:

- the thermocouples measuring the external surface temperatures were shielded from solar radiation using semi-cylindrical plastic tubes covered with aluminium tape (*Figure 4.2 (a)*);
- the thermocouples measuring the internal surface temperatures were covered with a piece of aluminium tape (*Figure 4.3*);
- the probes measuring the internal air temperatures were placed inside cardboard cylinders, so to allow air to freely circulate while shading the thermocouple (*Figure 4.3*);
- the heat flux plates on the opaque components were shielded using aluminium tape on their exposed face (*Figure 4.2 (c)*);
- the heat flux plates on the IGUs were shielded both on their exposed face (toward the inside of the test cell) and on their face toward the outside, using aluminium tape on the external surface of the IGU (*Figure 4.2 (e)* and *Figure 4.3*);
- the internal pyranometers were shielded using a funnel internally covered with a matt black foil (*Figure 4.2 (d)*).

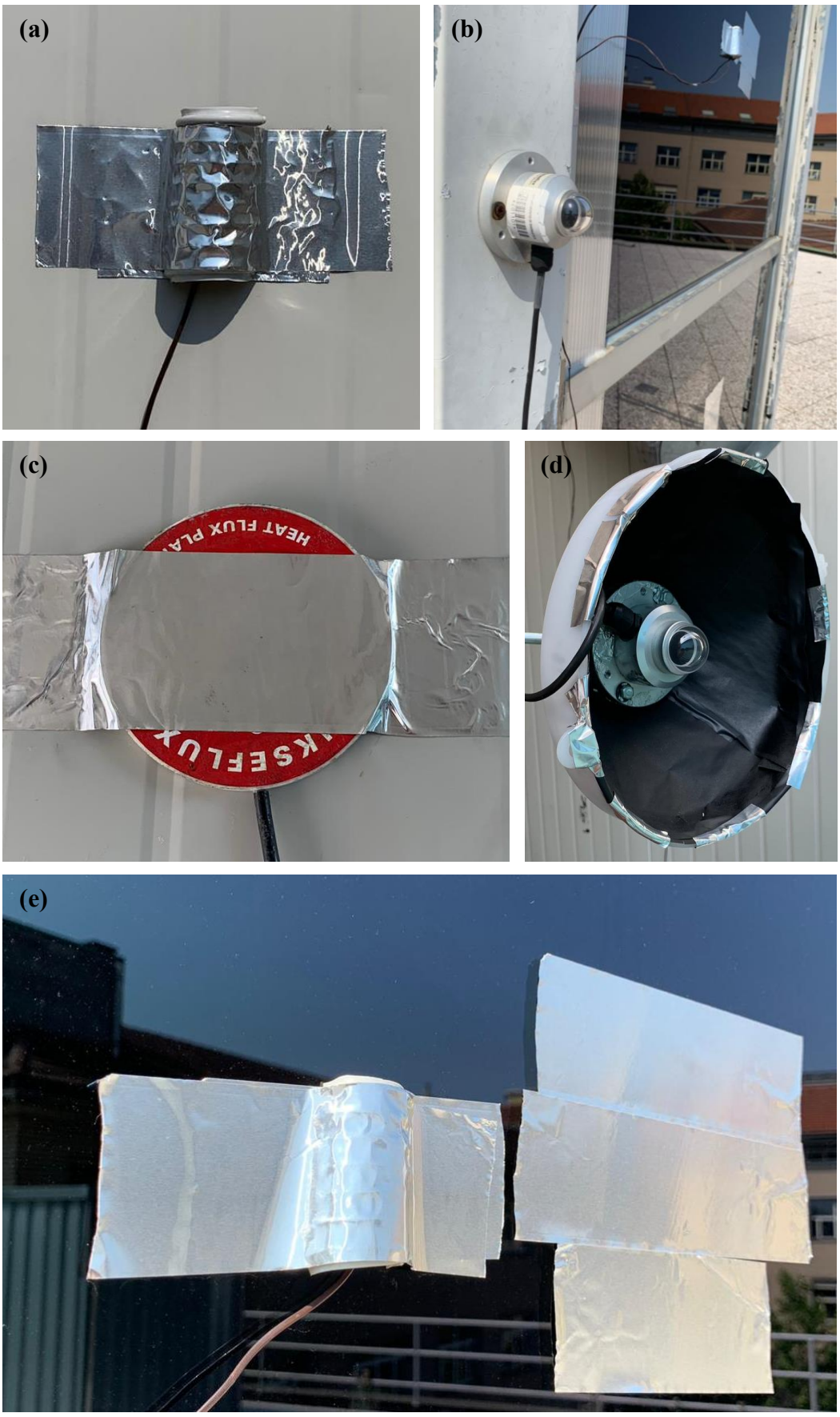

Figure 4.2. (a) External surface temperature probe; (b) External vertical pyranometer; (c) Internal heat flux plate on an opaque envelope component; (d) Internal pyranometers with the funnel shield; (e) Thermocouple on the external IGU face and aluminium tape shielding the heat flux plate place on the internal face of the IGU.

Figure 4.3. Sensors placed on the internal side of the test cell. In each IGU are visible a surface thermocouple (on the right), a heat flux plate (in the centre) and a pyranometer (on the left). In correspondence of the central pyranometer is visible the cardboard cylinder shielding one of the internal air temperature probes.

A DataTaker DT85 [93] was used to acquire and record the readings from all the above mentioned sensors. In order to avoid data-loss and to allow a feedback control to be implemented, the DataTaker was connected to the Politecnico di Torino local network so that the measurements files could be transferred in a protected folder regularly. An automatized structure was designed to have, on one hand, the measured data to be transferred from the DataTaker to the network folder, where data would be pre-processed and saved in daily files, and on the other hand to frequently read the current measurements (e.g. every minute) to allow feedback control strategies to be applied.

4.2.3. Test cell characterization

The aim of the test cell characterization is assessing the most important thermo-physical characteristics of the opaque components and to confirm the thermo-optical properties of the transparent ones (with already known and detailed characteristics) using in-situ measurements. In this section, the results obtained during the characterization are summarised.

Data was gathered from the 18th to the 22nd of February, at 5-minutes intervals. This data was used to characterize all the test cell components, in accordance with EN ISO 9869-1:2014 [94] and UNI EN ISO 6946:2008 [95].

The thermal characteristics of the opaque components are summarised in *Table 4.1*.

Table 4.1. Thermal conductance and transmittance of the opaque components

Opaque component	$\boldsymbol{C}$ $(\boldsymbol{W/m^2K})$	$\boldsymbol{U}$ $(\boldsymbol{W/m^2K})$
West Wall	0.523	0.480
East Wall	0.523	0.481
North wall	0.523	0.480
Roof	0.523	0.487
Floor	0.816	0.696

The static IGU is a double glazing made of an external clear glass pane (6 mm thick), an internal low-e coated pane (8 mm thick) and a 16 mm gap filled with argon 90%. The electrochromic IGUs are made as the static one, but the external pane is made of a laminated glass (10 mm thick) with an electrochromic device in between (*Figure 4.4*).

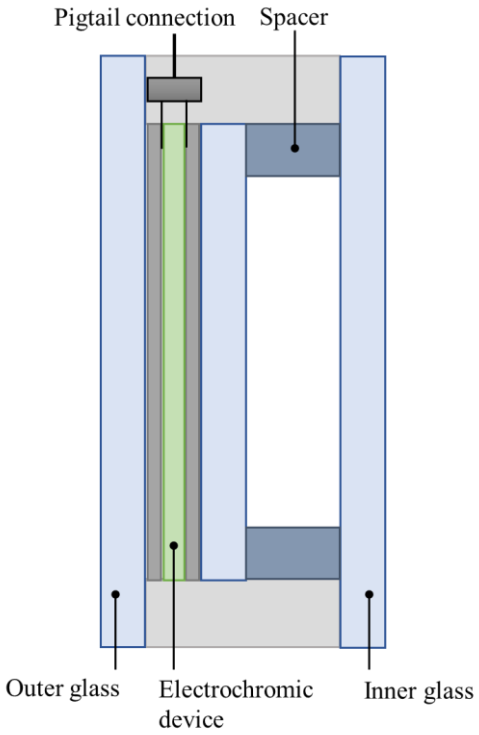

Figure 4.4. Electrochromic IGU section

The electrochromic glass optical properties were exported from the International Glazing Database (IGDB), while the thermos-optical properties of the IGUs were evaluated using the LBNL Window program [96].

Table 4.2. Optical properties of the electrochromic glass

State	τ_{vis} [−]	$\rho_{vis\,1}$ [−]	$\rho_{vis\,2}$ [−]	τ_{sol} [−]	$\rho_{sol\,1}$ [−]	$\rho_{sol\,2}$ [−]
EC73	0.731	0.142	0.119	0.529	0.176	0.173
EC46	0.456	0.090	0.101	0.264	0.139	0.124
EC28	0.278	0.071	0.078	0.138	0.133	0.112
EC14	0.143	0.640	0.069	0.064	0.130	0.109
EC8	0.083	0.061	0.069	0.036	0.129	0.112
EC5	0.050	0.059	0.071	0.021	0.129	0.118
EC2	0.023	0.058	0.075	0.010	0.129	0.126

Table 4.3. Thermo-optical properties of the electrochromic IGU

State	τ_{vis} [−]	$\rho_{vis\,f}$ [−]	$\rho_{vis\,b}$ [−]	τ_{sol} [−]	$\rho_{sol\,f}$ [−]	$\rho_{sol\,b}$ [−]	g [−]	U $[W/m^2K]$
EC73	0.671	0.158	0.162	0.393	0.232	0.324	0.471	
EC46	0.414	0.097	0.133	0.211	0.148	0.301	0.321	
EC28	0.249	0.074	0.117	0.113	0.134	0.293	0.237	
EC14	0.127	0.063	0.111	0.053	0.130	0.291	0.186	1.2
EC8	0.074	0.058	0.108	0.029	0.128	0.289	0.166	
EC5	0.045	0.055	0.107	0.017	0.123	0.290	0.156	
EC2	0.021	0.059	0.101	0.008	0.139	0.293	0.146	

In *Table 4.2* the optical properties of the electrochromic glass are summarised for seven different glass states, named using the visible transmission value. Similarly, in *Table 4.3* the thermo-optical properties of the whole electrochromic IGU are reported, considering the same tint states.

Using the external incident solar radiation and the transmitted ones, it was possible to evaluate the solar transmission using the following equation:

$$\tau_{sol,i}(\varphi) = \frac{Q_{in}}{Q_{inc,out}} \tag{4.1}$$

Where $Q_{inc,out}$ is the outside incident solar radiation and Q_{in} the vertical internal one (transmitted through the IGU). The solar transmission depends on the incident angle φ, which is equal to 0° (normal incidence) for the values in *Table 4.2* and *Table 4.3*, and changes depending on the sun position for the measured data.

Experimental data was used to confirm that the windows optical properties matched with those stored in the database. Firstly, for each window state as in *Table 4.3*, the solar transmission curves were calculated as a function of the incident angle using empirical polynomial regressions [97]. This enabled to generalize the solar transmission value stored in the database and valid only for solar radiation incident to the plane at a normal angle. Finally, measured solar transmission data obtained using Equation (4.1) was compared with the previously obtained curves. This comparison allowed the IGU characterization to be verified and to find a correspondence between the real tinting range and the one considered in the LBNL Window database. It was found that the bleached state perfectly corresponds to the state EC73 and the most tinted to EC5. These two states were considered as the extremes of the range for the successive simulations and calculations. The equivalence of the optical properties of the EC73 IGU and the static IGU was also confirmed.

The test cell characterization was completed with a blower door test, which enables to assess the airtightness of the environment [98] (*Figure 4.5*). Air changes at 50 Pa in pressure and depression were assessed, and dividing results by a factor of 20, the average Air Changes per Hour (ACH) of the test cell were found to be of

around 1.5 h^{-1} (pressurization test) and 2.1 h^{-1} (depressurization test). These values were used as baseline when building the EnergyPlus model.

Figure 4.5. Blower door test set-up

4.3. Control infrastructure setup

This Section presents the solutions adopted to implement real-time data acquisition, pre-processing and management, paramount for control applications.

4.3.1. Real-time data acquisition and management

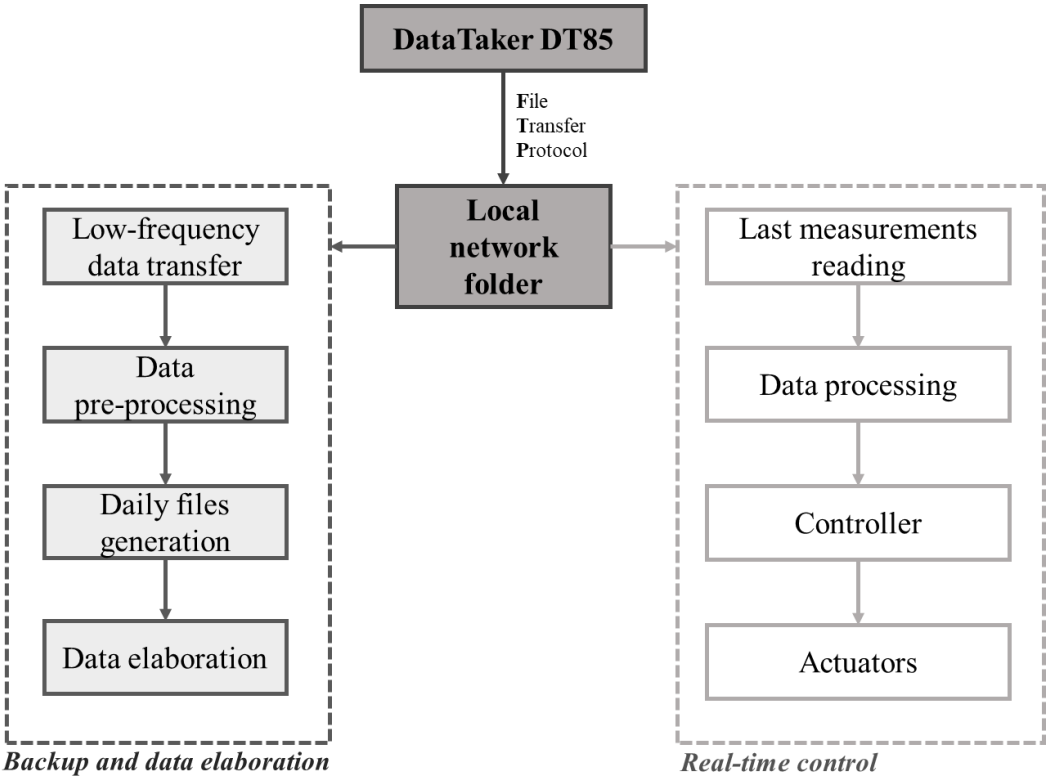

Figure 4.6. Control and data acquisition architecture

In *Figure 4.6* a schematic of the architecture used for data acquisition and control is shown. As previously introduced, the DataTaker transfer its measurement files to a protected folder at a variable frequency, chosen in function of the specific needs. For example, for the test cell characterization or monitoring (left part of *Figure 4.6*), a typical approach was to set-up the DataTaker to register the measurements every 15 minutes (with a scan rate of 1 minute). It is worth to be mentioned that the data logger acquires data at a frequency equal to the scan rate, but it averages this data and registers it at a lower rate (15 minutes in this case).

A Python script automatically retrieves this data directly from the local network folder and pre-process it into daily files, to allow faster analyses afterwards. In particular, the measured air temperatures are averaged in order to get one mean air temperature and the IGUs solar transmission properties are assessed to have feedbacks on the actual glass state.

4.3.2. Control application

The right section of *Figure 4.6* presents the control system. The controllable equipment includes the electrochromic windows and a convection heater.

The 2 kW convection heater was plugged to a power supply through a relay, controlled via a Raspberry Pi to allow remote control of the heater. The Raspberry Pi was also equipped with air temperature sensors, placed in the same position as the T-type thermocouples. These sensors were calibrated and were useful to enable the heater to operate "offline". However, since Raspberry Pi features Wi-Fi connectivity, it was possible to read and write data in real-time.

The electrochromic windows were controlled through a Python script provided by the manufacturer, which received the tint-level command on their server and send the command to the electrochromic windows (each identified with a unique code). The IGUs have a pigtail connection (as visible in *Figure 4.3* and the scheme in *Figure 4.4*) which goes directly into a control box (*Figure 4.7*)

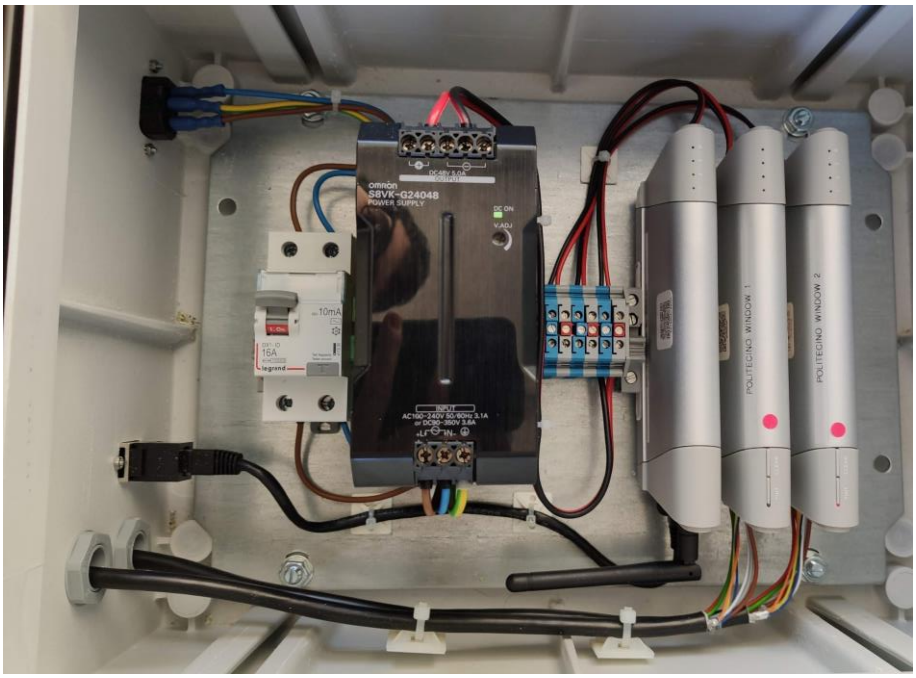

Figure 4.7. Electrochromic windows control box

4.4. Simulation setup

As in the previous case study, the simulation setup involves the interaction between different software and the definition of different working pieces.

Firstly, a physical model was defined in EnergyPlus and validated using experimental data. Then, this model was simplified using the R-C network analogy and the state-space representation, creating a grey-box model that was then identified. An evaluation of the required energy for lighting at each time of the year and for each electrochromic window state was performed, enabling the controller to consider also this factor.

4.4.1. EnergyPlus model definition and validation

An EnergyPlus model of the test cell was developed. The geometrical model was built in SketchUp, where all the main components were defined: the opaque envelope components, the IGUs, the Plexiglas strips, the west-side obstruction, etc. *Figure 4.8* shows the 3D model developed in SketchUp.

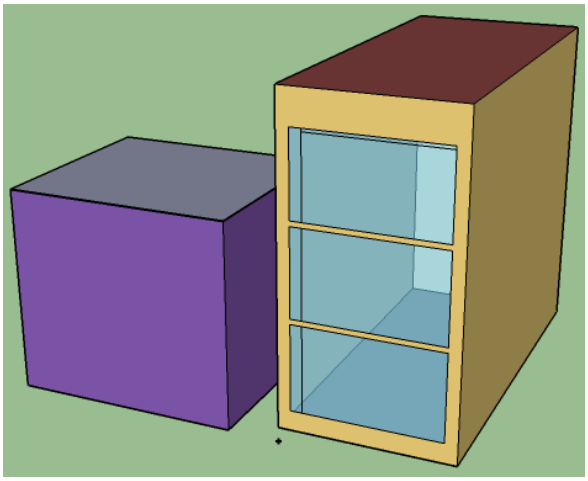

Figure 4.8. SketchUp geometrical model

All the characteristics of the test cell components were initially defined based on the results obtained during the characterization phase. Some uncertainties on the measured values are always present, and some not-negligible aspects as thermal bridges could not be measured beforehand. For these reasons, the test cell properties as defined in EnergyPlus needed to be tuned. This process lead to a validated white-box model. The validation process was supported by the experimental data and was based on the internal mean air temperature.

The validation was carried out considering experimental measurements with the test cell in free running and the electrochromic IGUs firstly in bleached state (EC74) and then in the most tinted state (EC5). It was then verified and adjusted using experimental data in heating conditions, where random schedules were given to both the convective heater and the electrochromic windows. The validation was based on the internal mean air temperature. However, also surface temperatures and transmitted solar radiations were considered, assessing the fit between the simulated

evolution of these physical quantities and the relative experimental measurements. In *Figure 4.9* and *Figure 4.10* [87], results from the model validation are shown.

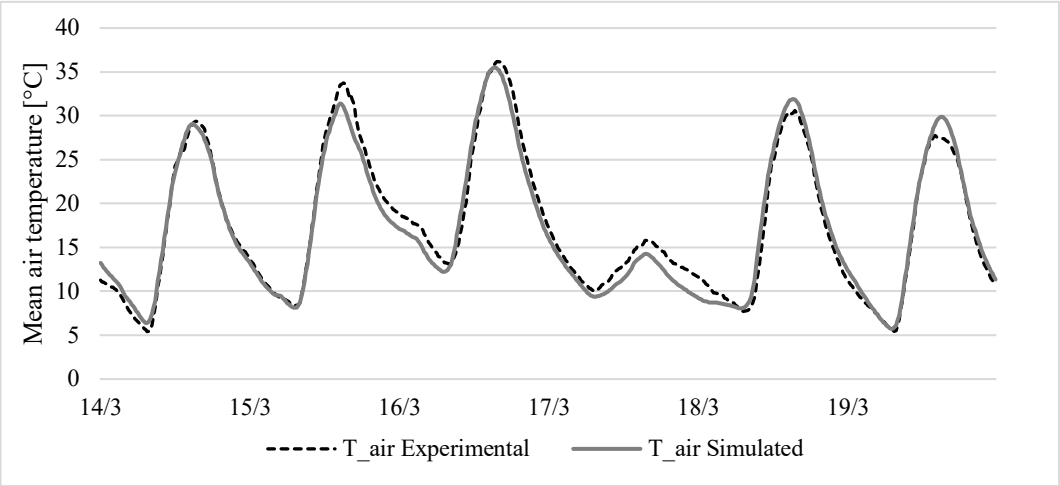

Figure 4.9. Internal air temperature comparison between experimental and simulated data - Tinted state (EC5)

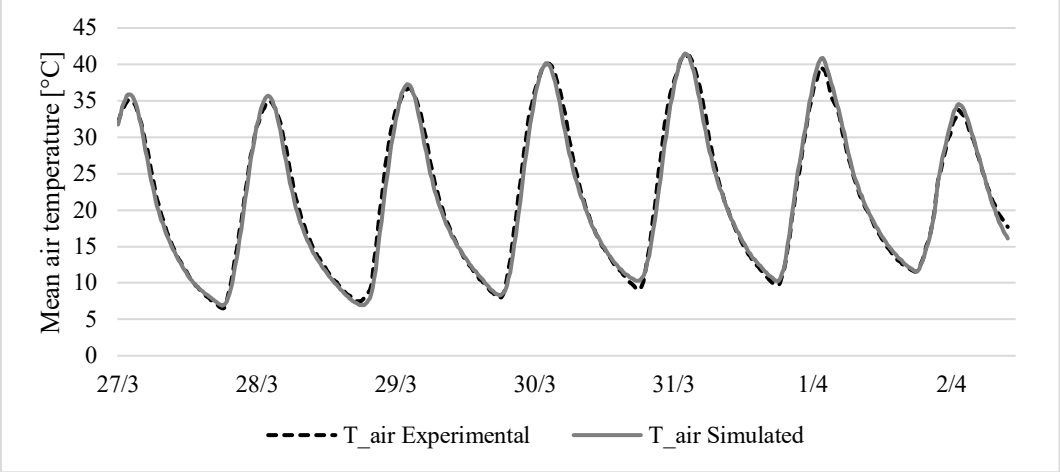

Figure 4.10. Internal air temperature comparison between experimental and simulated data - Bleached state (EC73)

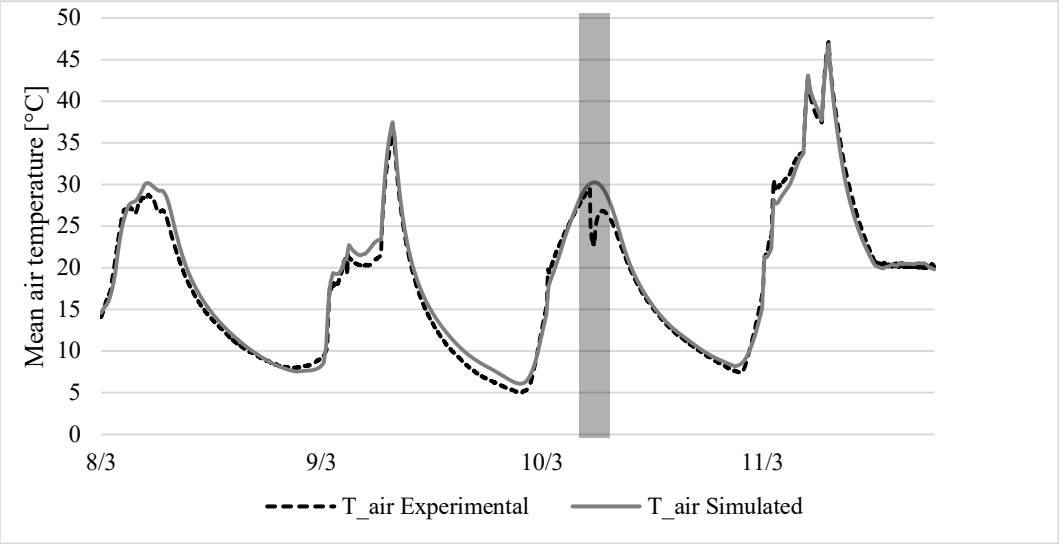

Figure 4.11. Internal air temperature comparison between experimental and simulated data – Changing glass states and heating power

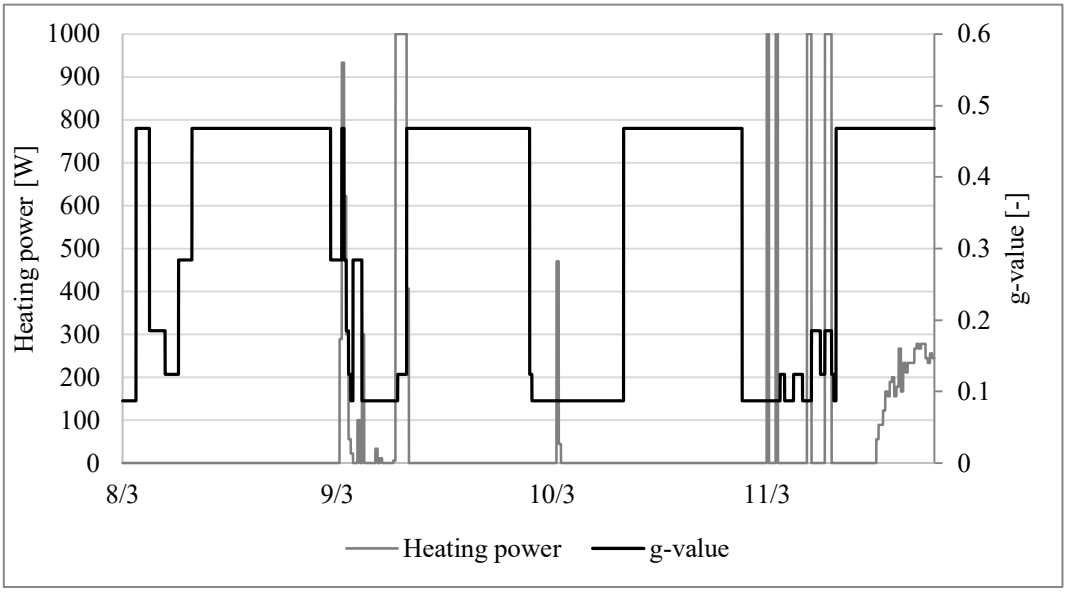

Figure 4.12. Controlled variables values during model validation shown in Figure 4.11

The highlighted band in *Figure 4.11* corresponds to a period in which the test cell door was opened because the access to the test facility was needed for small problem fixing. For this reason, the experimental air temperature curve drops, while the simulated one (which cannot take into account this event) does not.

In accordance with ASHRAE Guideline 14:2002 [99], the NMBE (Normalised Mean Biased Error) and CV(RMSE) (Coefficient of the root-mean-square error) values were calculated and verified (*Table 4.4*).

Table 4.4. Statistical parameters of the model validation

Tint state	Related figures	Statistical index	Model	ASHRAE limits
Bleached (EC73)	*Figure 4.9*	NMBE	-1.3%	±10%
		CV(RMSE)	5%	30%
Tinted (EC5)	*Figure 4.10*	NMBE	-1.7%	±10%
		CV(RMSE)	8%	30%
Variable	*Figure 4.11* *Figure 4.12*	NMBE	-2.5%	±10%
		CV(RMSE)	7%	30%

The statistical parameters evaluated in the last case (variable g-value and heating power) consider all the above shown data, also the biased period with the door opened. Since the values are within the limits, the model was considered validated.

4.4.2. Simplified model and System Identification

As in Chapter 3, a grey-box model was developed for this case study, with the aim of enabling the application of a Model Predictive Control strategy. The same approach of the previous case study was followed: an R-C network was chosen to describe the thermal behaviour of the case study in a simplified way, its dynamics are described through a state-space representation and its lumped parameters are identified via a system identification.

R-C network definition

As a first approach, the R-C network presented in *Figure 4.13* was considered.

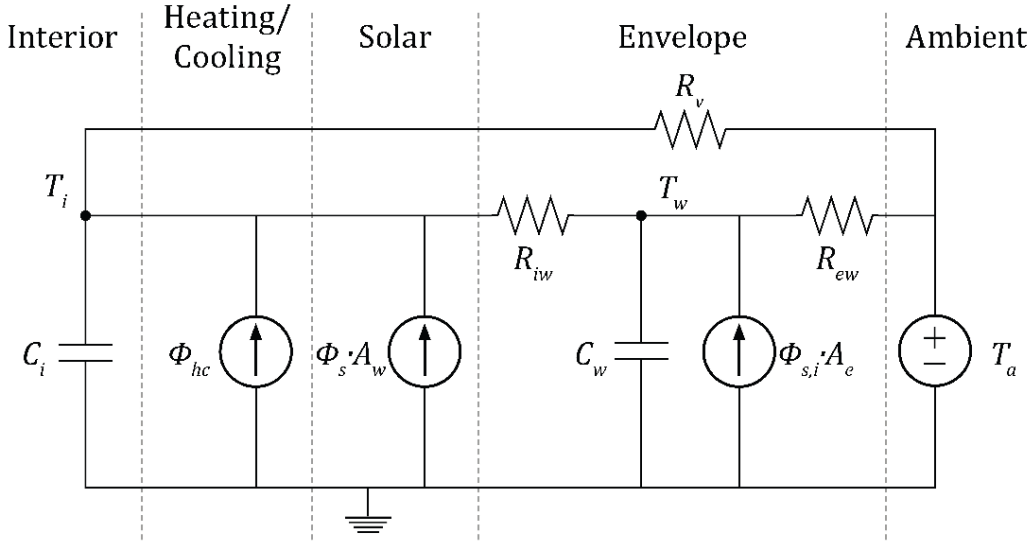

Figure 4.13. R-C network considering solar radiation on the opaque envelope

It consists of a II order R-C network, which was found to be the best performing in the previous case study, with the following parameters:

- T_i – average inside temperature;
- T_w – equivalent wall temperature;
- T_a – ambient temperature;
- R_v – equivalent infiltration resistance;
- R_{iw} – internal half of the wall equivalent resistance;
- R_{ew} – external half of the wall equivalent resistance;
- C_i – equivalent internal capacitance;
- C_w – equivalent wall capacitance;
- ϕ_{hc} – energy flux from the heating/cooling system;
- ϕ_s – energy flux from solar radiation through the transparent components;
- A_w – effective window area;
- $\phi_{s,i}$ – energy flux from the incident solar radiation on the opaque envelope components;
- A_e – effective opaque envelope area.

Therefore, the equations describing the system dynamics are:

$$\frac{dT_i}{dt} = \frac{1}{R_{iw}C_i}(T_w - T_i) + \frac{1}{R_vC_i}(T_a - T_i) + \frac{1}{C_i}\phi_s A_w + \frac{1}{C_i}\phi_{hc} \tag{4.2}$$

$$\frac{dT_w}{dt} = \frac{1}{R_{iw}C_w}(T_i - T_w) + \frac{1}{R_{ew}C_w}(T_a - T_w) + \frac{1}{C_w}\phi_{s,i}A_e \tag{4.3}$$

The system identification process, however, highlighted an over-parametrization problem. Considering the thermal dynamics occurring in the test cell, the R-C network was simplified by eliminating the $\phi_{s,i} \cdot A_e$ element: amongst the other elements of the network, the incident solar radiation on the opaque test cell components was considered the least influencing the overall dynamics. This because of two main reasons:

- the first is that incident solar radiation acts only on the east façade, the roof and a small portion of the west façade (given the above-described obstruction);
- the second is that the envelope external surface are smooth and light-coloured, hence characterised by a low solar absorptance value.

Moreover, the internal and external halves of the wall equivalent resistance were considered equal, given the perfect symmetry of the opaque test cell components. Therefore, instead of the parameters R_{ew} and R_{iw}, a unique parameter (R_w), which represents half of the wall equivalent resistance was introduced.

The II order R-C network taken into account is the one shown in *Figure 4.14*.

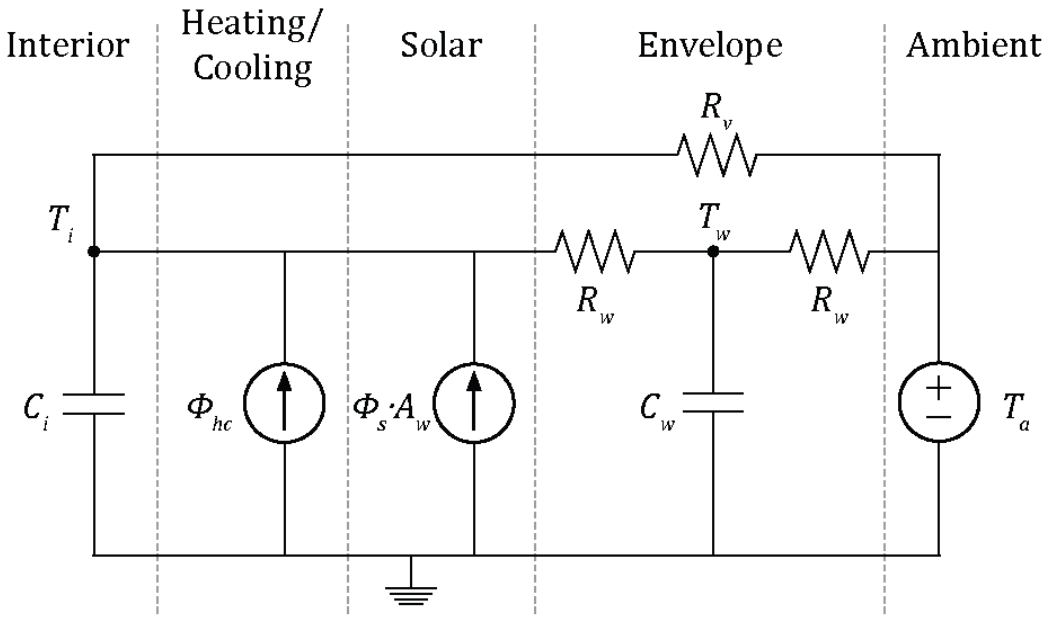

Figure 4.14. R-C network considered in this case study

The system dynamics of the network shown in *Figure 4.14* are characterised by the following equations:

$$\frac{dT_i}{dt} = \frac{1}{R_w C_i}(T_w - T_i) + \frac{1}{R_v C_i}(T_a - T_i) + \frac{1}{C_i}\phi_s A_w + \frac{1}{C_i}\phi_{hc} \quad (4.4)$$

$$\frac{dT_w}{dt} = \frac{1}{R_w C_w}(T_i - T_w) + \frac{1}{R_w C_w}(T_a - T_w) \quad (4.5)$$

This simplification leads to a considerable improvement in terms of stability and equivalence between the R-C network and the real thermal dynamics, as demonstrated by the System Identification process.

State-space representation

The following state-space equations are used to describe the system dynamics:

$$\dot{x}(t) = Ax(t) + Bu(t) \quad (4.6)$$

$$y(t) = Cx(t) + Du(t) \quad (4.7)$$

Where:

$$x = [T_i,\ T_w]^T \tag{4.8}$$

$$u = [T_a, \phi_s, \phi_{hc}]^T \tag{4.9}$$

$$A = \begin{bmatrix} -\left(\frac{1}{R_w C_i} + \frac{1}{R_v C_i}\right) & \frac{1}{R_w C_i} \\ \frac{1}{R_w C_w} & -\left(\frac{2}{R_w C_w}\right) \end{bmatrix} \tag{4.10}$$

$$B = \begin{bmatrix} \frac{1}{R_v C_i} & \frac{A_w}{C_i} & \frac{1}{C_i} \\ \frac{1}{R_w C_w} & 0 & 0 \end{bmatrix} \tag{4.11}$$

$$C = [1 \quad 0] \tag{4.12}$$

$$D = [0 \quad 0 \quad 0] \tag{4.13}$$

Where:

- $\dot{x}(t)$ - state vector;
- $y(t)$ - output vector;
- $u(t)$ – input vector;
- A, B, C, D – time invariant matrices.

The parameters to be identified are: R_w, R_v, C_i, C_w and A_w.

System Identification

Since the test cell only allowed free-running and heating conditions, it was not possible to obtain experimental during cooling. Therefore, the previously presented EnergyPlus validated model was used to generate the data-set needed for the System Identification process.

As in the previous case study, a four-week period was considered, where the first two weeks were used to estimate the lumped parameters and the last two weeks were used to test the performance of the model. Being the controlled inputs the electrochromic state and the heating/cooling power, random schedules were generated in order to "train" the model on all the possible conditions. Heating, cooling and free-running were alternated and the heating or cooling power inputs were set so to have different durations and magnitude; the electrochromic state changed throughout the entire duration of the dataset.

Figure 4.15 shows the heating/cooling system and electrochromic state schedules.

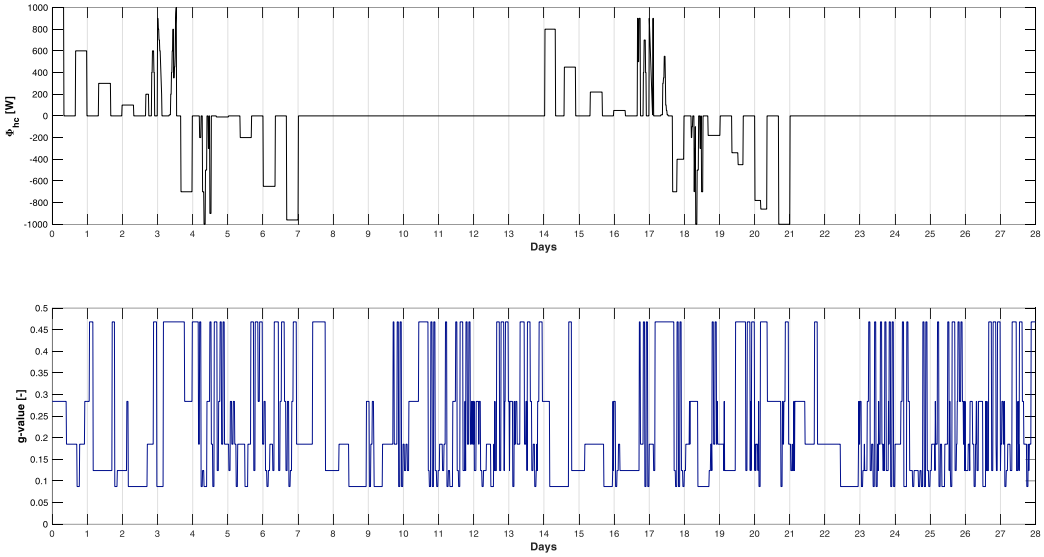

Figure 4.15. Heating/cooling system and electrochromic state schedule used to generate the input dataset

The resulting input dataset used for the identification is shown in *Figure 4.16*.

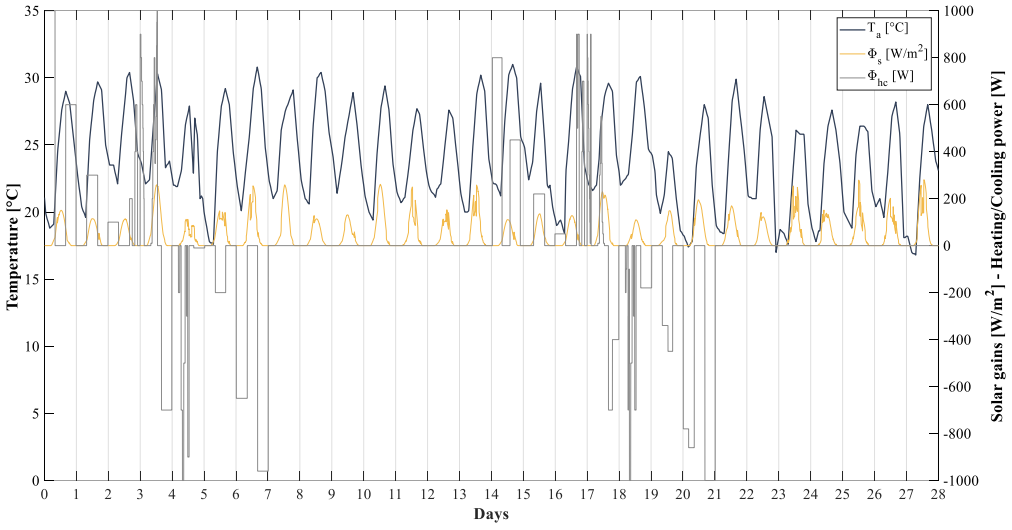

Figure 4.16. Input dataset for system identification

The input dataset shown in *Figure 4.16* includes the ambient temperature (T_a), the heating/cooling power (ϕ_{hc}) and solar gains (ϕ_s). Solar gains, as in the previous Chapter, are calculated as the solar radiation incident to the test façade multiplied by the transparent component g-value. In this case, since the façade is composed of one static unit and two electrochromic units, the g-value is calculated as a weighted average of the three IGUs. The g-value shown in *Figure 4.15* is only related to the electrochromic windows.

Using the Linear Grey-Box Models (in Matlab), fed with the above defined dataset, the lumped parameters where identified (*Table 4.5*).

Table 4.5. Parameters identification

	R_w (K/kW)	R_v (K/kW)	C_i (kWh/K)	C_w (kWh/K)	A_w (m^2)
Identified value	**91.69**	**45.73**	**0.073**	**0.286**	**3.30**
Upper boundary	103.80	22.90	0.014	0.079	2.10
Initial guess	25.95	68.71	0.041	0.236	3.16
Lower boundary	6.49	206.12	0.122	0.709	4.74

In *Table 4.5* the identified parameters are shown along with the relative first guess value and its boundaries.

Using the second half of the dataset, then, the grey-box model response was tested, and the graphical comparison is shown in *Figure 4.17*.

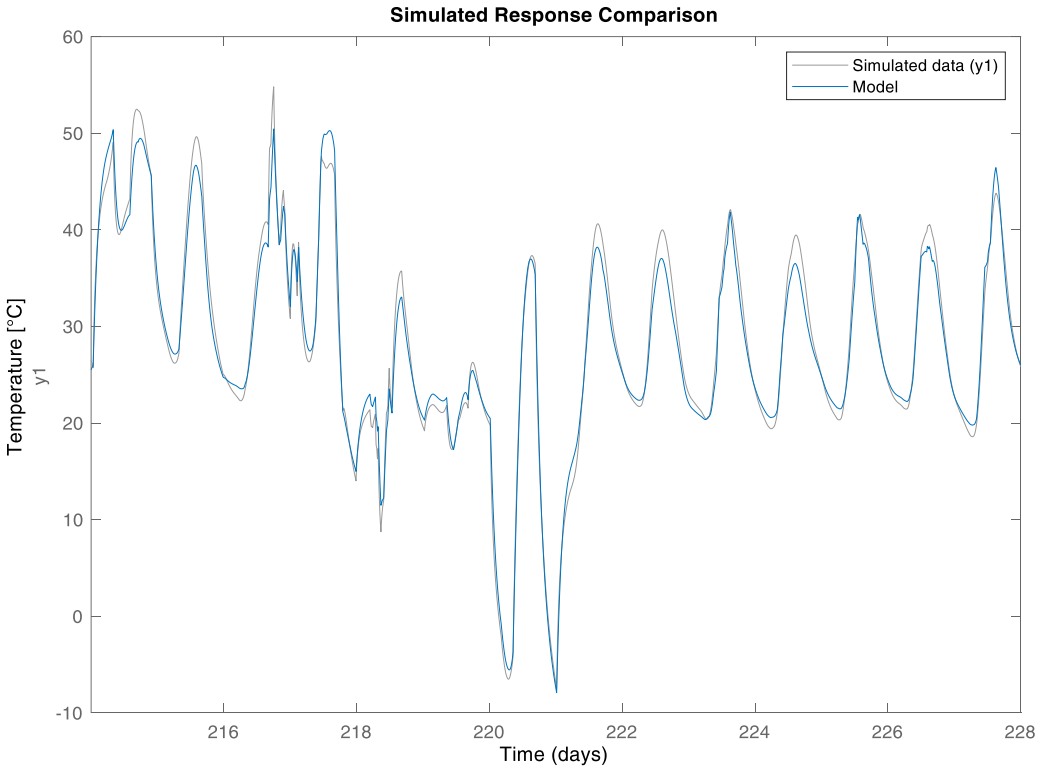

Figure 4.17. Simulated response comparison

The Matlab System Identification Toolbox was used to evaluate the fit between the grey-box model response and the simulated dataset. In particular, it evaluates the Normalised Root Mean Square Error (NRMSE), in this case equal to 86.08%.

4.4.3. Energy consumption for lighting evaluation

In collaboration with a researcher of the TEBE group, expert in lighting evaluations, the energy need for lighting throughout the year for different electrochromic glazing states was identified.

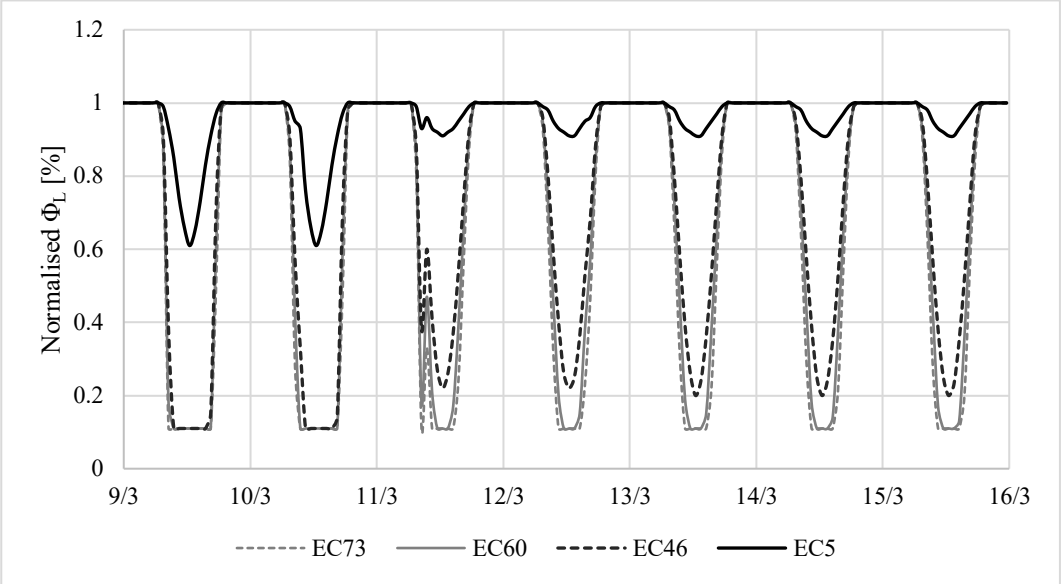

Figure 4.18. Normalised power need for lighting during a week

Figure 4.18 shows, in a random week, the normalised results of ϕ_L, which can be described as the power absorbed by the lighting system. It is normalised with respect to the nominal power of the lighting system, considered equal to 62 W.

These results were obtained using the software DIVA for Rhino [100], where the geometrical characteristics of the test cell were the same as the one used in EnergyPlus. All the transparent envelope optical properties were taken into account, along with the optical parameters of the internal surfaces, since once the light enters the environment, it bounces multiple times along the internal surfaces in relationship with its optical characteristics (colour, specularity, etc). The goal of the lighting system is to keep 500 lx of illuminance in a hypothetical horizontal task area considered to be in the middle of the test cell [101]. These values were organized in a table, used by the MPC as a look-up table to take into account the effect of an electrochromic state choice on the lighting energy consumption. In this way, the controller can quantify and predict the implications of a sequence of glass state choices on the energy need for lighting. This is particularly interesting because of the contrasting nature that often exists between the thermal and lighting needs: during a cooling period, while solar gains need to be minimised (electrochromic in dark states) in order to save cooling energy consumption, the opposite would be desirable to save lighting energy (electrochromic in clear states).

4.4.4. Co-simulation infrastructure

Figure 4.19 shows the workflow describing the co-simulations infrastructure.

On the left, the *white-box* model developed in Energy Plus simulates the system dynamics, and given its validation can be considered representative of the real system. At each control time-step, the simulation is paused and states measurements are passed to the controller via BCVTB. The controller, developed in Matlab, uses the received states measurements as inputs, along with the prediction of future disturbances and information on the energy need for lighting. This last information consists of pre-calculated values stored in a look-up table. Specifically, the values related with energy need for lighting predictions up to the control horizon and related to every possible window state are passed to the controller. This set of data allows the controller to solve the optimization problem, using the *grey-box* model to perform the needed predictions. Once a solution is found, the control actions relative to the first control time-step are passed to EnergyPlus via BCVTB. Finally, the control actions are implemented in the model and the *white-box* simulation continues until the following control time-step.

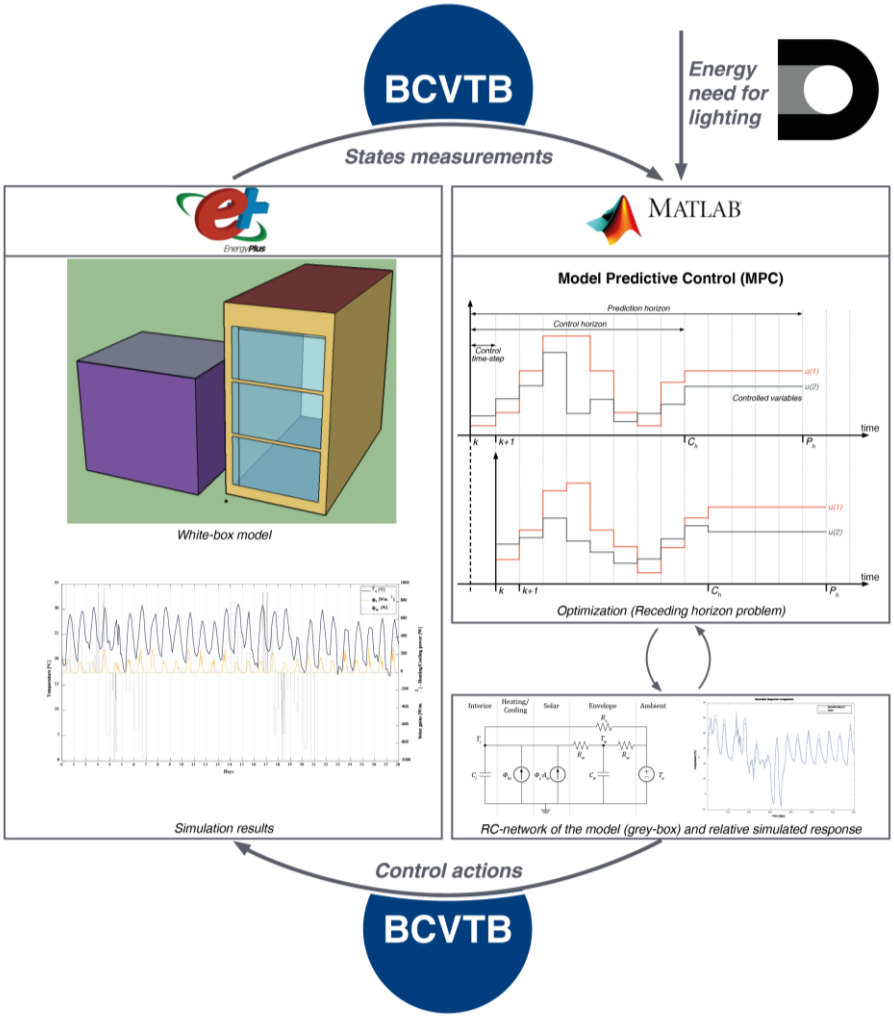

Figure 4.19. Simulation Workflow

4.5. Controller definition

In this Section, the developed MPC strategy is presented. Moreover, the RBC strategies used as baseline are described.

4.5.1. MPC formulation and simulative application

Constraints

A Hybrid Model Predictive Control (HMPC) was defined, because of the necessity to deal with continuous and Boolean variables.

Both hard and soft constraints were used in this case study:

$$\phi_{hc,min} \leq \phi_{hc} \leq \phi_{hc,max} \tag{4.14}$$

$$\sim (\delta_1 \,\&\, \delta_2) \,\&\, \sim (\delta_1 \,\&\, \delta_3) \,\&\, \sim (\delta_2 \,\&\, \delta_3) \tag{4.15}$$

$$\sim (\delta_1 \,\&\, night) \,\&\, \sim (\delta_2 \,\&\, night) \,\&\, \sim (\delta_3 \,\&\, night) \tag{4.16}$$

$$T_{i,min} - e \leq T_i \leq T_{i,max} + e \tag{4.17}$$

$$\phi_L \leq \phi_{L,min} + e_L \tag{4.18}$$

Equation (3.12) sets an upper and a lower boundary to the heating/cooling load (assuming heating as positive and cooling as negative).

Equation (3.13) avoids the switching of two different states of the electrochromic glass at the time (see *Table 4.6* to infer the window state from the Boolean variable $\delta_1, \delta_2, \delta_3$ combination).

Table 4.6. Correspondence between the Boolean variables and the relative states action

δ_1	δ_2	δ_3	State	Glass g-value	Façade average g-value
0	0	0	EC73	0.468	0.468
1	0	0	EC60	0.284	0.342
0	1	0	EC46	0.185	0.275
0	0	1	EC5	0.087	0.208

Equation (3.14) avoids the selection of states other than the bleached one at night time, where $night$ is defined as when solar radiation is below a certain threshold.

In Equation (3.15), a soft constraint on the internal temperature T_i is defined, allowing the system to violate the boundaries $T_{i,min}$ and $T_{i,max}$ using the slacking variable e, that penalizes the objective function.

To consider the lighting energy consumption, the slacking variable e_L was used as in Equation (4.18). The system will be provided with the minimum energy need

for lighting in that particular moment, which always corresponds with the bleached state. Therefore, if the bleached state is chosen, $\phi_L = \phi_{L,min}$, hence $e_L = 0$; if a different state is chosen, ϕ_L will necessarily be higher than $\phi_{L,min}$ ($\phi_L > \phi_{L,min}$), so e_L will be higher than 0 ($e_L = \phi_L - \phi_{L,min}$). The higher the energy need for lighting ϕ_L with respect to its minimum possible value $\phi_{L,min}$, the higher will be e_L, in turns negatively affecting the cost function. The controller will thus prefer ϕ_L values to be as close as possible to $\phi_{L,min}$, finding a trade-off between this need and the one relative to heating/cooling energy need, often contrasting.

HMPC formulation

As in Chapter 3, a Mixed Logic Dynamical formulation was required [50,82]:

$$x(t+1) = Ax(t) + B_1u(t) + B_2\delta(t) + B_3z(t) \quad (4.19)$$
$$y(t) = Cx(t) + D_1u(t) + D_2\delta(t) + D_3z(t) \quad (4.20)$$

Where:

- $x(t) = [x_c^T(t)\, x_d^T(t)]$ is the state vector, with a continuous part ($x_c(t) \in \mathbb{R}^n$) and a discrete part ($x_d(t) \in \{0,1\}^{n_d}$);
- $y(t) = [y_c^T(t)\, y_d^T(t)]$ is the output vector, with $y_c(t) \in \mathbb{R}^m$ and $y_d(t) \in \{0,1\}^{m_d}$ the respective continuous and discrete parts;
- $u(t) = [u_c^T(t)\, u_d^T(t)]$ with $u_c(t) \in \mathbb{R}^l$ and $u_d(t) \in \{0,1\}^{l_d}$ the respective continuous and discrete parts;
- $z(t) \in \mathbb{R}^r$ is a continuous auxiliary and $u_d(t) \in \{0,1\}^{r_d}$ represents discrete variables;
- A, B_i, C, D_i are the real constant matrices

Objective function

The objective function can be written as:

$$min_{\{u\}_0^{N-1}} J = \sum_{t=1}^{N-1} \|Q(x(t) - x_r)\|_p + \|R(u(t) - u_r)\|_p \quad (4.21)$$

Where:

- Q is the weighted matrix of the states;
- R is the weighted matrix of the controlled inputs;
- $x(t)$ is the state vector, x_r the reference state vector;
- $u(t)$ the controlled inputs vector and u_r the reference controlled input vector.

As in Chapter 3, the controlled inputs are considered for the cost function. The controlled input vector is $u = [e,\ \phi_{hc}, \phi_L, \delta_1, \delta_2, \delta_3]^T$, where e is a slacking

variable used to define a soft constraint, ϕ_{hc} is the heating/cooling energy, ϕ_L is the lighting energy, δ_1, δ_2, δ_3 are three Boolean variables related to the electrochromic glass state (as in *Table 4.6*).

The input variable characteristics and associated weights are summarised in *Table 4.7*.

Table 4.7. Input variables description and weights

Variable	Description	Variable typology	Limits		Weights
			Lower	Upper	
$\boldsymbol{e}$	Slacking	Continuous	0 °C	2 °C	0.1 W/K
$\boldsymbol{\phi_{hc}}$	Heating/Cooling	Continuous	-1000 W	1000 W	1 [-]
$\boldsymbol{\phi_L}$	Lighting	Continuous	0 W	62 W	1 [-]
$\boldsymbol{\delta_1}$	State: EC60	Boolean	0	1	0.00025 W
$\boldsymbol{\delta_2}$	State: EC46	Boolean	0	1	0.00050 W
$\boldsymbol{\delta_3}$	State: EC5	Boolean	0	1	0.00075 W

Due to the complexity of the problem to be solved and the limitation of the machine used to solve it, the control horizon (correspondent to the prediction horizon) was fixed to 6 hours, while the control time-step at 30 minutes.

Hardware and software setup

The Mixed Logic Dynamical System was formulated in HYSDEL [83]. The Multi-Parametric Toolbox 3.0 (MPT3) [84] was used to design the MPC algorithm. CPLEX was used as the optimizer to solve the Mixed Linear Programming (MILP) problem. The machine used is a DELL XPS15, with an Intel Core i7 @ 2.8 GHz processor and 16GB of RAM.

4.5.2. Baseline control strategies

As in Chapter 3, baseline control strategies were used to compare the MPC results.

Firstly, a base case study with static windows (equivalent to the electrochromic in the bleached state) was considered. Then, considering the possibility to change the electrochromic windows states, RBC strategies were applied based on the incident solar radiation ($\phi_{s,i}$) and on the average indoor temperature (T_i). The applied threshold are summarised in *Table 4.8*:

Table 4.8. RBC strategies summary

RBC strategy	Thresholds	Electrochromic state
$\boldsymbol{\phi_{s,i}}$	$\phi_{s,i} \leq 100$ W/m^2	EC73
	100 W/m^2 < $\phi_{s,i} \leq 150$ W/m^2	EC60
	100 W/m^2 < $\phi_{s,i} \leq 400$ W/m^2	EC46
	$\phi_{s,i} > 400$ W/m^2	EC5
$\boldsymbol{T_i}$	$T_i \leq 24.5$ °C	EC73
	24.5 °C < $T_i \leq 25$ °C	EC60
	25 °C < $T_i \leq 25.5$ °C	EC46
	$T_i > 26$ °C	EC5

4.6. Results

In this section, the presented results provide an exhaustive picture of the strategies adopted by the designed control strategies in different periods of the year. Moreover, comparisons between MPC and baseline strategies will be provided.

For a summer, an intermediate and a winter week period, results in the time domain are shown for the different control strategies, while in a radar chart the key performance indicators are compared.

Results in the time domain will show the weather disturbances and the output, in particular the incident solar radiation $\phi_{s,i}$, the ambient temperature T_a and the indoor temperature T_i, along with the controlled inputs, which are the electrochromic state (*g-value*), the heating and cooling power (ϕ_h and ϕ_c) and the lighting power (ϕ_L).

The radar charts comparing the control strategies are based on five Key Performance Indicators (KPIs):

- *total energy consumption [Wh]*: the energy request of the heating/cooling system over the week period;
- *peak power [W]*: the peak load of the heating/cooling system over the week period;
- *dark states [%]*: the amount of time in which the window was in dark states (i.e. EC28 or EC5) with respect to the total simulation period;
- *Percentage of Discomfort Hours (PDH) [h]*: as defined in EN 16978-1:2019[86], the percentage amount of time in which the operative temperature T_{op} is above or below given threshold values, in this case 20°C and 26°C respectively (Category II)
- *glass state changes [-]*: total number of times in which the electrochromic glass state changes.

As in Chapter 3, the normalised area of each polygon represented in the radar chart is used as KPI to compare the control strategies. It needs to be read along with the other KPIs to correctly perform the comparison, but its simplicity and directness make it a useful tool for this purpose

4.6.1. Summer week

From *Figure 4.20* to *Figure 4.23*, results of RBC and MPC strategies are shown for a summer week in Torino (July 20th – 27th). In *Figure 3.39*, a radar chart is shown to compare these strategies.

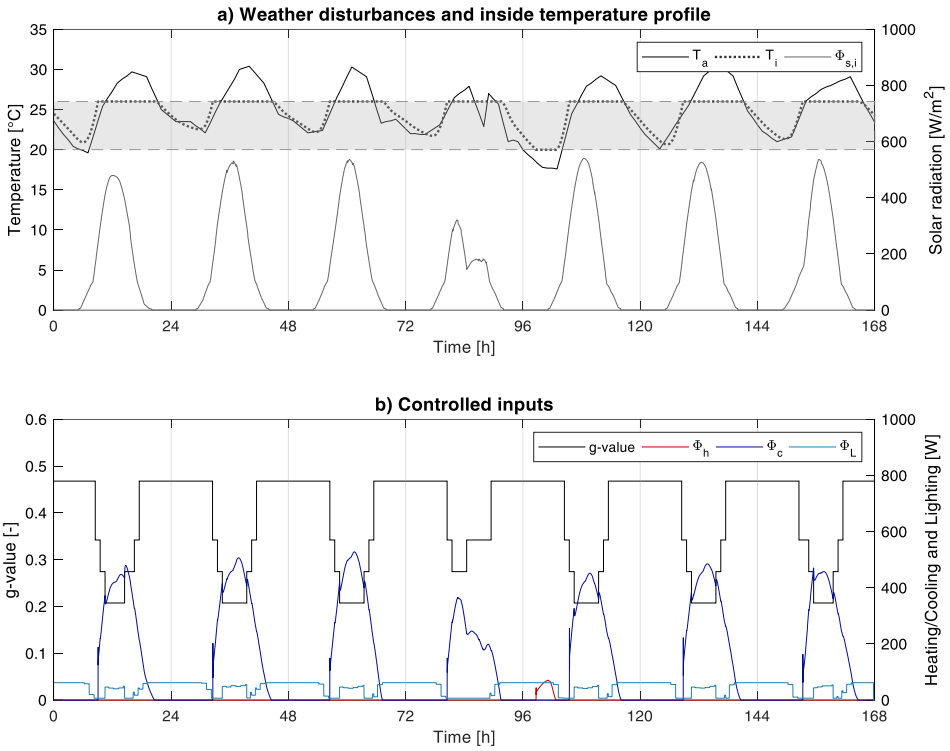

Figure 4.20. Rule Base Control based on the incident solar radiation ($\phi_{s,i}$) – Summer week

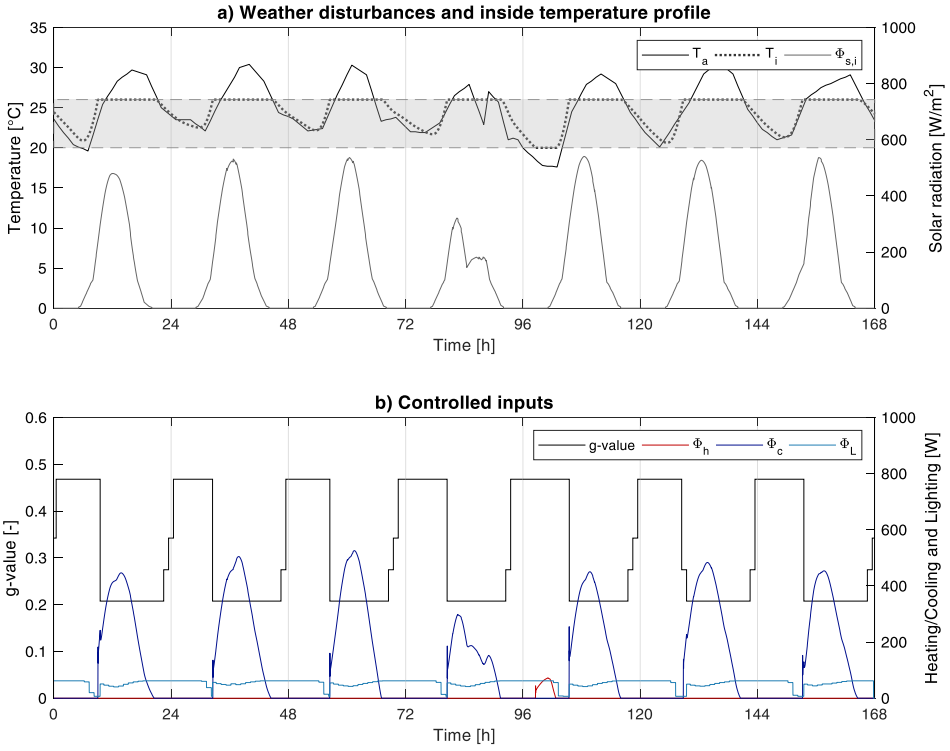

Figure 4.21. Rule Based Control based on indoor temperature (T_i) - Summer week

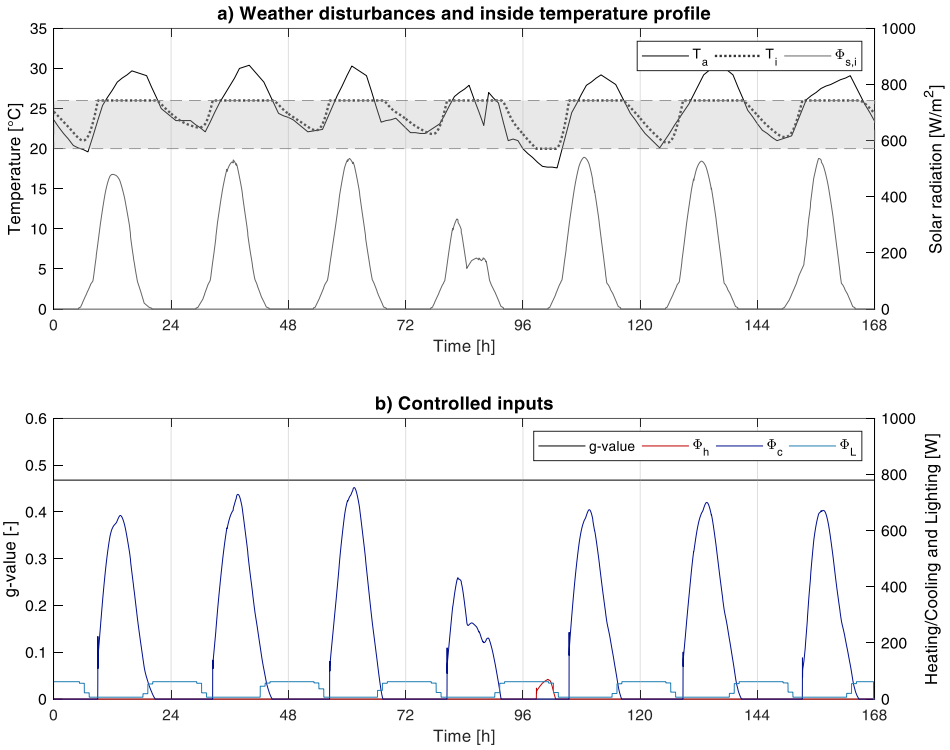

Figure 4.22. Bleached state - Summer week

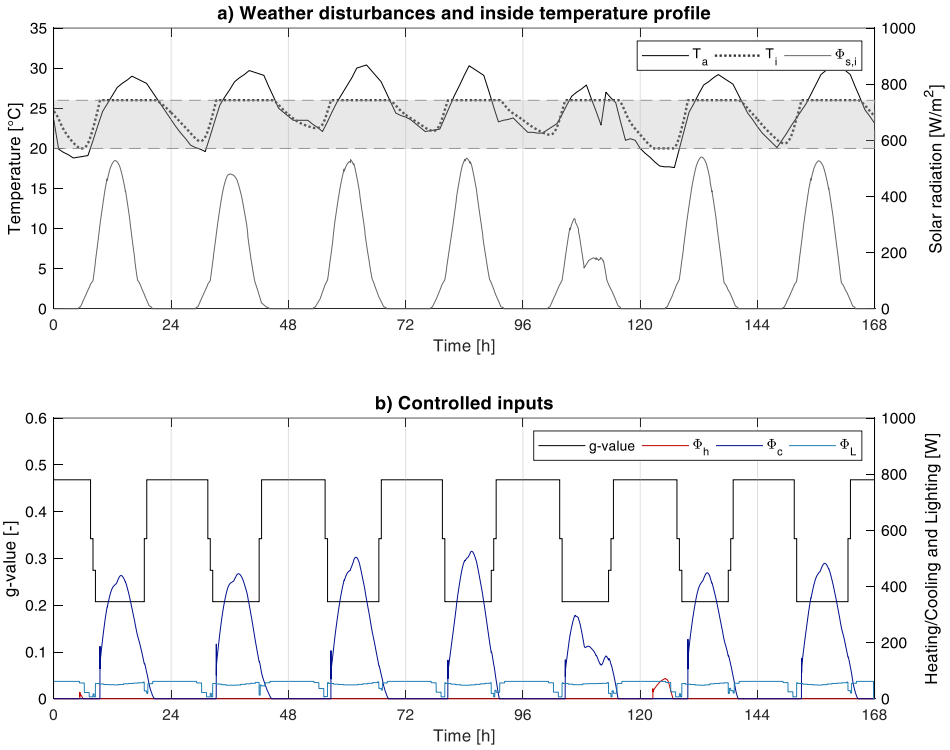

Figure 4.23. MPC control - Summer week

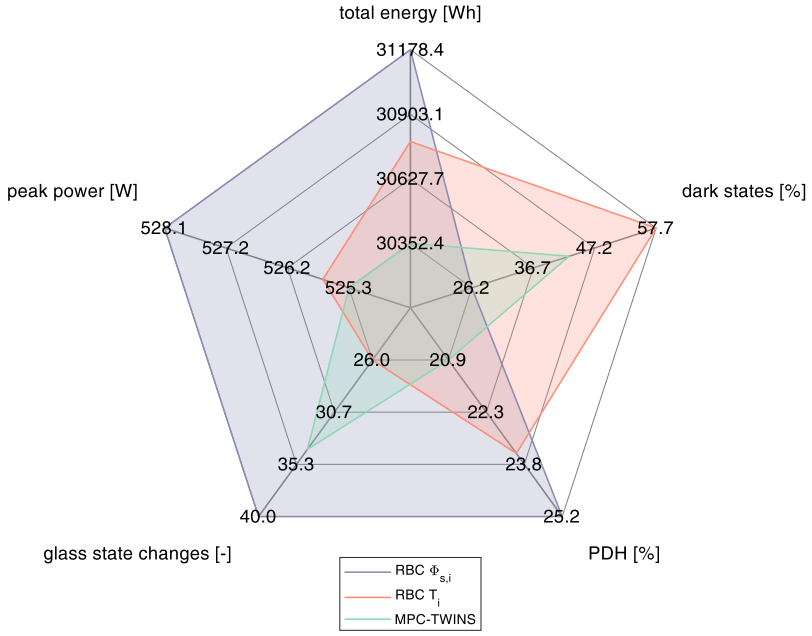

Figure 4.24. Comparison between MPC and RBC control strategies - Summer week

Table 4.9 summarises the KPI represented in *Figure 3.39*, along with the normalised polygon areas.

Table 4.9. Performance parameters and polygon areas – Summer week

	Total Energy [kWh]	**Peak Power [W]**	**Dark States [%]**	**PDH [%]**	**State changes [-]**	**Polygon Area [-]**
RBC $\phi_{s,i}$	31.18	528.07	26.19	25.20	40	2.09
RBC T_i	30.79	525.72	57.74	23.48	26	1.98
MPC	30.35	525.33	42.86	20.92	34	1.83

Results show that the MPC strategy seems to merge the advantages of the two RBC strategies: from one side it anticipates the solar radiation increase and it protects the indoor environment by choosing darker states; on the other side it considers the indoor air temperature, thus reacting faster when temperature increases are foreseen. Since the case study consists of a test cell built with lightweight materials and not particularly airtight, these anticipations result in lower advantages from the energy consumption perspective than what could be achieved in other cases. However, it is clear how the predictive abilities of the MPC strategy enable the system to not only consume less energy than the other cases, but also to guarantee better indoor conditions (lower percentage of discomfort hours), and more time with the glazing system in clear states. This last aspect also affects the

indoor comfort conditions, since it results in a decreased use of the lighting system in favour of natural daylight and a better view-out.

It is also worth to be noted that the adaptation range of the transparent façade is greatly reduced with respect to its full potential because of the static IGU.

4.6.2. Spring week

From *Figure 4.25* to *Figure 4.28*, results of RBC and MPC strategies are shown for a spring week in Torino (March 30th – April 5th). In *Figure 4.29*, a radar chart is reported to compare these strategies.

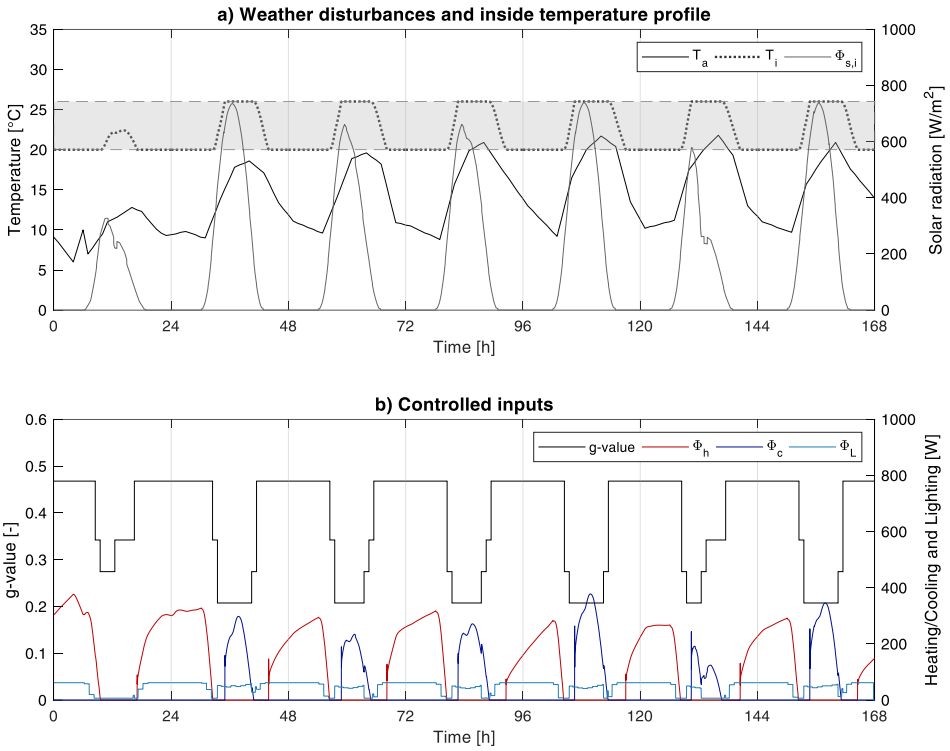

Figure 4.25. Rule Base Control based on the incident solar radiation ($\phi_{s,i}$) – Spring week

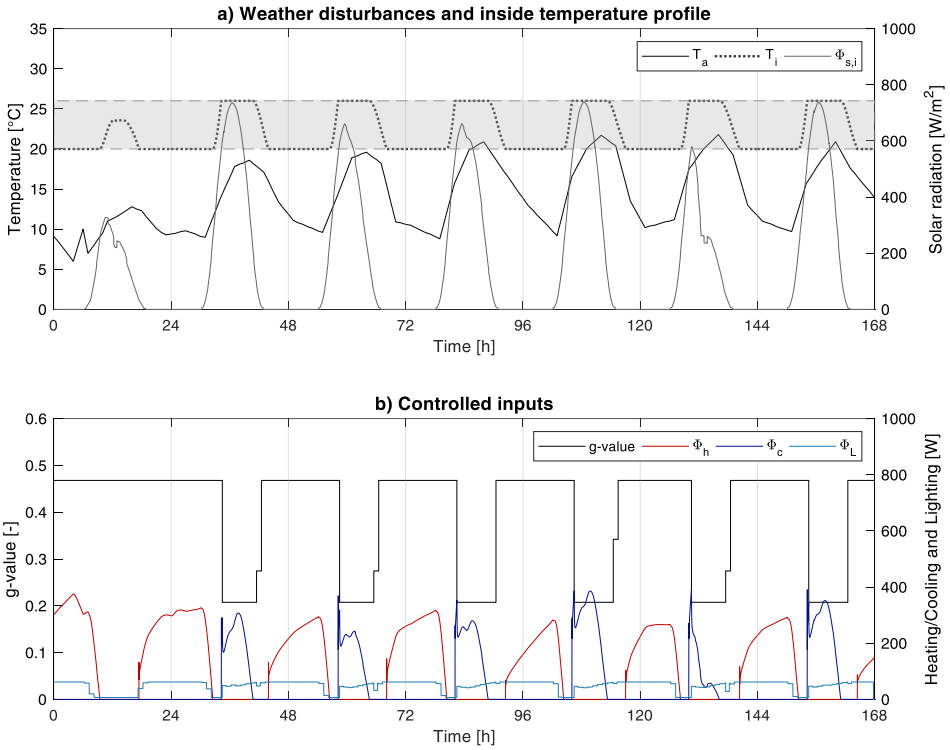

Figure 4.26. Rule Based Control based on indoor temperature (T_i) - Spring week

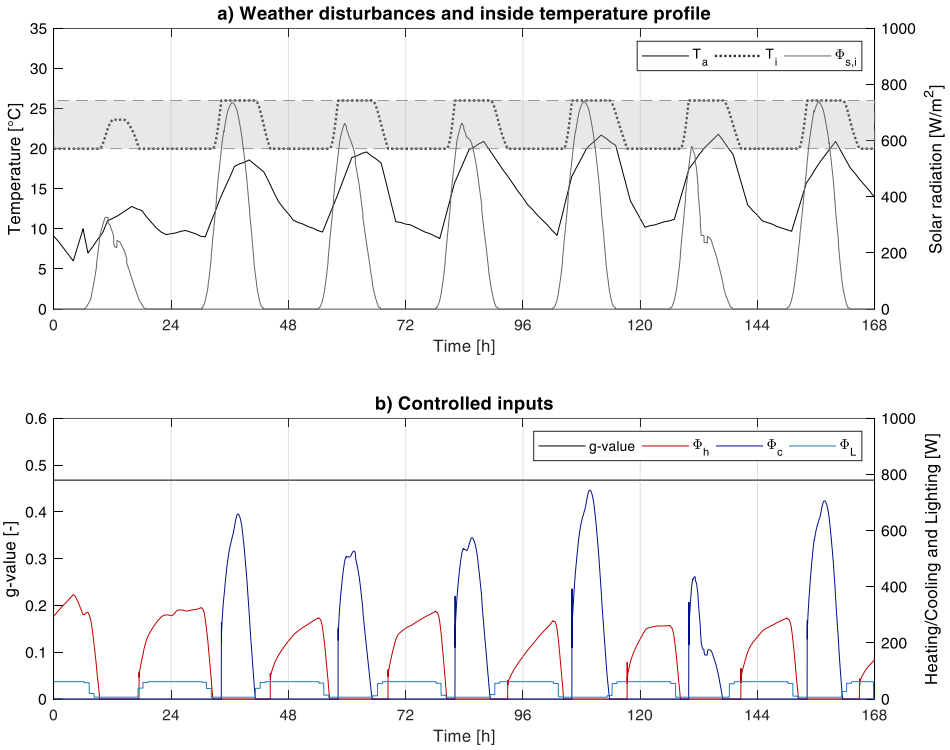

Figure 4.27. Bleached state - Spring week

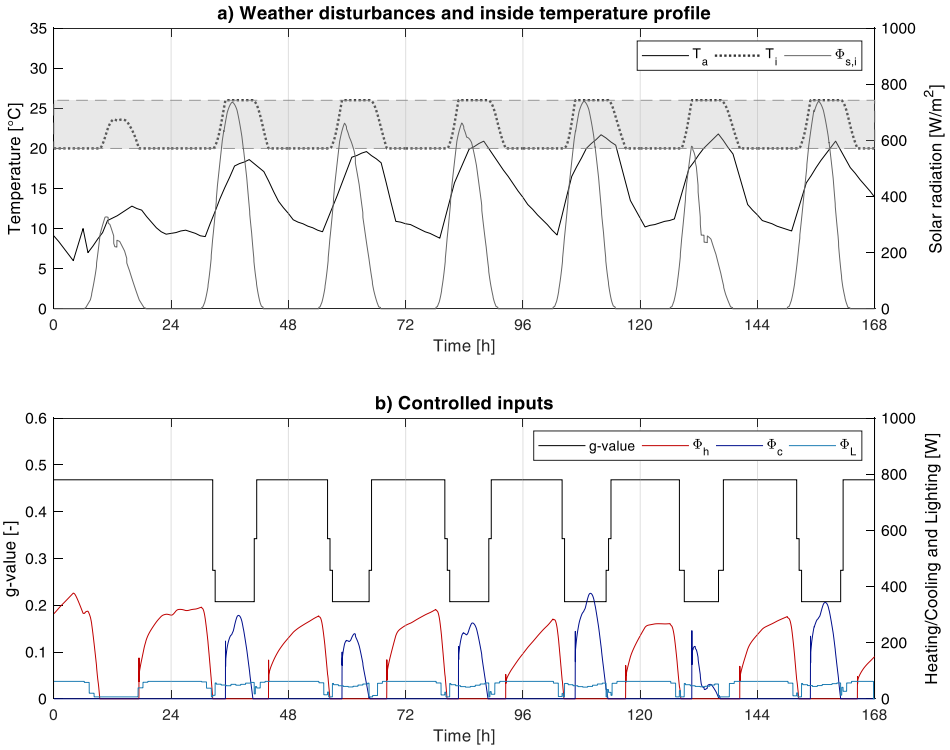

Figure 4.28. MPC control - Spring week

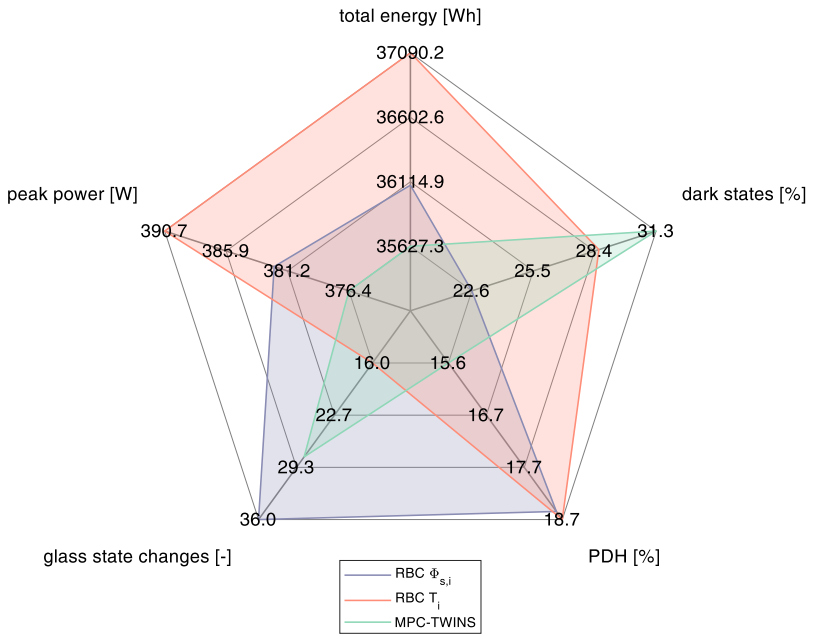

Figure 4.29. Comparison between MPC and RBC control strategies - Spring week

Table 4.10 summarises the KPI represented in *Figure 4.29*, along with the normalised polygon areas.

Table 4.10. Performance parameters and polygon areas – Spring week

	Total Energy [kWh]	**Peak Power [W]**	**Dark States [%]**	**PDH [%]**	**State changes [-]**	**Polygon Area [-]**
RBC $\phi_{s,i}$	36.09	382.23	23	18.5	36	2.07
RBC T_i	37.09	390.69	29	18.7	16	1.96
MPC	35.63	376.45	31	15.6	28	1.77

Because of the low ambient temperatures and high solar radiation, the spring period poses a challenge to the control strategies. In facts, a glazed south can cause overheating during the day due to the high solar gains, and heating can be needed when solar radiation is not present, due to the low ambient temperatures. Given the low thermal mass and airtightness of the test cell, as stated before, these alternating behaviours can be exacerbated. In contrast to the previous case, RBC base on solar radiation works better during spring, since protection from solar radiation is key to lower cooling energy consumption. As before, the MPC strategy seems merging the positive behaviours of the two RBC strategies and its anticipations seem smoothing the peaks (especially present in the RBC based on the indoor temperature). The

overall advantages are hampered by the low thermal capacity of the test cell, which is translated in a rapidly changing indoor temperature.

Since the MPC strategy is characterised by higher weights on the energy consumption and lower ones on the glass states, darker states are preferred during high solar radiation values to protect the indoor environment from excessive solar gains, resulting in higher percentage period with dark states. The advantages of this strategies would be more evident if the entire façade would have been characterised by the same adaptation range as the electrochromic IGUs and if the indoor environment would be more suitable to predictive strategies (higher capacity and airtightness).

4.6.3. Winter week

From *Figure 4.30* to *Figure 4.33*, results of RBC and MPC strategies are shown for a winter week in Torino (January 22nd – 28th). In *Figure 4.34*, a radar chart is reported to compare these strategies.

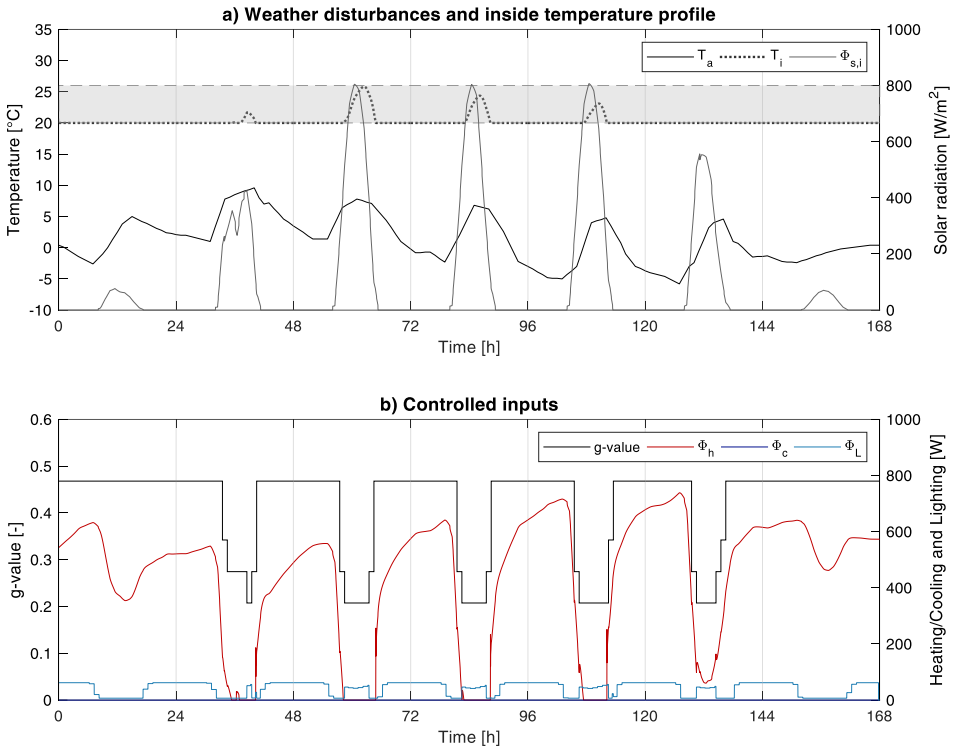

Figure 4.30. Rule Base Control based on the incident solar radiation ($\phi_{s,i}$) – Winter week

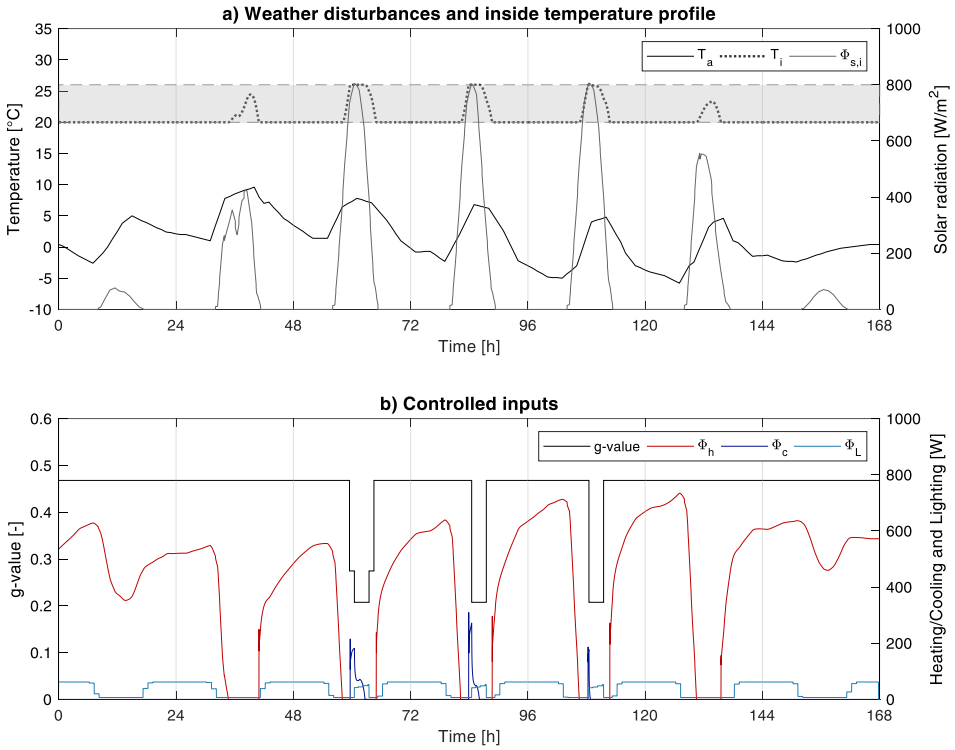

Figure 4.31. Rule Based Control based on indoor temperature (T_i) – Winter week

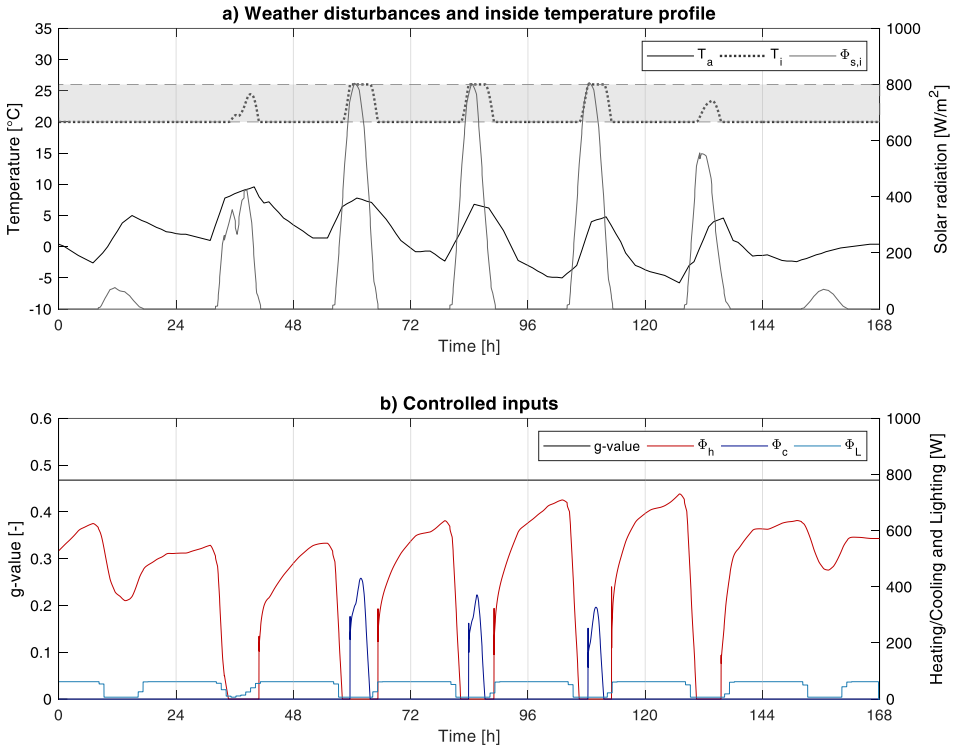

Figure 4.32. Bleached state - Winter week

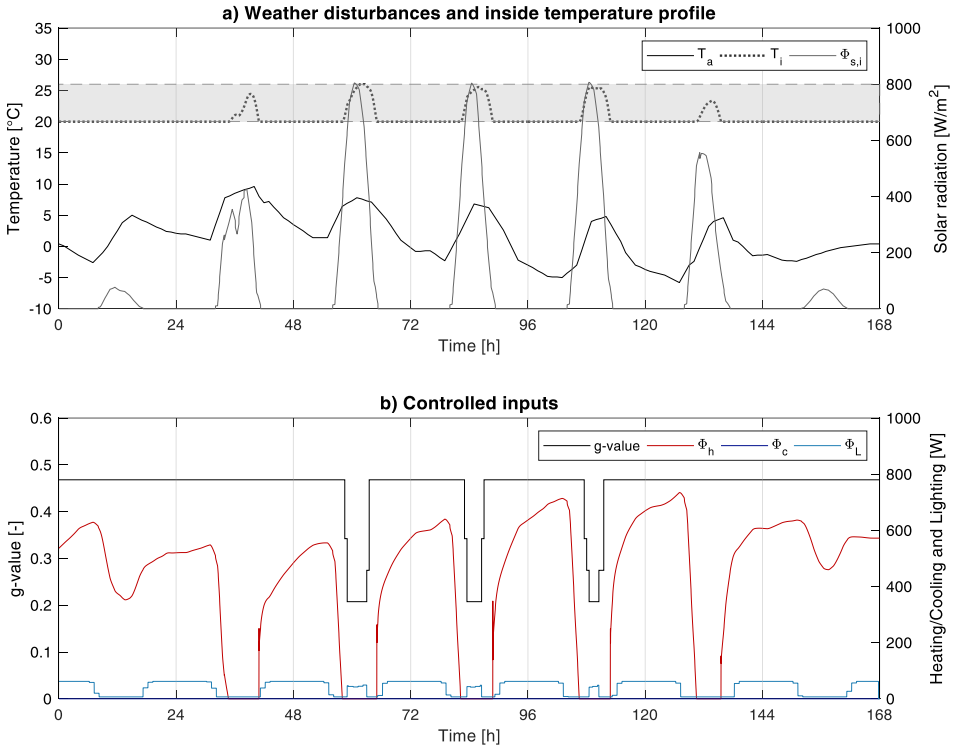

Figure 4.33. MPC control - Winter week

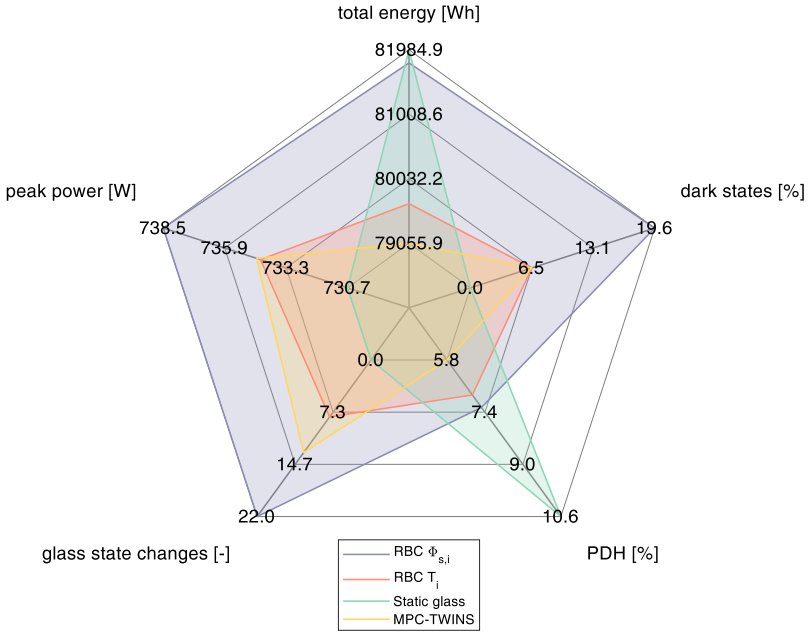

Figure 4.34. Comparison between MPC and RBC control strategies - Winter week

Table 4.11 summarises the KPI represented in *Figure 4.34*, along with the normalised polygon areas.

Table 4.11. Performance parameters and polygon areas – Winter week

	Total Energy [kWh]	**Peak Power [W]**	**Dark States [%]**	**PDH [%]**	**State changes [-]**	**Polygon Area [-]**
RBC $\phi_{s,i}$	81.79	738.48	19.64	7.27	22	2.08
RBC T_i	79.66	734.55	6.75	6.89	8	1.13
Static clear	81.98	730.71	0.00	10.56	0	1.05
MPC	79.05	734.38	6.55	5.84	13	1.00

Winter is obviously characterised by heating needs, hence solar gains can be seen as a resource. However, high solar radiation values occur even in the presented "extreme winter week", as defined in Torino IWEC file. This can result in the necessity to protect the indoor environment through solar gain modulation, especially in environments with high Window to Wall Ratios (WWR).

This allows the RBC strategy based on the incident solar radiation to protect the environment from over-heating risks, but it also causes an increased need in heating the environment, furthermore with a rougher heating curve. RBC based on the indoor temperature better exploits the solar gains, but the lack of ability to modulate the solar gains causes over-heating during the central hours of the days characterised by high solar radiation values. If compared to the *bleached state*

reference, the RBC based on the T_i value is able to lower the cooling needed caused by the over-heating occurring in the central hours of the same days. However, the lack of ability to completely protect the environment from the overheating phenomenon is unacceptable.

The MPC strategy cannot lower much the heating requirement during the hours without solar radiation, since on one side, in those ours is clearly impossible to exploit the solar gains and on the other side, because the low thermal mass curbs the predictive potential that could lead to higher thermal storages. However, the prediction abilities allow the controller to avoid over-heating during the central hours while decreasing the heating energy need. The smoother transitions are also reflected in a lower period outside comfort conditions.

4.7. Discussion

The present Chapter described a research activity path involving experimental activities, complex numerical simulations and design of advanced control strategies.

The experimental activity has seen the implementation of next-generation electrochromic glazing systems in Politecnico di Torino TWINS test facility. The nature of the collaboration with the smart glass manufacturer allowed this research activity to be carried out, even with the downside of not having a completely adaptive façade (given the static IGU). The experimental activity started with the implementation of the necessary equipment to measure all the necessary thermo-optical parameters and to gather the acquired data. An automatized structure and Python scripts were used to automatically save and process the data, with significant advantages (first and foremost avoiding data-loss) and crucial to enable real-time control applications.

Great importance was given to the test cell characterization, the white-box model validation and the grey-box model identification, since a reliable control-oriented model is paramount for a well-functioning MPC strategy [51,102].

A similar methodological approach to what described in Chapter 3 was followed to set-up the co-simulation infrastructure that needs to synchronize the physical model simulation with the controller, with its underlying management of weather data and the grey-box model, used to predict the future states. Considering the energy need for lighting incremented the complexity by adding a new contrasting need, impossible to be managed by standard RBC strategies.

As described in the results, limitations include the low thermal capacity of the test cell, which worked against the predictive abilities of the controller. Moreover, the static nature of part of the façade resulted in a not completely exploitable adaptation range.

However, the knowledge on the system thermal behaviour within the control-oriented model, allowed the controller to perform better than the widely used RBC strategies, by reducing energy consumption while keeping clear states for longer

periods, or avoiding over-heating problems by anticipating and modulating solar gains or simply smoothening transition, which often resulted in improved comfort.

Recommendation for future works on this research include the application of the previously shown strategies in real-time. This translates to the installation of an appropriate and controllable HVAC system, whose energy consumption can be measured, a dimmerable lighting system and additional sensors to evaluate the indoor light conditions (as lux probes). The grey-box model could then be identified with monitored data. Weather forecast data could be easily implemented using the widely spread web services. Monitored data on the test cell controlled with an MPC strategy would provide precious information to improve the described methodological approach.

In the presented chapter, a new methodological approach was applied, and allowed the design and implementation of a Hybrid Model Predictive Control, used in many industrial or system-related applications but new for adaptive building façade components. The improvements in the smart-glass manufacturing, demonstrated by the improved aesthetics (tinting toward neutral colours) and fast-changing tinting levels (under 3 minutes between the two extremes), need to meet improved control strategies to justify the higher costs compared to traditional solar radiation modulation systems. This work was a first attempt to merge two consolidated realities to create new possibilities for adaptive building components.

Chapter 5

5. Conclusions

This Chapter outlines the conclusions, states the limitations and illustrates the future outlook

5.1. Conclusions outline

The current share of building energy consumption, along with the increasing standards in terms of indoor comfort requirements, need to be faced with novel approaches. The outdated strategy of seeking a disconnection between the indoor and outdoor environments must be replaced with the smarter idea of exploiting the available resources in a dynamic and adaptive manner. This change of paradigm opens a whole new set of possibilities: for example, exploiting the building thermal dynamics and weather conditions, use information on energy pricing or RES generation to consequently manage the building system, or change comfort requirements based on various factors, as the presence of occupants or energy pricing. The ability to adapt to changing environmental conditions and requirements, moreover, can improve building energy flexibility, which is recently gaining importance. As a consequence, demand response strategies can be faced, answering the increasingly important need to support the electric grid requirements. The possibilities are virtually infinite, and tailored solutions can be designed for each particular case.

Adaptive building components play a central role in allowing this transition to become reality, but real-case applications are still (by far) a minority. *Hardware* technological solutions are already available and growing in terms of possibilities and adaptation ranges. However, market penetration is curbed by the high initial cost of these technologies (especially if compared with traditional building components) and the failure to fully exploit their potential during operation. This last issue can be addressed be tackled by using advanced *software* solutions, which would thus allow adaptive building components to improve their cost-effectiveness.

The presented PhD thesis was developed in this framework. Innovative building components were explored along with advanced control strategies that could enhance their applications. The research activity focused, from the *hardware* side, on electrochromic glazing, which can change its thermo-optical properties by means of an electric control. This technology is characterized by a wide adaptability range and high potential in future applicability due to decreasing costs and continuous improvements in the manufacturing. Model Predictive Control, on the other side, was identified as a promising control strategy to be used, due to its predictive nature that allows the system dynamics to be taken into account and its intrinsic capability of managing contrasting requirements, essential for a better exploitation of the adaptive components' possibilities. Moreover, MPC enables to design strategies aimed not only at reducing the energy consumption while guaranteeing the indoor comfort, but it can consider additional factors to increase the energy flexibility of the building with respect to the overall electric grid. Demand side management strategies can be implemented. Factors as the energy pricing, the availability of energy produced by renewable resources or the possibility to exploit thermal or electric storages can be taken into account. This is not a trivial characteristic, since it would not be achievable with simpler, rule-based strategies.

Following a pragmatic approach, a simulative case study was first taken into account. The first challenging step was that of translating a complex energy model in a simple and *agile* version of itself, reliable enough to provide consistent and accurate results, but requiring low computational effort to be solved. Completing this task allowed the opportunity to design a Model Predictive Controller for the management of the electrochromic glazing states and the heating/cooling system for the indoor air temperature control. Given the discrete nature of the electrochromic glazing states and the continuous nature of the heating/cooling system, a Hybrid Model Predictive Controller (HMPC) was considered the most preferable solution. In this way, no simplifications were needed: the precise thermos-optical properties of the electrochromic glazing at each state could be taken into account into the controller numerical optimization along with the continuous states of the heating/cooling system. Hard constraints were used to set the boundaries on the controlled variables and states and soft constraints to penalize undesirable conditions. Different weight matrices were defined to tune the HMPC in different ways, pushing the controller to act differently according to the preferred configuration. The possibility to use the same controller with different weight matrices allows to tune it in order to face different needs, enhancing different factors according to the needs. In order to implement the controller, a *co-simulation toolchain* was developed. Data exchange at time-step level between the physical model simulation and the controller allowed the needed benchmarking and feedback. Rule Based Controllers (RBC) were conceived with comparable logics to the most widespread control strategies found in literature. Moreover, different weather periods and climatic conditions were taken into account, with the aim of assessing the overall controller/adaptive system behaviour in different scenarios. Results obtained from the application of different HMPC strategies and baseline strategies were compared, demonstrating how the advanced HMPC outperformed simple RBC strategies. Specifically, the predictive abilities of the HMPC allowed better *solar gains modulation* that resulted in decreasing the system energy need and peak load while preserving comfort conditions and avoiding trivial, undesirable solutions (as maintaining tinted states for long periods). The success in the application of this control strategy is due to the facts that on one side solar gains greatly affect the indoor thermal conditions, and on the other side are strictly dependant on solar radiation and its evolution over time. The first element is translated in the fact that controlling solar gains has a big impact on the indoor thermal conditions, while the second element points at the prediction abilities of the HMPC as an important benefit.

A second case study has involved the installation of next-generation electrochromic glazing in an outdoor experimental test cell (TWINS). The extensive experimental activity carried out allowed the characterization of the test cell in that specific configuration and the numerical validation of the relative energy model. An automatized structure was designed and implemented with the twofold objective of automatically managing the experimental data and real-time controlling of the system (electrochromic glazing and convection heater). This activity resulted in a better insight on all the working pieces of a real-case adaptive

system and provided key information for the model validation. Following a similar methodological approach designed in the first case study, a *grey-box model* was defined and its parameters were identified using the validated energy model. A *co-simulation toolchain* was essential for linking all the working pieces of the MPC implementation. While in the first case study the lighting requirements were not taken into account, in this case they were assessed using ad-hoc simulation programs, and the relative results were implemented in the toolchain by means of a look-up table. This implementation required a different methodological approach with respect to what done for the other considered variables. The HMPC was thus designed to manage the additional lighting requirement, which often caused contrasting needs with the heating/cooling system. This aspect is particularly interesting due to the often contrasting nature of lighting and heating/cooling requirements: considering a previously stated example, high transparency states of the switchable glazing lead to an increase of natural daylight entering the environment, thus lowering the energy need for lighting; on the other end, a direct consequence is that the heat gains via solar radiation increase, leading to a potential increase in cooling energy needs. This contrasting nature of the considered variables poses a challenge to the control strategy, which needs to find a balanced trade-off solution. RBC strategies were conceived respecting the most widespread in literature, and results were used as baseline. The HMPC strategy was compared with the baseline strategies: the predictive controller was able to exploit the physical phenomena driving the system evolution, which RBC strategies cannot take into account. Moreover, the opportunity to manage contrasting needs, demonstrated with the implementation of the lighting requirements, underline the virtually boundless possibilities provided by the MPC. The great effort required to conceive and implement all the working pieces of MPC strategies is translated in a flexible, customizable and adaptable control solution able to better exploit the active building component potential.

In conclusion, the outcomes of the research activities undertaken in this PhD highlight the importance of control strategies on active building components, showing how an advanced control strategy such as the Model Predictive Control, on the one hand opens a new set of possibilities (e.g. managing contrasting needs, account for constraints) and on the other hand enhances the performance of these systems. Moreover, the intrinsic flexibility and adaptability of MPC, along with the possibility of considering multiple variables at once, enables the opportunity of exploiting the gained building energy flexibility to implement strategies aimed at taking demand response actions. This feature is considered as increasingly important nowadays, given the growing building energy intensity due to higher and more widespread comfort requirements.

The increasing complexity of *adaptive building components* and the growing availability of *cheap electronic devices*, high *computational power* and *data* (e.g. weather forecast, sensors in the built environment) will necessarily lead to a future where a holistic approach is required. Building physics, computer science, data analytics and control competences need to work as a whole to tackle future challenges. Only in this context will innovative adaptive components be seen as a

viable and convenient solution, with positive repercussions on the future built environment, with better comfort conditions, added flexibility, lower energy consumptions and more capable of exploiting renewable energy sources. The present thesis approached this novel problem with a pragmatic approach, with the result of demonstrating and assessing the opportunities provided by merging *adaptive technologies* and *advanced control strategies*.

5.2. Limitations and future outlook

The present work has focused on the implementation of Hybrid Model Predictive Control for electrochromic glazing systems. Through the described methodological framework, this goal was achieved, demonstrating the opportunities brought by this approach.

In future works online weather forecasting can be considered to allow the online control of the electrochromic façade. Improvements can be identified in the consideration of occupancy, which thanks to state-of-the-art models can be reliably predicted, thus embedding additional potential to the MPC strategies. Energy pricing prediction can be used in massive and energy intensive buildings to pre-heat or pre-cool the indoor environment during low fares or in sight of increasing prices. Finally, information on RES generation can be implemented, when applicable, to better exploit clean energy generation.

References

[1] R.J. Zedalis, International Energy Law, Int. Energy Law. (2017). https://doi.org/10.4324/9781315252056.

[2] Energy and climate change, 10/12/2019. (n.d.). https://www.eea.europa.eu/signals/signals-2017/articles/energy-and-climate-change (accessed April 10, 2020).

[3] L. Pérez-Lombard, J. Ortiz, C. Pout, A review on buildings energy consumption information, Energy Build. 40 (2008) 394–398. https://doi.org/10.1016/j.enbuild.2007.03.007.

[4] A. Allouhi, Y. El Fouih, T. Kousksou, A. Jamil, Y. Zeraouli, Y. Mourad, Energy consumption and efficiency in buildings: Current status and future trends, J. Clean. Prod. 109 (2015) 118–130. https://doi.org/10.1016/j.jclepro.2015.05.139.

[5] S.Ø. Jensen, M. Henrik, R. Lopes, R.G. Junker, D. Aelenei, R. Li, S. Metzger, K.B. Lindberg, A.J. Marszal, M. Kummert, B. Bayles, E. Mlecnik, R. Lollini, W. Pasut, Annex 67: Energy Flexible Buildings - Energy Flexibility as a key asset in a smart building future - Contribution of Annex 67 to the European Smart Building Initiatives, (2017) 1–16. http://www.annex67.org/media/1470/position-paper-energy-flexibility-as-a-key-asset-i-a-smart-building-future.pdf.

[6] S.Ø. Jensen, A. Marszal-Pomianowska, R. Lollini, W. Pasut, A. Knotzer, P. Engelmann, A. Stafford, G. Reynders, IEA EBC Annex 67 Energy Flexible Buildings, Energy Build. 155 (2017) 25–34. https://doi.org/10.1016/j.enbuild.2017.08.044.

[7] M. Perino, V. Serra, Switching from static to adaptable and dynamic building envelopes: A paradigm shift for the energy efficiency in buildings, J. Facade Des. Eng. 3 (2015) 143–163. https://doi.org/10.3233/fde-150039.

[8] M. Juaristi, T. Gómez-Acebo, A. Monge-Barrio, Qualitative analysis of promising materials and technologies for the design and evaluation of Climate Adaptive Opaque Façades, Build. Environ. 144 (2018) 482–501. https://doi.org/10.1016/j.buildenv.2018.08.028.

[9] F. Favoino, Q. Jin, M. Overend, Design and control optimisation of adaptive insulation systems for office buildings. Part 1: Adaptive technologies and simulation framework, Energy. 127 (2017) 301–309. https://doi.org/10.1016/j.energy.2017.03.083.

[10] D. Saelens, J. Carmeliet, H. Hens, Energy performance assessment of multiple-skin facades, HVAC R Res. 9 (2003) 167–185. https://doi.org/10.1080/10789669.2003.10391063.

[11] F. Favoino, F. Goia, M. Perino, V. Serra, Experimental assessment of the energy performance of an advanced responsive multifunctional façade module, Energy Build. 68 (2014) 647–659.

https://doi.org/10.1016/j.enbuild.2013.08.066.
[12] R. Baetens, B.P. Jelle, A. Gustavsen, Properties, requirements and possibilities of smart windows for dynamic daylight and solar energy control in buildings: A state-of-the-art review, Sol. Energy Mater. Sol. Cells. 94 (2010) 87–105. https://doi.org/10.1016/j.solmat.2009.08.021.
[13] N. Aste, M. Manfren, G. Marenzi, Building Automation and Control Systems and performance optimization: A framework for analysis, Renew. Sustain. Energy Rev. 75 (2017) 313–330. https://doi.org/10.1016/j.rser.2016.10.072.
[14] R.C.G.M. Loonen, M. Trčka, D. Cóstola, J.L.M. Hensen, Climate adaptive building shells: State-of-the-art and future challenges, Renew. Sustain. Energy Rev. 25 (2013) 483–493. https://doi.org/10.1016/j.rser.2013.04.016.
[15] C.M. Lai, S. Hokoi, Solar façades: A review, Build. Environ. 91 (2015) 152–165. https://doi.org/10.1016/j.buildenv.2015.01.007.
[16] F. Fiorito, M. Sauchelli, D. Arroyo, M. Pesenti, M. Imperadori, G. Masera, G. Ranzi, Shape morphing solar shadings: A review, Renew. Sustain. Energy Rev. 55 (2016) 863–884. https://doi.org/10.1016/j.rser.2015.10.086.
[17] B.P. Jelle, A. Hynd, A. Gustavsen, D. Arasteh, H. Goudey, R. Hart, Fenestration of today and tomorrow: A state-of-the-art review and future research opportunities, Sol. Energy Mater. Sol. Cells. 96 (2012) 1–28. https://doi.org/10.1016/j.solmat.2011.08.010.
[18] M. Casini, Active dynamic windows for buildings: A review, Renew. Energy. 119 (2018) 923–934. https://doi.org/10.1016/j.renene.2017.12.049.
[19] J. Al Dakheel, K.T. Aoul, Building applications, opportunities and challenges of active shading systems: A state-of-the-art review, Energies. 10 (2017). https://doi.org/10.3390/en10101672.
[20] S.D. Rezaei, S. Shannigrahi, S. Ramakrishna, A review of conventional, advanced, and smart glazing technologies and materials for improving indoor environment, Sol. Energy Mater. Sol. Cells. 159 (2017) 26–51. https://doi.org/10.1016/j.solmat.2016.08.026.
[21] A. Holstov, B. Bridgens, G. Farmer, Hygromorphic materials for sustainable responsive architecture, Constr. Build. Mater. 98 (2015) 570–582. https://doi.org/10.1016/j.conbuildmat.2015.08.136.
[22] C.G. Granqvist, Transparent conductors as solar energy materials: A panoramic review, Sol. Energy Mater. Sol. Cells. 91 (2007) 1529–1598. https://doi.org/10.1016/j.solmat.2007.04.031.
[23] P. Hoes, J.L.M. Hensen, The potential of lightweight low-energy houses with hybrid adaptable thermal storage: Comparing the performance of promising concepts, Energy Build. 110 (2016) 79–93. https://doi.org/10.1016/j.enbuild.2015.10.036.
[24] M. Oltean, Switchable glass: A possible medium for Evolvable Hardware, Proc. - First NASA/ESA Conf. Adapt. Hardw. Syst. AHS 2006. 2006 (2006) 81–87. https://doi.org/10.1109/AHS.2006.69.
[25] D. Cupelli, F.P. Nicoletta, S. Manfredi, G. De Filpo, G. Chidichimo, Electrically switchable chromogenic materials for external glazing, Sol. Energy Mater. Sol. Cells. 93 (2009) 329–333. https://doi.org/10.1016/j.solmat.2008.11.010.
[26] F. Favoino, F. Fiorito, A. Cannavale, G. Ranzi, M. Overend, Optimal control and performance of photovoltachromic switchable glazing for building integration in temperate climates, Appl. Energy. 178 (2016) 943–961. https://doi.org/10.1016/j.apenergy.2016.06.107.

[27] A. Cannavale, F. Fiorito, D. Resta, G. Gigli, Visual comfort assessment of smart photovoltachromic windows, Energy Build. 65 (2013) 137–145. https://doi.org/10.1016/j.enbuild.2013.06.019.
[28] I.B. Pehlivan, R. Marsal, E. Pehlivan, E.L. Runnerstrom, D.J. Milliron, C.G. Granqvist, G.A. Niklasson, Electrochromic devices with polymer electrolytes functionalized by SiO 2 and In2O3:Sn nanoparticles: Rapid coloring/bleaching dynamics and strong near-infrared absorption, Sol. Energy Mater. Sol. Cells. 126 (2014) 241–247. https://doi.org/10.1016/j.solmat.2013.06.010.
[29] C. Dulgerbaki, N.N. Maslakci, A.I. Komur, A.U. Oksuz, Electrochromic strategy for tungsten oxide/polypyrrole hybrid nanofiber materials, Eur. Polym. J. 107 (2018) 173–180. https://doi.org/10.1016/j.eurpolymj.2018.07.050.
[30] L.M. Huang, C.Y. Peng, C.W. Hu, H.C. Lu, C.H. Chen, D.J. Yang, C.C. Kuo, K.C. Ho, Spectroelectrochemical and adhesion properties of chemically synthesized ion conducting poly (vinyl butyral) in Prussian blue and poly (3, 4-ethylenedioxythiophene) laminated electrochromic glazing, Sol. Energy Mater. Sol. Cells. 171 (2017) 258–266. https://doi.org/10.1016/j.solmat.2017.06.051.
[31] N. Aste, F. Leonforte, A. Piccolo, Color rendering performance of smart glazings for building applications, Sol. Energy. 176 (2018) 51–61. https://doi.org/10.1016/j.solener.2018.10.026.
[32] F. Favoino, M. Overend, Q. Jin, The optimal thermo-optical properties and energy saving potential of adaptive glazing technologies, Appl. Energy. 156 (2015) 1–15. https://doi.org/10.1016/j.apenergy.2015.05.065.
[33] C.G. Granqvist, Electrochromics and Thermochromics: Towards a New Paradigm for Energy Efficient Buildings, Mater. Today Proc. 3 (2016) S2–S11. https://doi.org/10.1016/j.matpr.2016.01.002.
[34] F. Gugliermetti, F. Bisegna, Visual and energy management of electrochromic windows in Mediterranean climate, Build. Environ. 38 (2003) 479–492. https://doi.org/10.1016/S0360-1323(02)00124-5.
[35] M.N. Assimakopoulos, A. Tsangrassoulis, M. Santamouris, G. Guarracino, Comparing the energy performance of an electrochromic window under various control strategies, Build. Environ. 42 (2007) 2829–2834. https://doi.org/10.1016/j.buildenv.2006.04.004.
[36] M.N. Assimakopoulos, A. Tsangrassoulis, G. Guarracino, M. Santamouris, Integrated energetic approach for a controlable electrochromic device, Energy Build. 36 (2004) 415–422. https://doi.org/10.1016/j.enbuild.2004.01.040.
[37] V. Ritter, C. Matschi, D. Schwarz, Assessment of five control strategies of an adjustable glazing at three different climate zones, J. Facade Des. Eng. 3 (2015) 129–141. https://doi.org/10.3233/fde-130036.
[38] M. Scorpio, G. Ciampi, A. Rosato, L. Maffei, M. Masullo, M. Almeida, S. Sibilio, Electric-driven windows for historical buildings retrofit: Energy and visual sensitivity analysis for different control logics, J. Build. Eng. 31 (2020) 101398. https://doi.org/10.1016/j.jobe.2020.101398.
[39] J. González, F. Fiorito, Daylight design of office buildings: Optimisation of external solar shadings by using combined simulation methods, Buildings. 5 (2015) 560–580. https://doi.org/10.3390/buildings5020560.
[40] A. Jonsson, A. Roos, Evaluation of control strategies for different smart window combinations using computer simulations, Sol. Energy. 84 (2010)

1–9. https://doi.org/10.1016/j.solener.2009.10.021.
[41] P.F. Tavares, A.R. Gaspar, A.G. Martins, F. Frontini, Evaluation of electrochromic windows impact in the energy performance of buildings in mediterranean climates, Energy Policy. 67 (2014) 68–81. https://doi.org/10.1016/j.enpol.2013.07.038.
[42] P. Tavares, H. Bernardo, A. Gaspar, A. Martins, Control criteria of electrochromic glasses for energy savings in mediterranean buildings refurbishment, Sol. Energy. 134 (2016) 236–250. https://doi.org/10.1016/j.solener.2016.04.022.
[43] L.L. Fernandes, E.S. Lee, G. Ward, Lighting energy savings potential of split-pane electrochromic windows controlled for daylighting with visual comfort, Energy Build. 61 (2013) 8–20. https://doi.org/10.1016/j.enbuild.2012.10.057.
[44] J. Karlsson, Control System and Energy Saving Potential for Switchable Windows, Build. Simul. 2001. (2001) 199–206.
[45] E.S. Lee, A. Tavil, Energy and visual comfort performance of electrochromic windows with overhangs, Build. Environ. 42 (2007) 2439–2449. https://doi.org/10.1016/j.buildenv.2006.04.016.
[46] J. Hoon Lee, J. Jeong, Y. Tae Chae, Optimal control parameter for electrochromic glazing operation in commercial buildings under different climatic conditions, Appl. Energy. 260 (2020) 114338. https://doi.org/10.1016/j.apenergy.2019.114338.
[47] N. Aste, M. Manfren, G. Marenzi, Building Automation and Control Systems and performance optimization: A framework for analysis, Renew. Sustain. Energy Rev. 75 (2017) 313–330. https://doi.org/10.1016/j.rser.2016.10.072.
[48] A. Mahdavi, Simulation-based control of buildings systems operation, Build. Environ. 36 (2001) 789–796. https://doi.org/10.1016/S0360-1323(00)00065-2.
[49] G. Serale, M. Fiorentini, A. Capozzoli, D. Bernardini, A. Bemporad, Model Predictive Control (MPC) for enhancing building and HVAC system energy efficiency: Problem formulation, applications and opportunities, Energies. 11 (2018). https://doi.org/10.3390/en11030631.
[50] E.F. Camacho, C. Bordons, Model Predictive Control - Second edition, 2007.
[51] S. Prívara, J. Cigler, Z. Váňa, F. Oldewurtel, C. Sagerschnig, E. Žáčeková, Building modeling as a crucial part for building predictive control, Energy Build. 56 (2013) 8–22. https://doi.org/10.1016/j.enbuild.2012.10.024.
[52] X. Li, J. Wen, Review of building energy modeling for control and operation, Renew. Sustain. Energy Rev. 37 (2014) 517–537. https://doi.org/10.1016/j.rser.2014.05.056.
[53] American Society of Heating Refrigerating and Air-Conditioning Engineers :: ASHRAE, 2013 ASHRAE handbook: Fundamentals, American Society of Heating, Refrigerating and Air-Conditioning Engineers Inc, 2009.
[54] J.J. Bloem, System identification applied to building performance data / ed. by J.J. Bloem, Joint Research Centre European Commission, Luxembourg, 1994.
[55] D. Gyalistras, M. Gwerder, Use of weather and occupancy forecasts for optimal building climate control (OptiControl): Two years progress report, 2009.
https://doi.org/http://www.sysecol.ethz.ch/publications/pdfs/Gy024.pdf.
[56] S. Prívara, Z. Vana, E. Zacekova, J. Cigler, Building modeling: Selection of

the most appropriate model for predictive control, Energy Build. 55 (2012) 341–350. https://doi.org/10.1016/j.enbuild.2012.08.040.
[57] Y. Ma, F. Borrelli, B. Hencey, B. Coffey, S. Bengea, P. Haves, Model Predictive Control for the Operation of Building Cooling Systems, IEEE Trans. Control Syst. Technol. 20 (2012) 796–803. https://doi.org/10.1109/TCST.2011.2124461.
[58] P. Bacher, H. Madsen, Identifying suitable models for the heat dynamics of buildings, Energy Build. 43 (2011) 1511–1522. https://doi.org/10.1016/j.enbuild.2011.02.005.
[59] Blum D, Wetter M, MPCPy: An Open-Source Software Platform for Model Predictive Control in Buildings, Proc. 15th IBPSA Conf. (2017) 1381–1390. https://doi.org/10.26868/25222708.2017.351.
[60] F. Oldewurtel, A. Parisio, C.N. Jones, D. Gyalistras, M. Gwerder, V. Stauch, B. Lehmann, M. Morari, Use of model predictive control and weather forecasts for energy efficient building climate control, Energy Build. 45 (2012) 15–27. https://doi.org/10.1016/j.enbuild.2011.09.022.
[61] D. Sturzenegger, D. Gyalistras, M. Morari, R.S. Smith, Model Predictive Climate Control of a Swiss Office Building, Implementation, Results, Cost–Benefit Anal. 24 (2016) 1–12. https://doi.org/10.1109/TCST.2015.2415411 Y3 - 07.01.2016 U6 - http://ieeexplore.ieee.org/ielx7/87/7361777/07087366.pdf?tp=&arnumber=7087366&isnumber=7361777 M4 - Citavi.
[62] S. Privara, J. Siroky, L. Ferkl, J. Cigler, Model predictive control of a building heating system: The first experience, Energy Build. 43 (2011) 564–572. https://doi.org/10.1016/j.enbuild.2010.10.022.
[63] J. Siroky, F. Oldewurtel, J. Cigler, S. Privara, Experimental analysis of model predictive control for an energy efficient building heating system, Appl. Energy. 88 (2011) 3079–3087. https://doi.org/10.1016/j.apenergy.2011.03.009.
[64] J. Siroky, Hybrid MPC approach to reconfiguration of building heating system, Eur. Control Conf. (2013) 2675–2680.
[65] P.-D. Morosan, R. Bourdais, D. Dumur, J. Buisson, Distributed model predictive control for building temperature regulation, Am. Control Conf. (ACC), 2010. (2010) 3174–3179.
[66] Y. Ma, F. Borrelli, Fast stochastic predictive control for building temperature regulation, 2012 Am. Control Conf. (2012) 3075–3080. https://doi.org/10.1109/ACC.2012.6315347.
[67] Y. Ma, F. Borrelli, B. Hencey, A. Packard, S. Bortoff, Model Predictive Control of thermal energy storage in building cooling systems, Decis. Control. 2009 Held Jointly with 2009 28th Chinese Control Conf. CDC/CCC 2009. Proc. 48th IEEE Conf. (2009) 392–397. https://doi.org/10.1109/cdc.2009.5400677.
[68] OptiControl, (n.d.). https://opticontrol.ee.ethz.ch/index.html (accessed February 1, 2020).
[69] B. Coffey, Integrated Control of Operable Fenestration Systems and Thermally Massive HVAC Systems, (2012) 1–58.
[70] C. Gehbauer, D.H. Blum, T. Wang, E.S. Lee, Integrated Dynamic Facade Control with an Agent-based Architecture for Commercial Buildings, (2020). https://doi.org/10.20357/B7CP4S.
[71] C. Gehbauer, D.H. Blum, T. Wang, E.S. Lee, An assessment of the load modifying potential of model predictive controlled dynamic facades within

the California context, Energy Build. 210 (2020) 109762. https://doi.org/10.1016/j.enbuild.2020.109762.
[72] M. Wetter, Co-simulation of building energy and control systems with the building controls virtual test bed, J. Build. Perform. Simul. 4 (2011) 185–203. https://doi.org/10.1080/19401493.2010.518631.
[73] A. Janssens, Reliable building energy performance characterisation based on full scale dynamic measurements, Build up Web Webinar. (2016) 1–11.
[74] G. Cattarin, F. Causone, A. Kindinis, L. Pagliano, Outdoor test cells for building envelope experimental characterisation - A literature review, Renew. Sustain. Energy Rev. 54 (2016) 606–625. https://doi.org/10.1016/j.rser.2015.10.012.
[75] A.L. León-Rodríguez, R. Suárez, P. Bustamante, M.A. Campano, D. Moreno-Rangel, Design and performance of test cells as an energy evaluation model of facades in a mediterranean building area, Energies. 10 (2017). https://doi.org/10.3390/en10111816.
[76] D.B. Crawley, L.K. Lawrie, F.C. Winkelmann, W.F. Buhl, Y.J. Huang, C.O. Pedersen, R.K. Strand, R.J. Liesen, D.E. Fisher, M.J. Witte, J. Glazer, EnergyPlus: Creating a new-generation building energy simulation program, Energy Build. 33 (2001) 319–331. https://doi.org/10.1016/S0378-7788(00)00114-6.
[77] EnergyPlus™, (2017). https://doi.org/10.11578/dc.20171025.2028 (accessed April 7, 2020).
[78] L. Berkeley, O.A.K. Ridge, M.B.Y. Ut-battelle, A. For, S. Energy, D. Or, T. In, A.N.Y. Form, O.R. By, A.N.Y. Means, W. The, Application Guide for EMS, in: 2019.
[79] L. Berkeley, O.A.K. Ridge, M.B.Y. Ut-battelle, A. For, S. Energy, D. Or, T. In, A.N.Y. Form, O.R. By, A.N.Y. Means, W. The, External Interface (s) Application Guide, in: 2018: pp. 1–31.
[80] K.K. Andersen, H. Madsen, L.H. Hansen, Modelling the heat dynamics of a building using stochastic differential equations, Energy Build. 31 (2000) 13–24. https://doi.org/10.1016/S0378-7788(98)00069-3.
[81] C. Ghiaus, I. Hazyuk, Calculation of optimal thermal load of intermittently heated buildings, Energy Build. 42 (2010) 1248–1258. https://doi.org/10.1016/j.enbuild.2010.02.017.
[82] A. Bemporad, M. Morari, Control of systems integrating logic, dynamics, and constraints, Automatica. 35 (1999) 407–427. https://doi.org/10.1016/S0005-1098(98)00178-2.
[83] F.D. Torrisi, A. Bemporad, HYSDEL - A tool for generating computational hybrid models for analysis and synthesis problems, IEEE Trans. Control Syst. Technol. 12 (2004) 235–249. https://doi.org/10.1109/TCST.2004.824309.
[84] M. Toolbox, M. Herceg, M. Kvasnica, C.N. Jones, M. Morari, Multi-Parametric Toolbox 3.0, (2013).
[85] D.L. Arnold, Performance Assessment of SageGlass Electrochromic Coatings and Control Scenarios, City. 1 (2010) 35–35.
[86] E. 16798-1, Energy performance of buildings - Ventilation for buildings - Part 1: Indoor environmental input parameters for design and assessment of energy performance of buildings addressing indoor air quality, thermal environment, lighting and acoustics, (2019).
[87] G. Gennaro, Strategie di controllo avanzate di vetri elettrocromici per il risparmio energetico negli edifici: caratterizzazione sperimentale e analisi

numeriche, Politecnico di Torino, 2019.
[88] D. Pepe, Controllo dinamico della radiazione solare con smart glazing per il comfort termico ambientale: caratterizzazione sperimentale e analisi numeriche, Politecnico di Torino, 2019.
[89] F. Goia, V. Serra, Analysis of a non-calorimetric method for assessment of in-situ thermal transmittance and solar factor of glazed systems, Sol. Energy. 166 (2018) 458–471. https://doi.org/10.1016/j.solener.2018.03.058.
[90] S.P. Corgnati, M. Perino, V. Serra, Experimental assessment of the performance of an active transparent façade during actual operating conditions, Sol. Energy. 81 (2007) 993–1013. https://doi.org/10.1016/j.solener.2006.12.004.
[91] V. Serra, F. Zanghirella, M. Perino, Experimental evaluation of a climate façade: Energy efficiency and thermal comfort performance, Energy Build. 42 (2010) 50–62. https://doi.org/10.1016/j.enbuild.2009.07.010.
[92] F. Favoino, F. Goia, M. Perino, V. Serra, Experimental analysis of the energy performance of an ACTive, RESponsive and Solar (ACTRESS) façade module, Sol. Energy. 133 (2016) 226–248. https://doi.org/10.1016/j.solener.2016.03.044.
[93] DataTaker DT85, (n.d.). https://www.thermofisher.com.au/show.aspx?page=/ContentAUS/Manufacturing-Processing/Industrial-Loggers/DataTaker/DataTaker-DT85.html (accessed April 17, 2020).
[94] ISO 9869-1:2014- Thermal insulation — Building elements — Insitu measurement of thermal resistance and thermal transmittance; Part 1: Heat flow meter method, (2014) 48.
[95] UNI EN ISO 6946:2008 - Building Components and Building Elements-thermal Resistance and Thermal Trasmittance – Calculation Method, (n.d.).
[96] LBNL Window, (n.d.). https://windows.lbl.gov/software/window (accessed April 10, 2020).
[97] United States Department of Energy, EnergyPlus Version 8.9.0 Documentation: Engineering Reference, (2018) 1716. https://energyplus.net/sites/all/modules/custom/nrel_custom/pdfs/pdfs_v8.9.0/EngineeringReference.pdf.
[98] UNI EN ISO 9972:2015 - Thermal performance of buildings - Determination of air permeability of buildings - Fan pressurization method, (2015).
[99] ASHRAE Guideline 14- 2002 Measurement of Energy and Demand Savings, (2002).
[100] DIVA software, (n.d.). https://solemma.com/Diva.html (accessed April 15, 2020).
[101] UNI EN 12464-1:2011 - Light and lighting. Lighting of work places. Part 1: Indoor work places, (2011).
[102] X. Li, J. Wen, Review of building energy modeling for control and operation, Renew. Sustain. Energy Rev. 37 (2014) 517–537. https://doi.org/10.1016/j.rser.2014.05.056.